ON LINEAR ELASTIC STRAIN ENERGY-RELEASE RATE AND THE J-INTEGRAL

BY

ALIYU, ABDU ABDULLAHI (B.Eng.Mechanical, A.B.U.; M.Eng. Mechanical, A.B.U.; M.Sc. Mechanical, I.I.T., Chicago).

Submitted in Partial Fulfillment of the Requirements for the Degree of Doctor of Philosophy (Ph.D.) in Mechanical Engineering of Ahmadu Bello University, Zaria, Nigeria.

1986

CERTIFICATION

This thesis entitled, "On Linear Elastic Strain Energy-Release Rate and the J-Integral", by A. A. Aliyu, meets the regulations governing the award of the degree of Ph.D. of Ahmadu Bello University, Zaria, and is approved for its contribution to knowledge and literacy presentation.

1. Professor S. Y. Aku — Date: 5/12/85
CHAIRMAN, SUPERVISORY COMMITTEE.

2. Dr. W. Rychwalski — Date: 5/12/1985
MEMBER, SUPERVISORY COMMITTEE.

3. Dr. C. O. Folayan — Date: 5th Dec 1985
HEAD, MECHANICAL ENGR. DEPT.

4. Professor G. Osuide — Date: _____
DEAN, POST-GRADUATE SCHOOL.

ACKNOWLEDGEMENTS

I very much acknowledge the encouragement and helpful suggestions of my main adviser, Professor S. Y. Aku. I also appreciate the helpful discussions of my co-adviser, Dr. W. Rychwalski. The cooperation of many technical staff of the Mechanical Engineering Department is very much acknowledged.

I would also like to express my sincere gratitude to the Administrators of Ahmadu Bello University, for awarding a study fellowship to me between June, 1982 to September, 1985, to work on my Ph.D. degree programme. Finally, I do not even know how to best express my deep pleasure and gratitude to Professor A. Abdullahi, the Vice-Chancellor of A.B.U. and Professor S. Y. Aku, the then Head of Mechanical Engineering Department, A.B.U., Zaria, for their excellent cooperation with me during the period of my study fellowship.

ABSTRACT

A brief review of the trend in Fracture Mechanics studies was provided. Some solutions of elementary fracture mechanics problems were re-investigated. Many of those solutions were shown to have some limitations. These limitations were in the form of introducing some unrealistic stress and displacement distributions. The general applicability of the strain energy-release rate and the J-integral as crack tip parameters are based on viewing the stress and strain fields at the crack tip with an appropriate rationale. Therefore, based on the elementary problems considered and their reported solutions, some inconsistencies in the application and interpretation of the Irwin crack extension force, G and the J-integral as crack tip parameters, were pointed out.

For the purpose of eliminating some of the limitations noted in the review, a plane quasi-static problem was reconsidered. By employing the well-known Kolosov-Muskhelishvili equations, some new formulae were derived. The new formulae are, in fact, the generalized Westergaard formulae. It was furthermore proved that the new formulae satisfy all necessary equations of motion and conditions of plane elasticity.

Applying the new formulae, some special problems in both the main body of the thesis and the appendix, were solved. From the problems considered, the crack extension force, G, was evaluated from the new solutions developed. Furthermore, a new crack tip characterizing parameter, denoted by I, (after G.R. Irwin) was developed. The effect of biaxial loading

on the Irwin crack tip parameter, I, was investigated. It was furthermore shown that characterization via the crack extension force concept is equivalent to crack tip characterization via the Irwin parameter.

Also from the problems considered, the J—integral was investigated. For all the cases considered, it was shown that the J-integral at a crack tip is not equal to the Irwin crack extension force, G, at the same crack tip. From the solutions again, by consi—dering some appropriate rationale, the J-integral was shown to yield unrealistic results for some loadings.

Finally, some experiments were conducted on glass to determine its fracture toughness values. All the experiments were conducted at room temperature and a loading rate of 2.0 cm/min. From the different experiments conducted, consistent values of the fracture toughness values were obtained. A critical strain energy-release rate, G_1 = 6.93 N/m and a critical Irwin parameter, $I_{1c} = 997.6 \times 10^3$ N/m for the glass were obtained.

TABLE OF CONTENTS

	Page
CERTIFICATION	i
ACKNOWLEDGEMENTS	ii
ABSTRACT	iii
LIST OF SYMBOLS	vii
LIST OF FIGURES	ix
LIST OF TABLES	xi
CHAPTER:	
I. LITERATURE REVIEW	1
1.1. Introduction	1
1.2. Some Notable Results	6
1.3. Crack-tip Characterizing Parameters	15
1.4. Aims and Scope of the Thesis ...	19
II. SOLUTIONS OF CRACK PROBLEMS BY COMPLEX POTENTIALS (1)	21
2.1. Introduction	21
2.2. The Westergaard Formulae ...	23
2.3. Derivation of The New Formulae ...	24
2.4. Proof of the Correctness of the New Formulae	27
2.5. Conclusions	30
III. SOLUTIONS OF CRACK PROBLEMS BY COMPLEX POTENTIALS (2)	32
3.1. Introduction	32
3.2. The New Formulae Applied to Some Mode I Problems	32
3.3. Some Comments About the New Solutions	43
3.4. Conclusions	56

CHAPTER: Page

IV. THE STRAIN ENERGY-RELEASE RATE ... 63

4.1. Introduction 63

4.2. Evaluation of the Strain Energy-Release Rate 65

4.3. Some Applications of the Concept of The Strain Energy-Release Rate 68

4.4. The New Irwin Crack-tip Characterizing Parameter ... 74

4.5. Conclusions 80

V. THE J-INTEGRAL 81

5.1. Introduction 81

5.2. Evaluation of the J-Integral 86

5.3. Some Discussions on the J-Integral 92

5.4. Conclusions 96

VI. EXPERIMENTAL PROGRAMME 98

6.1. Introduction 98

6.2. Specimens Preparation ... 105

6.3. Tests Procedure 107

6.4. Results, Evaluations and Discussions 112

6.5. Conclusions 125

VII. SUMMARY, CONCLUSIONS AND SUGGESTIONS FOR FUTURE WORK 128

7.1. Summary 128

7.2. Conclusions 132

7.3. Discussions and Suggestions for Future Work 133

7.4. New and Major Contributions to Knowledge 142

APPENDIX A: Solutions of Some Other Problems 144

APPENDIX B: Sample Calculations of G and J 158

R E F F E R E N C E S 163

LIST OF SYMBOLS

A, A_o = Functions of biaxial loading in the old stress and displacement distributions.

$2a$ = Crack length.

$2b_o$ = Width of specimen.

E = Young's Modulus.

$e_{xx}, e_{yy}, \gamma_{xy}$ = Strain components, in a 2-D body.

$f\sigma$ = Material fringe value.

G, G_1, G_{11} = Strain energy-release rate.

G_{1c} = Critical strain energy-release rate.

h = Thickness of plane body.

i = $\sqrt{-1}$ or 1,2.

J = Rice J-integral.

j = 1,2.

I, I_1 = Irwin crack-tip parameter.

I_{1c} = Critical Irwin crack-tip characterizing parameter.

$\bar{I}, \bar{I}_1, \bar{I}_{1c}$ = Non-dimensional I, I_1 and I_{1c} respectively.

K_1 = Opening mode stress intensity factor.

K_{11} = In plane shear mode stress intensity factor.

L = Length of specimen.

M = Moment.

$n_i = n_1, n_2$ = Components of unit vector.

n = Number of crack-tips.

N = Constant, in the new formulae.

$Re(f), Im(f)$ = Real and Imaginary parts of a complex function f.

r, θ = Polar coordinates at the crack-tip.

p = Concentrated load.

P = Maximum principal stress density factor.

Q = Maximum principal strain density factor.

R = Maximum shear stress density factor.

S = Maximum strain energy density factor.

T = Maximum distortion energy density factor.

u,v,w = Displacements in the x,y and z directions respectively.

U = Airy stress function.

W = Strain energy density.

x,y = Rectangular coordinates.

Y = Width correction factor.

z = $x + iy$

$Z_1=Z_1(z)$, $Z_{11}=Z_{11}(z)$ = Complex stress functions.

$\phi = \phi(z)$ = Complex stress function.

$\phi' = \phi'(z)$ = Differentiation of ϕ with respect to z.

$\sigma_{xx}, \sigma_{yy}, \tau_{xy}$ = Stress components.

σ_o, σ_o^P, τ_o = Applied stresses.

σ_1 σ_2 = Principal stresses.

$(\sigma_o)\alpha$ = Applied stress for a given value of α.

σ_f = Fracture strength of a material.

μ,ν = Shear Modulus and Poissions Ratio, respectively.

κ = Constant (function of ν)

α = Biaxility coefficient.

Γ = Path of integration of J.

LIST OF FIGURES

Fig. 1: The Modes I, II and III crack propagation.

Fig. 2: Some elementary problems.

Fig. 3: The distribution of α_{xx} along the x-axis.

Fig. 5: The path Γ.

Fig. 6: The plots of $(2\sigma_1\sqrt{2\pi r})/K_1$ and $(2\sigma_2\sqrt{2\pi r})/K_1$ against angular Position θ at the crack tip.

Fig. 7: Some Reported Experimental fringes, I.

Fig. 8: Some Reported Experimental fringes, II.

Fig. 9: Some Reported Experimental fringes, III.

Fig.10: The plots of $\sigma^c_{xx}/\sigma^a_{xx}$, $\sigma^c_{yy}/\sigma^a_{yy}$ and τ^c_{xy}/τ^a_{xy}.

Fig.11: The theoretical shapes of fringes from the new solution for uniaxial loading.

Fig.12: The plot of the biaxial factor α against N.

Fig.13: The plot of $(\sigma_o)\alpha/\sigma_o$ against α for $\nu = .3$.

Fig.14: The J-integral evaluation for a crack in a large plate.

Fig.15: The plots of $4EJ/K_1^2$ and $4EG/K_1^2$ against α for plane stress, $\nu = .3$.

Fig.16: A sketch of the centre cracked specimen.

Fig.17: The plots of the width correction factor Y against a/b_o.

Fig.18: Simple tension tests specimens for statically characterizing the glass.

Fig.19: Some unsuccessful broken specimens.

Fig.20: Set up of the specimen on the Denison Testing Machine.

Fig.21: Some broken specimens for fracture toughness measurements (i) and cross-sectional area of specimen showing initial crack length a (ii).

Fig.22: The plot of the applied stress against axial strain.
Fig.23: The plot of the applied stress against transverse strain.
Fig.24: The plot of the transverse strain against the axial strain.
Fig.25: A large plate with a central crack of length 2a loaded by point loads.
Fig.26: A large plate with a central crack of length 2a loaded by moments.
Fig.27: A large plate with two equal collinear cracks.
Fig.28: A large plate with three cracks along the x-axis.
Fig.29: A large plate with infinite row of cracks along the x-axis.

x

LIST OF TABLES

TABLE 1: The maximum load recorded for some simple tension test specimens.

TABLE 2: The load and the strains recorded for an S6 specimen.

TABLE 3: Values of Young's modulus and Poisson's ratio from S6, S7 and S9 specimens.

TABLE 4: The average values of some mechanical properties of glass.

TABLE 5: Maximum load and initial crack length for six centre cracked specimens.

TABLE 6: Some crack-tip parameters for glass evaluated without width corrections.

TABLE 7: Some crack-tip parameters for glass evaluated with width corrections.

TABLE 8: Some mechanical properties of the glass.

CHAPTER I

LITERATURE REVIEW

1.1. Introduction

Fracture Mechanics is a relatively new branch of solid mechanics which began attracting research interest during the World War II. The major reason for the interest was as a result of the observations that structures designed on yield strength concept and with the applied tensile stresses known to be in the safe regions, still failed by propagation of brittle cracks. When the subject was originally introduced, because the materials that fail in brittle fashion, i.e. fracturing with limited plastic extent, under normal conditions, are few, the theory was neglected. It was later on revived when it was noticed that independently of temperature, structural elements that display ductile properties in standard tensile tests in some cases fail by brittle process.

In the revived theory, the basic foundation is that the stress and the strain fields surrounding a brittle crack are characterized by a parameter called the 'stress intensity factor' multiplied by a $\frac{1}{\sqrt{r}}$ singularity, where r is the distance from the brittle crack-tip. The foundation was introduced in the 1950's. To date, all theories of brittle fracturing are based on viewing the stress and strain fields at the tip of a crack and incorporating some appropriate rationale and or a hypothesis. Before describing some of the theories it is

therefore necessary to calculate the distribution of stress in the neighbourhood of a crack in an elastic solid. The discussions are restricted to plane, quasi-static problems.

Some of the most important analytical methods for flawed structures, include the complex potential technique, the integral transforms technique, the singular integral equations technique and the numerical method. A description of these techniques can be found in the works of Erdogan (1983), Muskhelishvili (1953), Sneddon and Lowengrub (1969), Sokolnikoff (1956) and Williams (1956).

Common to all these techniques is that one is solving a problem in which the solution must satisfy the equilibrium conditions, the compatibility conditions, the stress-strain relations and the boundary conditions of the problem. One can therefore employ any of these techniques for a particular problem and the results must be the same for all the techniques. Furthermore, as mentioned earlier, it is from these solutions with some appropriate rationale that useful concepts in fracture mechanics are developed. For structural members with cracks, crack-tip characterizing parameters are the most useful concepts that have already been developed.

The concepts of the crack-tip characterizing parameters to be fully studied here, are the strain-energy release rate and the J-integral. The series of works of Griffith (1920), Muskhelishvili (1953), Westergaard(1939),

Sneddon (1946) and Irwin (1957, 1960) adequately introduced the strain energy release rate concept while Rice (1968) introduced the J-integral concept.

The concept of the strain energy release rate (originally surface tension force per unit area) was introduced by Griffith (1920). He argued that, like liquids, solids possess surface tension. He then formulated a criterion which states that, a crack will begin to spread when the rate of change with respect to crack length of the strain energy stored in the structure equals the rate of change of the surface energy of the crack. He conducted some experiments to prove his theory but the results were not totally successful. Although not totally successful, that historical work was among the first useful experimental results which indicate the usefulness of the subject as an engineering tool for design. It has proved that the fracture behaviour of one cracked body may be predicted on the basis of the observed behaviour of another body.

The major development to date in fracture mechanics can be attributed to Muskhelishvili's (1953) work on the complex form of two-dimensional equations of elasticity. With the aid of the work of Kolosov, G.B., Muskhelishvili obtained what are now called the Kolosov-Muskhelishvili formulae.

Furthermore, Westergaard (1939) employed the Kolosov equations and obtained the solutions of some two-dimensional problems by employing the now called

Westergaard stress functions.

Then Sneddon (1946) employed the Westergaard formulae and obtained the asymptotic stress distribution at the neighbourhood of a crack.

Irwin (1957, 1960), by employing the Sneddon's work, obtained the asymptotic stress and displacement distributions in the neighbourhood of a crack in terms of a characterizing parameter called the stress intensity factor. He then classified the stress intensity factor into three modes. These are: the mode I or the opening mode stress intensity factor, K_1, the mode II or the in-plane shear mode stress intensity factor, K_{11} and the mode III or the tearing mode stress intensity factor, K_{111}. (See Fig. 1). Furthermore, Irwin (1960) by employing the Griffith (1920) work, proposed that in the Griffith theory of brittle fracture, the rate of plastic work at the crack tip should also be considered as a dissipative energy component. That term introduced by Irwin is called the strain energy release rate, G (G after Griffith) or the crack extension force.

For some further additional information about the stress intensity factors and the strain energy release rate, one can refer to the works of Atkinson and Eshelby (1968), Clausing (1969), Dally and Sanford (1978), Erdogan (1983), Hayes (1975), Heyer (1973), Irwin et al (1978), Sanders (1960) and Wheeler et al (1982).

Another characterizing parameter which has currently been used is the J-integral, which was interpreted as the rate of change of potential energy in the body, Rice(1968).

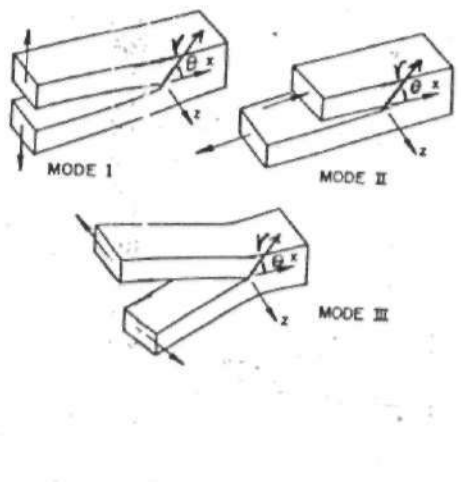


Fig. 1: Modes I, II and III Crack Propagation

When it was proposed, it was accepted as a universal tool to be applied to linear elastic, non-linear elastic and elastic-plastic fracture mechanics problems, Rice (1968) and Paris (1977). At least for the linear elastic case it has been generally accepted by many researchers to be equal to the strain energy release rate. More information about the J-integral can be obtained from the works of Aoki et al (1981), Begley and Landes (1972), Budiasky and Rice (1973), Herrmans (1981), Paris et al (1979) and Turner (1975).

1.2. Some Notable Results

It was stated by Irwin (1957) and proved by Eftis and Liebowitz (1972) and Sanford (1979) and used in many reported studies of the stress intensity factors and the strain energy-release rate, that when a structure which has a flaw in the form of a crack, is subjected to some generalized symmetric opening mode loadings, with the crack along the x-axis, the z-axis perpendicular to the crack border and r, θ are polar coordinates at the crack tip in the xy-plane, then the stress distribution in the neighbourhood of the crack-tip could be written as, see Figs. 1 and 2 for K_1 and r,θ coordinates.

$$xx = \frac{K_1}{\sqrt{2\ \pi\ r}} \text{Cos } \tfrac{1}{2}\ \theta[1 - \text{Sin } \tfrac{1}{2}\ \theta \text{ Sin } \tfrac{3}{2}\ \theta]-2A \qquad \text{----------(1.2.1)}$$

$$\sigma_{yy} = \frac{K_1}{\sqrt{2\pi r}} \text{Cos } \tfrac{1}{2}\theta[1+\text{Sin } \tfrac{1}{2}\theta\text{Sin } \tfrac{3}{2}\theta], \quad \text{----(1.2.2)}$$

$$\tau_{xy} = \frac{K_1}{\sqrt{2\pi r}} \text{Cos } \tfrac{1}{2}\theta\text{Sin } \tfrac{1}{2}\theta \text{ Cos } \tfrac{3}{2}\ \theta, \quad \text{------(1.2.3)}$$

and

$$\sigma_{zz} = [{}^{\nu(\sigma_{xx}+\sigma_{yy}),\ \text{for plane strain}}_{0,\ \text{for plane stress}}]], \quad \text{---(1.2.4)}$$

where K_1 is the mode I stress intensity factor which is

a function of the applied stress and crack size, A is a real constant and ν is the Poisson's ratio of the material.

Equations (1.2.1- 4) were assumed to be valid for a number of problems including a large plate with a straight central crack along the x-axis loaded by far field stresses in both the x and y directions; a series of equally spaced cracks on the x-axis in an infinite plate also loaded by far field generalized mode I forces; a single crack along the x-axis in an infinite plate with a wedge action applied to produce a pair of splitting forces and an edge-notch plate subjected to some mode I loadings, etc. The stress intensity factor, K_1 and the constant A, depend on the nature of the problem.

As an example, for an infinite plate with a finite central crack of length 2a, along the x-axis, the stress intensity factor, K_1, becomes, Irwin (1957),

$$K_1 = \sigma_o \sqrt{\pi a}, \quad \text{----------(1.2.5)}$$

where σ_o is the far field applied stress in the y-direction. If the far field applied stress in the x-direction is $\sigma_{xx} = \alpha\sigma_o$ where α is some constant, then

$$2A = (1 - \alpha)\sigma_o, \quad \text{---------- --(1.2.6)}$$

Equations (1.2.1-6) are accepted to be the solution of the problem shown in Fig. 2(i). In the next paragraphs, it is shown that these equations are solutions to the problem only when A = 0.

The constant 2A in equations (1.2.1) was intentionally added to satisfy the far field boundary condition of the problem but unfortunately, it has violated

the boundary conditions along the free crack surface. As for example, from Eftis and Liebowitz (1972) and Sanford (1979), one can write the stress σ_{xx} distribution as

$$\sigma_{xx} = \text{Re } Z_1 - y \text{ Im } Z_1' - 2A, \quad \text{----------(1.2.7)}$$

where Z_1 is the Westergaard stress function and the prime denotes differentiation with respect to Z. Re( ) and Im( ) represent the real and the imaginary parts of a complex function, respectively.

For the infinite plate considered above

$$Z_1 = \sigma_\infty \frac{Z}{\sqrt{Z^2-a^2}}, \quad \text{----------(1.2.8)}$$

and

$$z = x + iy, \quad \text{----------(1.2.9)}$$

Along the x-axis, one obtains from equations (1.2.7), (1.2.8) and (1.2.9)

$$\sigma_{xx} = \sigma_\infty \text{ Re } \frac{x}{\sqrt{x^2-a^2}} - 2A, \quad \text{--------(1.2.10)}$$

Fig. 3 shows the non-dimensional σ_{xx} distribution.

There are two immediate discrepancies in equation (1.2.10). First, the skin stress, $\sigma_{xx} \neq 0$ for some loadings and zero for some others, for $|x| \leq a$. Secondly, a material point at $x = a$, say, is subjected to some finite stress of $-2A$ at $x = a^-$ and an infinite stress at $x = a^+$. Note that in the limit, a^-, $a^+ \to a$. Naturally, both the observations may not be possible.

Let us next consider the displacement distribution. From Eftis and Liebowitz (1972) and Sanford (1979), one can derive the displacement in the x-direction, u, as

$$2\mu u = \text{Re}\left[\left(\frac{\kappa-1}{2}\right)\int Z_1 dz - \left(\frac{\kappa-1}{2}\right)Az - \bar{C}_\infty\right] - y \text{ Im}[Z_1 - A]$$

$$\text{-------(1.2.11)}$$

where μ is the shear modulus, Z_1 is given by equation (1.2.8) and C_o is some constant to be determined from the displacement boundary condition of the problem, while

$$\kappa = \begin{cases} 3-4\nu, & \text{for plane strain} \\ \frac{3-\nu}{1+\nu}, & \text{for plane stress} \end{cases}, \quad \text{-------(1.2.12)}$$

A careful study of equation (1.2.11) reveals that there is either a separation (tearing) of the plate along the y-axis ($x = 0$) when $\bar{C}_o \neq 0$ or some unrealistic displacement at the crack tip $x = a$ results. Both of these are not possible.

Similarly for all A, which means for different biaxial loadings from Muskhelishvili (1953) and some others, one obtains the vertical displacement V along the x-axis as $2\mu v = (\kappa+1)/4\ \sigma_o\sqrt{a^2 - x^2}$ for $|x| \leq a$ and zero for $|x| \geq a$. This means that the displacement is a function of only some selected loading, which naturally cannot be so.

Furthermore, by employing the stress-optic law and the whole field stress distribution of the problem, along the x-axis, gives

$$A = \frac{N_o f_\sigma}{h}, \quad \text{-------(1.2.13)}$$

where N_o is the fringe order, f_σ is the material fringe value and h is the model thickness. Experimentally, as for example from the works of Dally (1979), Fig. 9; Irwin et al (1978), Figs. 7, 9 and 10; Sanford (1979), Fig. 1; and William (1962), Figs. 3, 5 and 8, N_o was never observed to be a constant along the x-axis. Some of these fringes are shown in Figs. 7 - 9. It implies that equation (1.2.13) is not satisfied, which clearly

indicates that equations (1.2.1) do not give the correct stress distribution.

In addition to all of the above, a careful study of the stress distribution reported above would reveal that the theoretical fringes formed for uniaxial loading are as shown in Fig. 4 which is different from what has been observed experimentally. The tilting of the fringes is like so due to the existence of the skin stress at $|x| \leq a$ which introduced some unrealistic displacements.

From the above discussions, one concludes that equations (1.2.1) to (1.2.7) do not represent any stress state except when A = 0.

It should be noted that in the solutions noted above, there are no errors in the analysis, but that when these models are applied to the problems of Fig. 2, some stresses and displacements are introduced which violate the boundary conditions of the problem intended to be solved. These models could therefore be described as inadequate. The aim of this research therefore was to point out these limitations and to gear efforts towards improving on the limitations Note that in the discussions and improvements to follow, the coordinate systems x,y and r,θ are as shown in Figs. 1 and 2.

As a further example of a reported solution, consider the infinite plate shown in Fig. 2(ii), loaded by some uniform pressure of intensity σ_o along $-a \leq x \leq a$. By employing the modified Westergaard formulae, introduced by Eftis and Liebowitz (1972) and

the Westergaard stress function

$$Z_1 = \sigma_o \left[\frac{z}{\sqrt{z^2-a^2}} - 1\right], \text{ ----------(1.2.14)}$$

the stress distribution in the neighbourhood of the crack tip is given as

$$\sigma_{xx} = \frac{K_1}{\sqrt{2\pi r}} \text{Cos } \tfrac{1}{2}\theta[1-\text{Sin } \tfrac{1}{2}\theta \text{ Sin } \tfrac{3}{2}\theta]-\sigma_o, \text{---(1.2.15)}$$

$$\sigma_{yy} = \frac{K_1}{\sqrt{2\pi r}} \text{Cos } \tfrac{1}{2}\theta[1+\text{Sin } \tfrac{1}{2}\theta \text{ Sin } \tfrac{3}{2}\theta]-\sigma_o, \text{---(1.2.16)}$$

and

$$\tau_{xy} = \frac{K_1}{\sqrt{2\pi r}} \text{Cos } \tfrac{1}{2}\theta \text{ Sin } \tfrac{1}{2}\theta \text{ Cos } \tfrac{3}{2}\theta, \text{----(1.2.17)}$$

Where K_1 is given by equation (1.2.5). The same stress distribution was reported by Sneddon and Lowengrub(1969). Inspecting equations (1.2.15), it is observed that there is a normal stress of magnitude $-\sigma_o$, along the crack surface. That is naturally impossible and cannot be acceptable. Furthermore, a careful examination of the solution would reveal that at the crack tips $x = \pm a$, some unrealistic displacements of magnitude $\pm(\kappa-1)\sigma_o a/4\mu$ exist. These displacements are not acceptable in Fig. 2(ii) problem.

Another problem of interest is that shown in Fig. 2(iii). The reported solution could be found in Irwin (1957). These solutions are not acceptable for the following reasons. First, in almost all reported solutions of the problem of concentrated force in elasticity, such as in Muskhelishvili (1953) and Sokolnikoff (1956), the stress must be infinite at the point of application of the load. This is not so in

the solution of this problem. Secondly, the solution predicts some unrealistic displacements of magnitude $u = \pm(\kappa - 1)P/4\mu a$ at the crack tips. Thirdly, for any applied load P, the vertical displacement is always zero. Finally, when one employs these solutions and evaluates the total strain energy of the loaded system, this is found to be zero. All these are indications that these models cannot be applied to the problem shown in Fig. 2(iii).

Now let us turn our attention to the reported solutions of a mode II problem. It is shown in Fig. 2(iv). These equations were also extensively reported in the literature of fracture mechanics. For some more information about the mode II problem, one can refer to Erdogan (1983), Sneddon and Lowengrub (1969) and Irwin (1960). Under mode II loading, the stress distributions in the neighbourhood of the crack tip are given by

$$\sigma_{xx} = -\frac{K_{11}}{\sqrt{2\pi r}} \text{Sin } \tfrac{1}{2}\theta[2+\text{Cos } \tfrac{1}{2}\theta \text{ Cos } \tfrac{3}{2}\theta], \text{---(1.2.18)}$$

$$\sigma_{yy} = \frac{K_{11}}{\sqrt{2\pi r}} \text{Sin } \tfrac{1}{2}\theta \text{ Cos } \tfrac{1}{2}\theta \text{ Cos } \tfrac{3}{2}\theta, \text{ ------(1.2.19)}$$

and

$$\tau_{xy} = \frac{K_{11}}{\sqrt{2\pi r}} \text{Cos } \tfrac{1}{2}\theta[1-\text{Sin } \tfrac{1}{2}\theta \text{ Sin } \tfrac{3}{2}\theta], \text{ ---(1.2.20)}$$

where K_{11} is the mode II stress intensity factor which is a function of the applied stress and the crack size. Equations (1.2.18)can easily be obtained by employing the Westergaard formulae as, Sneddon and Lowengrub (1969),

$$\sigma_{xx} = 2\ \mathrm{Im}Z_{11} + y\ \mathrm{Re}\ Z'_{11}, \quad \text{----------(1.2. 21)}$$

$$\sigma_{yy} = -\ y\ \mathrm{Re}\ Z'_{11}, \quad \text{----------(1.2. 22)}$$

$$\tau_{xy} = \mathrm{Re}\ Z_{11} - y\ \mathrm{Im}Z'_{11}, \quad \text{----------(1.2. 23)}$$

$$2\mu u = \frac{(\kappa+1)}{2}\mathrm{Im}\int Z_{11}dz + y\ \mathrm{Re}\ Z_{11}, \quad \text{----(1.2. 24)}$$

and

$$2\mu v = \frac{(\kappa-1)}{2}\mathrm{Re}\int Z_{11}dz - y\ \mathrm{Im}\ Z_{11}, \quad \text{-----(1.2. 25)}$$

where $Z_{11} = Z_{11}(z)$ is a stress function, u and v are displacements in the x and y directions, respectively.

For an infinite plate with a central crack of length 2a,

$$Z_{11} = \tau_o \frac{z}{\sqrt{z^2-a^2}}, \quad \text{----------(1.2.26)}$$

and

$$K_{11} = \tau_o \sqrt{\pi a}, \quad \text{----------(1.2.27)}$$

where τ_o is the far field applied stress τ^{∞}_{xy}.

An important boundary condition for the mode II problem is that the displacement v along the axis y = 0 has to be zero. We expect that boundary condition to be satisfied even from the symmetry condition of the problem. Unfortunately, that boundary condition is violated by the solution in equations (1,2.18), because from equations (1.2. 21) to (1.2.26), one obtains

$$2\mu v = -\frac{(\kappa-1)}{2}\tau_o \sqrt{x^2-a^2}, \quad \text{----------(1.2.28)}$$

for $|x| \geq a$. Since the theoretical model violates the displacement boundary condition, it then means that the stresses are not the exact ones sought for the problem of Fig. 2(iv).

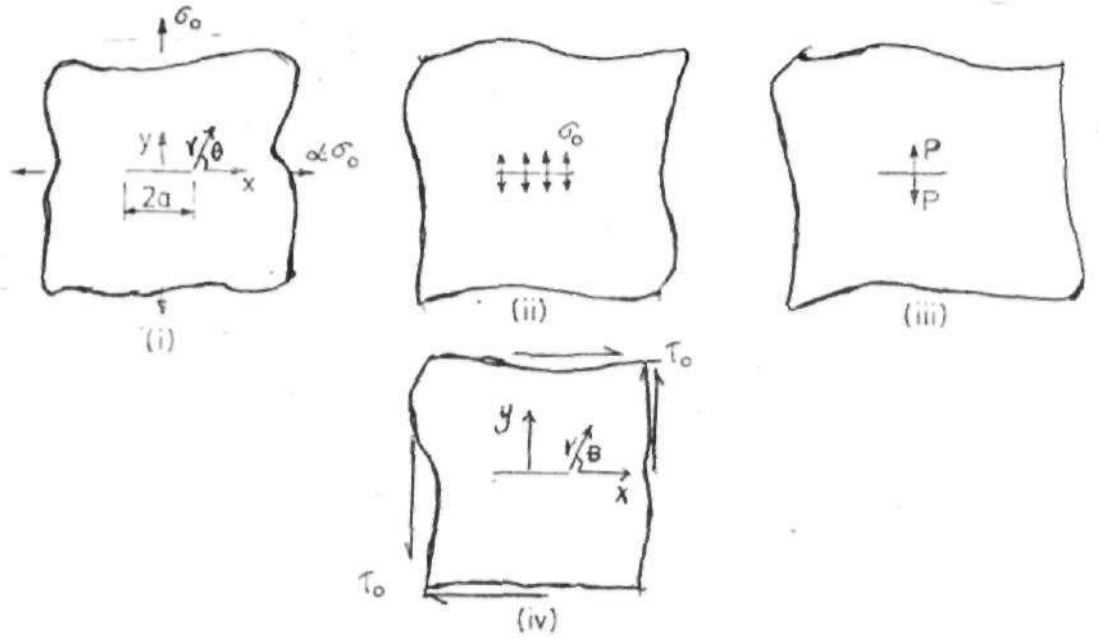


Fig .2: Some elementary problems.

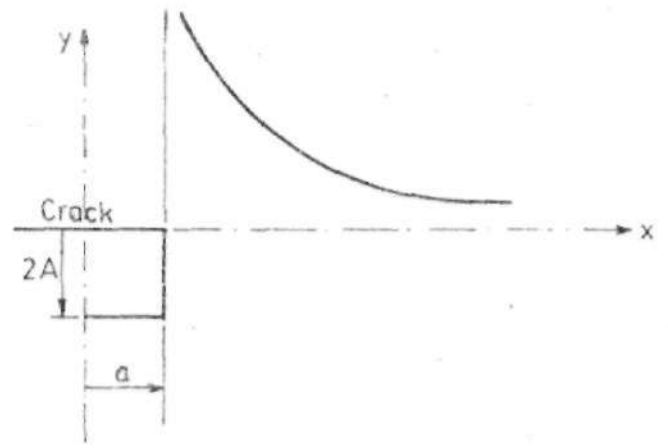


Fig .3: The distribution of σ_{xx} along the x-axis

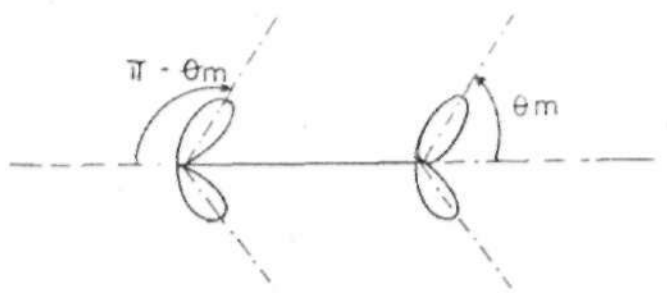


Fig .4: Shape of fringes from the reported solution of uniaxially loaded plate .

1.3. Crack-Tip Characterizing Parameters

A very significant development which has helped a lot towards the practical application of fracture mechanics is the introduction of some concepts in the form of crack-tip characterizing parameters. Some of these characterizing parameters are the stress intensity factor, the strain energy-release rate and the J-integral. For some additional information about the development of the concept and the application of the stress intensity factor and the strain energy-release rate, one is referred to Clausing (1969), Erdogan (1983), Irwin (1957, 1960, 1978), Hayes (1975) and Heyer (1973). And for the J-integral, one is referred to Begley and Landes (1972), Budiasky and Rice (1973), Paris et al (1979) and Rice (1968).

These parameters are defined as follows:

The modes I and II stress intensity factors, K_1 and K_{11} are

$$K_1 = \lim_{\substack{r\to o \\ \theta = o}} \sigma_{yy}(r,\theta)\sqrt{2\pi r}, \qquad \text{----------(1.3.1)}$$

and

$$K_{11} = \lim_{\substack{r\to o \\ \theta = o}} \tau_{xy}(r,\theta)\sqrt{2\pi r}, \qquad \text{----------(1.3.2)}$$

while the modes I and II strain energy-release rate originally formulated as crack extension force, G, are, Irwin (1957)

$$G_1 = \lim_{\Delta a \to o} \frac{n}{\Delta a} \int_o^{\Delta a} \tfrac{1}{2}\, \sigma_{yy}(r=r';\theta=0)\, v(r=\Delta a - r';\theta=\pi)\, dr'$$

.....(1.3.3.)

and

$$G_{11} = \lim_{\Delta a \to o} \frac{n}{\Delta a} \int_o^{\Delta a} \tfrac{1}{2}\tau_{xy}(r=r';\theta=0)\, u(r=\Delta a - r';\theta=\pi)\, dr'.$$

----------(1.3.4)

The J-integral is defined as, Rice (1968),

$$J = \int_{\Gamma}[Wn_x - T_i u_{i,x}]ds, \quad \text{----------(1.3.5)}$$

where Δa is an element of crack growth, n is the number of symmetric crack-tips, W is the strain energy density, T_i is the traction vector on Γ, $u_i = u,v$ are the displacements in the x and y directions, respectively, Γ is a curve surrounding the crack-tip, ds is an element of Γ and n_x, n_y are components of unit vector normal to the path Γ, transverse in the anti-clockwise direction as shown in Fig. 5. By employing the solutions used in Section 1.2 for an infinite plate with a central crack of length 2a, loaded by generalized mode I and mode II loadings, the stress intensity factors are given by equations (1.2.5) and (1.2.27), respectively. Further-more, by employing the definitions in equations (1.3.3) and (1.3.4) the strain energy-release rates are obtained as Irwin (1960), with κ as defined in equation (1.2.12),

$$G_1 = \frac{1+\kappa}{8\mu} K_1^2, \quad \text{----------(1.3.6)}$$

and

$$G_{11} = \frac{1+\kappa}{8\mu} K_{11}^2, \quad \text{----------(1.3.7)}$$

For the same problems, the J-integral was obtained by Rice (1968) as,

$$J = J_1 = \frac{1-\nu^2}{E} K_1^2, \quad \text{----------(1.3.8)}$$

and

$$J = J_{11} = \frac{1-\nu^2}{E} K_{11}^2, \quad \text{----------(1.3.9)}$$

both for plane strain condition, where ν is the Poisson's ratio and E is the Young's modulus for the material.

Some of the immediate conclusions from equations (1.2.5), (1.2.27) and (1.3.6) to (1.3.9) and which are

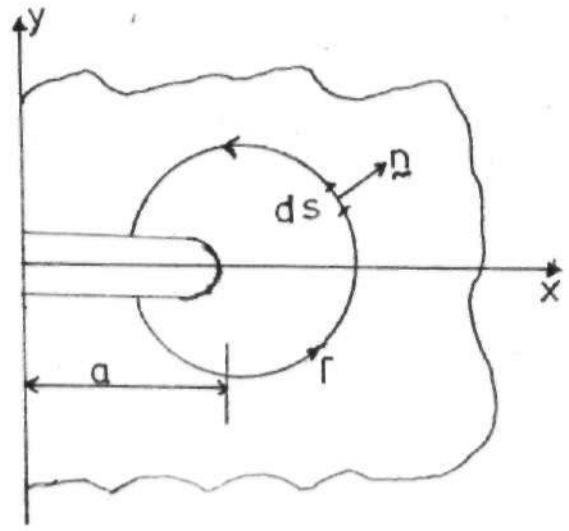


Fig. 5: The Path Γ

used as the backbone in the study of fracture mechnics are:

That the crack-tip characterizing parameters K, G and J are not effected by the far field applied stress σ^{∞}_{xx}. Secondly, that the strain energy-release rate is equal to the J-integral. Thirdly, that crack-tip characterization via the strain energy-release rate or the J-integral is equivalent to an approach via the stress intensity factor.

It has already been shown that the models from which equations (1.2.5), (1.2.27) and (1.3.6) to (1.3.9) are derived, have some limitations, thus, there is a need for more general theories. When some of of the problems are reconsidered, some detailed investigation of the strain energy-release rate and the J-integral as characterizing parameters will be conducted.

Before reconsidering the problems, let us carefully study the derivation of equation (1.3.8). For an infinite plate under biaxial loading and by employing equations (1.3.3) and (1.3.5) and the solutions noted in Section 1.2, stated in equations (1.2.1), one obtains at the crack-tip $x = +a$

$$G = \frac{1-\nu^2}{2E} K_1^2, \quad \text{----------(1.3.10)}$$

and

$$J = \frac{1-\nu^2}{E} K_1^2, \quad \text{----------(1.3.11)}$$

and at the crack-tip $x = -a$,

$$G = \frac{1-\nu^2}{2E} K_1^2, \quad \text{----------(1.3.12)}$$

and

$$J = -\frac{1-\nu^2}{E} K_1^2, \quad \text{----------(1.3.13)}$$

where E is the Young's modulus and ν is the Poisson's ratio of the material. K_1 is given by equation (1.2.5).

We cannot draw any dependable conclusion between the relationship of J and G from just one problem. For that purpose, many more problems are considered in the next chapter and in the appendix and then comparison between the J and G obtained are made.

1.4. Aims and Scope of this Research

As was noticed in Section 1.2, above, some important solutions of some elementary fracture mechanics problems from which vital information regarding some concepts in fracture mechanics can be drawn, are shown to have some limitations. Naturally, the aim of the research is to eliminate these limitations by obtaining new models of most of the elementary problems and introducing new concepts of fracture if possible. In particular, intensive studies on the crack extension force, G, henceforth defined as the strain energy-release rate and the J-integral would be conducted.

The complex potentials technique is employed for the solution of most of the problems. Plane, quasi-static, straight cracks in homogeneous isotropic in linearly elastic body are considered. Furthermore, although there are a number of specimens employed for the determination of the characterizing parameters, the centre cracked specimen is analytically and experimentally dealt with in this thesis. The calculations of the above mentioned parameters can be extended to the other geometries by modifying the presented procedures.

For the centre cracked specimens, loadings of the form

$$\sigma^{\infty}_{yy} = \sigma_o$$

$$\sigma^{\infty}_{xx} = \alpha\sigma_o$$

and

$$\tau^{\infty}_{xy} = o$$

and

$$\sigma_{yy}(x,0) = -\sigma_o, |x| \leq a$$

$$v(x,0) = 0, \quad |x| \geq a$$

are reconsidered both in the main body of thesis and in the appendix. From the solutions developed, crack-tip characterizing parameters are then investivated.

Furthermore, the solutions obtained are compared to those normally reported in the literature of fracture mechanics and noted in Section 1.2.

Finally, experiments are conducted on glass at the materials laboratory of Mechanical Engineering Department, to determine its fracture toughness.

CHAPTER II

SOLUTIONS OF CRACK PROBLEMS BY COMPLEX POTENTIALS (1)

2.1. Introduction

The complex potentials technique is one of the most general methods for obtaining the solution of a number of two-dimensional problems in elasticity. It involves the systematic use of the theory of complex variables. From the impetus of Kolosov's work (1909), Muskhelishvili (1953) obtained the solution of the biharmonic equation of elasticity in terms of two complex potentials, $\phi = \phi(z)$ and $\chi = \chi(z)$ as

$$\sigma_{xx} + \sigma_{yy} = 2[\phi'(z) + \overline{\phi'(z)}], \text{ ----------(2.1.1)}$$

$$\sigma_{yy} - \sigma_{xx} + 2i\,\tau_{xy} = 2[\bar{z}\,\phi''(z) + \chi'(z)], \text{---(2.1.2)}$$

and

$$2\mu(u + iv) = \kappa\,\phi(z) - z\,\overline{\phi'}(z) - \overline{\chi}(z), \text{---(2.1.3)}$$

where $z = x + i\,y$, $\bar{z} = x - i\,y$, $(\phi)'$ denotes differentiation with respect to z, $(\bar{\phi})$ denotes complex conjugate of (ϕ), and μ is the shear modulus of the material and as defined by equation (1.2.9) $\kappa = 3 - 4\nu$ for plane strain and $(3 - \nu)/(1 + \nu)$ for plane stress with ν as the Poisson's ratio of the material. Equations (2.1.1) to (2.1.3) are called the Kolosov-Muskhelishvili equations.

Equations (2.1.1) to (2.1.3) can be written in full as

$$\sigma_{xx} = 2\,\mathrm{Re}\,\phi' - x\,\mathrm{Re}\,\phi'' - y\,\mathrm{Im}\,\phi'' - \mathrm{Re}\,\chi', \text{---(2.1.4)}$$

$$\sigma_{yy} = 2\,\mathrm{Re}\,\phi' + x\,\mathrm{Re}\,\phi'' + y\,\mathrm{Im}\,\phi'' + \mathrm{Re}\,\chi', \text{---(2.1.5)}$$

$$\tau_{xy} = x\,\mathrm{Im}\,\phi'' - y\,\mathrm{Re}\,\phi'' + \mathrm{Im}\,\chi', \text{-------(2.1.6)}$$

$$2\mu u = \kappa \operatorname{Re}\phi - x \operatorname{Re}\phi' - y \operatorname{Im}\phi' - \operatorname{Re}\chi, \quad (2.1.7)$$

and

$$2\mu v = \kappa \operatorname{Im}\phi + x \operatorname{Im}\phi' - y \operatorname{Re}\phi' + \operatorname{Im}\chi, \quad (2.1.8)$$

where $\operatorname{Re}(\phi)$ and $\operatorname{Im}(\phi)$ represent the real and the imaginary parts of a complex function, respectively.

For some unique solutions and for the cases where stresses are applied, let the arbitrary nature of the complex functions ϕ and χ be investigated. Suppose that ϕ_1, χ_1 and ϕ_2, χ_2 are two sets of solutions. Since σ_{xx}, σ_{yy}, and τ_{xy} must be single valued, from equations (2.1.4) to (2.1.6) one obtains the relationship between the two sets of the complex functions as

$$\phi_2 = \phi_1 + a_1, \quad (2.1.9)$$

and

$$\chi_2 = \chi_1 + a_2, \quad (2.1.10)$$

where a_1 and a_2 are some constants.

Other useful equations that can be obtained from equations (2.1.1) and (2.1.2) are the resultant forces and moment exerted on an arc, AB say. These are given by Muskhelishvili (1953) as

$$F_x + i F_y = - i[\phi(z) + z \overline{\phi'}(z) + \bar{\chi}(z)]_A^B, \quad (2.1.11)$$

and

$$M = \operatorname{Re}[\int \chi(z)dz - z\chi(z) - z\bar{z}\phi'(z)]_A^B, \quad (2.1.12)$$

where F_x and F_y are respectively resultant forces in the x and y directions, M is the resultant moment and $[f]_A^B$ denotes the increase in f as z traverses the arc from A to B.

For some problems, depending on convenience, equations (2.1.1) to (2.1.12) can be written in coordinates other than the xy coordinates, by transformation. These can be found in Muskhelishvili (1953), Sneddon and Lowengrub (1969) and Sokolnikoff (1956).

For the present purpose, these equations are used without any further transformation.

2.2. The Westergaard Formulae

Westergaard (1939) obtained some specialized versions of equations (2.1.4) to (2.1.8) for certain crack problems, two of which are of interest here. The first problem is that of a large plate with a central crack of length 2a, loaded by far field stresses $\sigma^{\infty}_{yy} = \sigma_o$, $\sigma^{\infty}_{xx} = \sigma_o$ and $\tau^{\infty}_{xy} = 0$. This is shown in Fig.2(ii) with $\alpha = 1$. Assuming for this problem that

$$\phi'(z) = \tfrac{1}{2} Z_1, \quad \text{----------(2.2.1)}$$

and

$$\chi'(z) = -\tfrac{1}{2} z Z_1', \quad \text{----------(2.2.2)}$$

and substituting the above equations into the Kolosov-Muskhelishvili equations gives

$$\sigma_{xx} = \text{Re } Z_1 - y \text{ Im } Z_1', \quad \text{----------(2.2.3)}$$

$$\sigma_{yy} = \text{Re } Z_1 + y \text{ Im } Z_1', \quad \text{----------(2.2.4)}$$

and

$$\tau_{xy} = -y \text{ Re } Z_1', \quad \text{----------(2.2.5)}$$

Westergaard furthermore assumed

$$Z_1 = \sigma_o \frac{z}{\sqrt{z^2 - a^2}}, \quad \text{----------(2.2.6)}$$

Note that by substituting equation (2.2.6) into equations (2.2.3) to (2.2.5) one arrives at equations (1.2.1), wi out 2A.

The second problem solved by Westergard (1939) is for a large plate with a central crack of length 2a, loaded by $\tau^{\infty}_{xy} = \tau_o$, shown in Fig. 2(iv). Substituting,

$$\phi'(z) = -\tfrac{1}{2} i Z_{11}, \quad \text{----------(2.2.7)}$$

and

$$\chi'(z) = i Z_{11} + \tfrac{1}{2} i z Z_{11}', \quad \text{----------(2.2.8)}$$

into the Kolosov-Muskhelishvili equations, gives

$$\sigma_{xx} = z \text{ Im } Z_{11} + y \text{ Re } Z'_{11}, \text{----------(2.2.9)}$$

$$\sigma_{yy} = - y \text{ Re } Z'_{11} , \text{----------(2.2.10)}$$

and

$$\tau_{xy} = \text{Re } Z_{11} - y \text{ Im } Z'_{11}, \text{----------(2.2.11)}$$

Westergaard assumed that

$$Z_{11} = \tau_o \frac{z}{\sqrt{z^2-a^2}}, \text{----------(2.2.12)}$$

Equations (2.2.3) to (2.2.5) and equations (2.2.9) to (2.2.11) are called the Westergaard formulae while equations (2.2.6) and (2.2.12) are known as the Westergaard stress functions. $Z_1 = Z_1(z)$ relates to the opening or mode I problems and $Z_{11} = Z_{11}(z)$ relates to the inplane shear or mode II problems. Equations (2.2.3) to (2.2.5) and (2.2.9) to (2.2.11) are extensively employed for other related problems such as stress distribution for other plane geometries and derivation of the modified Westergaard formulae as in Irwin (1957), Sneddon and Lowengrub (1969), Eftis and Liebowitz (1972), Sanford (1979) and Erdogan (1983).

The next section deals with the derivation from the first principle of some new formulae for stresses and displacements, which are in fact the generalized Westergaard formulae.

2.3. Derivation of the New Formulae

It was proved by Kolosov and Muskhelishvili that the solutions of a certain class of plane elasticity problems can be obtained in terms of two complex potentials; $\phi = \phi(z)$ and $\chi = \chi(z)$. In what follows for crack problems in two-dimensions, the Kolosov-Muskhelishvili equations which are in terms of the two

complex functions are made to depend on only one complex potential. These equations are in fact the generalized Westergaard formulae. The derivation of the equations from the first principle now follows.

The solution of the bi-harmonic equation in a Region R can be written as

$$U = Re[\bar{Z}\phi + \psi], \quad \text{----------(2.3.1)}$$

where U is the Airy stress function and $\phi = \phi(z)$, $\psi = \psi(z)$ are complex analytic functions in R. Equation (2.3.1) can be written as

$$2U = \bar{Z}\phi + z\bar{\phi} + \psi + \bar{\psi}, \quad \text{----------(2.3.2)}$$

From the well known equations

$$\sigma_{xx} = \frac{\partial^2 U}{\partial y^2}, \quad \text{----------(2.3.3)}$$

$$\sigma_{yy} = \frac{\partial^2 U}{\partial x^2}, \quad \text{----------(2.3.4)}$$

$$\tau_{xy} = -\frac{\partial^2 U}{\partial x \partial y}, \quad \text{----------(2.3.5)}$$

and the stress-displacement relations, the Kolosov-Muskhelishvili formulae are obtained, with $\chi(z)$ substituted for $\psi'(z)$.

In the Kolosov-Muskhelishvili equations, let

$$\chi(z) = N\,\phi(z) - z\phi'(z), \quad \text{----------(2.3.6)}$$

where N is some real constant. Then, one obtains equations (2.1.4) to (2.1.8) as

$$\sigma_{xx} = (3-N)\,Re\,\phi'(z) - 2y\,I_m\,\phi''(z), \quad \text{-------(2.3.7)}$$

$$\sigma_{yy} = (1+N)\,Re\,\phi'(z) + 2y\,I_m\,\phi''(z), \quad \text{-------(2.3.8)}$$

$$\tau_{xy} = (N-1)\,I_m\,\phi'(z) - 2y\,Re\,\phi''(z), \quad \text{-------(2.3.9)}$$

$$2\mu u = (\kappa-N)\,Re\,\phi(z) - 2y\,Im\,\phi'(z), \quad \text{-------(2.3.10)}$$

and

$$2\mu v = (\kappa+N)\,Im\,\phi(z) - 2y\,Re\,\phi'(z), \quad \text{-------(2.3.11)}$$

Equations (2.3.7) to (2.3.11) are the new formulae and are in terms of only one complex potential, $\phi = \phi(z)$ and a constant N which can be obtained from

the far field boundary conditions of the plane problems.

As an example, by substituting N = 1 and

$$\phi'(z) = \tfrac{1}{2} Z_1, \quad \text{----------(2.3.12)}$$

in the new formulae, the Westergaard formulae, equations (2.2.3) to (2.2.5) are obtained. Similarly, by substituting, N = -1 and

$$\phi'(z) = -\frac{i}{2} Z_{11}, \quad \text{----------(2.3.13)}$$

into the new formulae, the Westergaard formulae, for the inplane shear problem, equations (2.2.9) to (2.2.11), are obtained. The new formulae are therefore shown to be the generalized Westergaard (1939) equations.

As will be shown in the next chapter by assigning an appropriate value of N and the stress function $\phi(z)$, the new formulae can give the solutions of a number of plane problems with the crack(s) along the x-axis and loaded by either far field stresses σ^{∞}_{xx}, σ^{∞}_{yy} and τ^{∞}_{xy} and or some pressure loading along the crack faces. In the next section, it will be shown that the new formulae satisfy some necessary equations of elasticity.

It should be noted that the basis of the so called new formulae was the substitution in equation (2.3.6). Many researchers would like to know how such substitution came about. There are certain standard methods for the formulation of boundary value problems described in detail in Muskhelishvili (1953) and Sokolnikoff (1956) in which the functions $\phi(z)$ and $\chi(z)$ could be determined. When these functions are determined through the above mentioned procedure, by hectic trial and error the

relationship between $\phi(z)$ and $\chi(z)$ could be obtained. In the trials I employed, the Saint-Venant semi-inverse method in which certain relationships on the basis of known cases are selected. A number of these trial functions were selected and only that in equation (2.3.6) satisfies all the conditions required by the expected solution. Some of the other simple relationships investigated include:

$$\chi(z) = \phi(z) - Z\,\phi'(z) + A,$$

$$\chi(z) = \phi(z) - BZ\,\phi'(z),$$

and

$$\chi(z) = C[\phi(z) - Z\,\phi'(z)],$$

where A, B, C are some constants.

2.4. Proof of the Correctness of the New Formulae

For a solution of an elasticity problem to be correct, it must satisfy the following four conditions:

(a) the equilibrium conditions,

(b) the stress-strain relations,

(c) the compatibility conditions, and

(d) the boundary conditions of the problem.

In this section, equations (2.3.7) to (2.3.11) are proved to satisfy conditions (a) to (c) for any real constant N, where $-\infty < N < +\infty$. The unknown constant N, as mentioned earlier, can only be determined from the

boundary conditions of the problem. Since the boundary conditions differ from problem to problem, the evaluation of the constant N and the proof that condition (d) is satisfied are left until specific problems are considered.

In the proof that follows, the following equations of complex variable theory are employed,

$$\phi(z) = \text{Re } \phi(z) + i \text{ Im } \phi(z), \text{ ----------(2.4.1)}$$

$$\frac{\partial \text{ Re } \phi(z)}{\partial x} = \frac{\partial \text{ Im } \phi(z)}{\partial y} = \text{Re } \phi'(z), \text{ -----(2.4.2)}$$

and

$$\frac{\partial \text{ Im } \phi(z)}{\partial x} = - \frac{\partial \text{ Re } \phi(z)}{\partial y} = \text{Im } \phi'(z), \text{---(2.4.3)}$$

where $z = x + i y$.

The equilibrium equations in two dimensions are,

$$\frac{\partial \sigma_{xx}}{\partial x} + \frac{\partial \tau_{xy}}{\partial y} = 0, \text{ ----------(2.4.4)}$$

and

$$\frac{\partial \sigma_{yy}}{\partial y} + \frac{\partial \tau_{xy}}{\partial x} = 0, \text{ ----------(2.4.5)}$$

From equations (2.3.7) to (2.3.9), one obtains

$$\frac{\partial \sigma_{xx}}{\partial x} = (3-N)\text{Re } \phi'' - 2y \text{ Im } \phi''', \text{ ----------(2.4.6)}$$

$$\frac{\partial \tau_{xy}}{\partial y} = (N-1)\text{Re } \phi'' - 2 \text{ Re } \phi'' + 2y \text{ Im } \phi''', \text{----(2.4.7)}$$

$$\frac{\partial \tau_{xy}}{\partial x} = (N-1)\text{Jm } \phi'' - 2y \text{ Re } \phi''', \text{ ----------(2.4.8)}$$

and

$$\frac{\partial \sigma_{yy}}{\partial y} = (1-N)\text{Im } \phi'' + 2y \text{ Re } \phi''', \text{ ----------(2.4.9)}$$

By adding equations (2.4.6) and (2.4.7) and equations (2.4.8) and (2.4.9), one concludes that equations (2.4.4) and (2.4.5) are identically satisfied for any constant N.

The plane stress, stress-strain relations are given by

$$2\mu(1+\nu)e_{xx} = \sigma_{xx} - \nu\sigma_{yy}, \quad \text{----------(2.4.10)}$$

$$2\mu(1+\nu)e_{yy} = \sigma_{yy} - \nu\sigma_{xx}, \quad \text{----------(2.4.11)}$$

$$2\mu(1+\nu)e_{zz} = -\nu(\sigma_{xx} + \sigma_{yy}), \quad \text{----------(2.4.12)}$$

and

$$\mu\gamma_{xy} = \tau_{xy}, \quad \text{----------(2.4.13)}$$

With the new formulae, equations (2.3.7) to (2.3.9), one obtains the strains as

$$2\mu(1+\nu)e_{xx} = (3-N-\nu-\nu N)\,\mathrm{Re}\,\phi' - 2(1+\nu)y\,\mathrm{Im}\phi'', \quad \text{--(2.4.14)}$$

$$2\mu(1+\nu)e_{yy} = (1+N-3\nu+\nu N)\,\mathrm{Re}\,\phi' + 2(1+\nu)y\,\mathrm{Im}\phi'', \quad \text{--(2.4.15)}$$

$$2\mu(1+\nu)e_{zz} = -4\,\mathrm{Re}\,\phi', \quad \text{----------(2.4.16)}$$

$$\mu\gamma_{xy} = (N-1)\,\mathrm{Im}\,\phi' - 2y\,\mathrm{Re}\,\phi'', \quad \text{----------(2.4.17)}$$

where, as defined earlier, μ is the shear modulus and ν the Poisson's ratio of the material.

With the definitions of the strains in terms of the displacements u, v and w, as

$$e_{xx} = \frac{\partial u}{\partial x}, \quad \text{----------(2.4.18)}$$

$$e_{yy} = \frac{\partial v}{\partial y}, \quad \text{----------(2.4.19}$$

$$e_{zz} = \frac{\partial w}{\partial z}, \quad \text{----------(2.4.20)}$$

and

$$\gamma_{xy} = \frac{\partial u}{\partial y} + \frac{\partial v}{\partial x}, \quad \text{----------(2.4.21)}$$

and equations (2.4.14) to (2.4.17), one arrives at the new formulae in equations (2.3.10) and (2.3.11). The condition (b) i.e. the stress-strain relations are therefore satisfied by the new formulae.

The next proof is for condition (c). The well established two-dimensional compatibility equation is

by

$$\frac{\partial^2 e_{xx}}{\partial y^2} + \frac{\partial^2 e_{yy}}{\partial x^2} - \frac{\partial^2 \gamma_{xy}}{\partial x \partial y} = 0, \quad \text{----------(2.4.22)}$$

Employing equations (2.4.2), (2.4.3) and equations (2.4.14) to (2.4.17), one obtains

$$\frac{\partial^2 e_{xx}}{\partial y^2} = -\frac{(3-N-\nu-\nu N)}{2\mu(1+\nu)} \text{Re } \phi''' - \frac{2}{\mu} \text{Re } \phi''' + \frac{y}{\mu} \text{Im}\phi^{iv},$$

--------(2.4.23)

$$\frac{\partial^2 e_{yy}}{\partial x^2} = \frac{(1+N-3\nu+\nu N)}{2\mu(1+\nu)} \text{Re } \phi''' + \frac{y}{\mu} \text{Im}\phi^{iv}, \text{-----(2.4.24)}$$

and

$$\frac{\partial^2 \gamma_{xy}}{\partial x \partial y} = \frac{(N-1)}{\mu} \text{Re } \phi''' - \frac{2}{\mu} \text{Re } \phi''' + \frac{2}{\mu} y \text{ Im}\phi^{iv}, \text{ ---(2.4.25)}$$

By substituting equations (2.4.23) to (2.4.25) into equations (2.4.22), one can conclude that the plane stress compatibility condition is also satisfied for all values of the constant, N.

2.5. Conclusions

In the chapter, the well established Kolosov-Muskhelishvili formulae were employed and new set of equations for stresses and displacements are derived. The new formulae are in terms of only one complex potential. These new formulae were also shown to be the generalized Westergaard equations.

It was also proved that the new formulae satisfy the conditions of equilibrium and compatibility and that the stress-strain relations are also satisfied. In the proof, the case of plane stress was considered but with the simple and well established procedure of solid mechanics, by transforming the elastic constants as

$$E \to \frac{E}{1-\nu^2}$$

and

$$\nu \to \frac{\nu}{1-\nu},$$

the case of plane strain can be obtained. By making the above changes into equations (2.4.10) to (2.4.25) one can conclude that all the proofs also hold for the plane strain problems.

The most important advantage of the new formulae, is that for the crack problems, one is left with the determination of only one complex analytic functions, unlike two functions when one employs the Kolosov-Muskhelishvili equations.

CHAPTER III

SOLUTIONS OF CRACK PROBLEMS

BY COMPLEX POTENTIALS (2)

3.1. Introduction

In this chapter, the new formulae, equations (2.3.7) to (2.3.11) are applied to some opening mode problems. The problems considered include that of a large plate with a straight central crack of length 2a, along the x-axis, as shown in Fig. 2, with the following loading conditions.

(i) $\sigma^{\infty}_{yy} = \sigma_o$, $\sigma^{\infty}_{xx} = \alpha\sigma_o$ and $\tau^{\infty}_{xy} = 0$

where $-\infty < \alpha < \infty$ and,

(ii) $\sigma_{yy}(x,o) = -\sigma_o, |x| < a$

$v(x,o) = 0, \quad |x| \geq a$

and $\sigma^{\infty}_{xx} = \sigma^{\infty}_{yy} = 0$, $\tau^{\infty}_{xy} = 0$.

Some other problems solved via the new formulae are discussed in the appendix. The solutions derived through the new formulae are then compared with the solutions normally reported in the literature of the subject.

Also, some studies are made on the distribution of the maximum and minimum principal stresses and the energy of distortion in tne neighbourhood of the crack-tip. The former are useful in photo-elastic studies.

3.2. The New Formulae Applied to Some Mode I Problems

Consider the problem shown in Fig. 2 in which

$$\left.\begin{aligned} \sigma^{\infty}_{yy} &= \sigma_o \\ \sigma^{\infty}_{xx} &= \alpha\sigma_o, \text{ and} \\ \tau^{\infty}_{xy} &= 0 \end{aligned}\right\}, \qquad \text{----------(3.2.1)}$$

The new formulae, equations (2.3.7) to (2.3.11), can be written as

$$\sigma_{yy} = \text{Re } \phi_1'(z) + \frac{2}{1+N} y \text{ Im } \phi_1''(z), \quad \text{-----(3.2.2)}$$

$$\sigma_{xx} = \frac{3-N}{1+N} \text{Re } \phi_1'(z) - \frac{2}{1+N} y \text{ Im } \phi_1''(z), \quad \text{---(3.2.3)}$$

$$\tau_{xy} = \frac{N-1}{1+N} \text{Im } \phi_1'(z) - \frac{2}{1+N} y \text{ Re } \phi_1''(z), \quad \text{--(3.2.4)}$$

$$2\mu u = \frac{(\kappa-N)}{1+N} \text{Re } \phi_1(z) - \frac{2}{1+N} y \text{ Im } \phi_1'(z), \quad \text{-(3.2.5)}$$

and

$$2\mu v = \frac{\kappa+N}{1+N} \text{Im } \phi_1(z) - \frac{2}{1+N} y \text{ Re } \phi_1'(z), \quad \text{-(3.2.6)}$$

In the above equations, one needs the function $\phi_1(z)$, in order to evaluate the stresses and displacements. For the problem under consideration, assume (a complex function similar to that of Westergaard),

$$\phi_1'(z) = A_o \frac{z}{\sqrt{z^2-a^2}}, \quad \text{----------(3.2.7)}$$

where A_o is some constant. Integrating and differentiating equation (3.2.7), gives respectively,

$$\phi_1(z) = A_o \sqrt{z^2-a^2}, \quad \text{----------(3.2.8)}$$

and

$$\phi_1''(z) = -A_o a^2 \frac{1}{(z^2-a^2)^{3/2}}, \quad \text{---------(3.2.9)}$$

Now, as $z \to \infty$, equations (3.2.7) and (3.2. 9) respectively give

and
$$\left.\begin{aligned} \phi_1'(z \to \infty) &\to A_o \\ \phi_1''(z \to \infty) &\to 0 \end{aligned}\right\}, \quad \text{----------(3.2.10)}$$

From equations (3.2.2) to (3.2.4), one obtains

$$\left.\begin{aligned} \sigma^{\infty}_{yy} &= \text{Re } \phi_1'(z \to \infty) \\ \sigma^{\infty}_{xx} &= \frac{3-N}{1+N} \text{Re } \phi_1'(z \to \infty) \\ \tau^{\infty}_{xy} &= \frac{N-1}{1+N} \text{Im } \phi_1'(z \to \infty) \end{aligned}\right\}, \quad \text{----------(3.2.11)}$$

and

Comparing equations (3.2.11), (3.2.10) and (3.2.1),

give

$$A_o = \sigma_o, \quad \text{----------(3.2.12)}$$

and

$$\alpha = \frac{3-N}{1+N}, \quad \text{----------(3.2.13)}$$

The equations for the stresses and displacements in terms of the biaxiality coefficient, α are then given by

$$\sigma_{yy} = \text{Re } \phi_1'(z) + \frac{(1+\alpha)}{2} y \text{ Im } \phi_1''(z), \quad \text{------(3.2.14)}$$

$$\sigma_{xx} = \alpha \text{ Re } \phi_1'(z) - \frac{(1+\alpha)}{2} y \text{ Im } \phi_1''(z), \quad \text{---(3.2.15)}$$

$$\tau_{xy} = \frac{(1-\alpha)}{2} \text{ Im } \phi_1'(z) - \frac{(1+\alpha)}{2} y \text{ Re } \phi_1''(z), \quad \text{--(3.2.16)}$$

$$2\mu u = \frac{(\kappa+\alpha\kappa-3+\alpha)}{4} \text{ Re } \phi_1(z) - \frac{(1+\alpha)}{2} y \text{ Im } \phi_1'(z), \quad \text{--(3.2.17)}$$

and

$$2\mu v = \frac{(\kappa+\alpha\kappa+3-\alpha)}{4} \text{Im } \phi_1(z) - \frac{(1+\alpha)}{2} y \text{ Re } \phi_1'(z), \quad \text{--(3.2.18)}$$

where $\phi_1'(z)$, $\phi_1(z)$ and $\phi_1''(z)$ are respectively given by equations (3.2.7) to (3.2.9) with $A_o = \sigma_o$.

From the above equations, the asymptotic stress and displacement at the crack can be obtained. These are obtained as

$$\sigma_{yy} = \frac{K_1}{\sqrt{2\pi r}}\left[\text{Cos } \tfrac{1}{2}\theta + \frac{(1+\alpha)}{4} \text{ Sin } \theta \text{ Sin } \tfrac{3}{2}\theta\right], \quad \text{--(3.2.19)}$$

$$\sigma_{xx} = \frac{K_1}{\sqrt{2\pi r}}\left[\alpha \text{ Cos } \tfrac{1}{2}\theta - \frac{(1+\alpha)}{4} \text{Sin } \theta \text{ Sin } \tfrac{3}{2}\theta\right], \quad \text{---(3.2.20)}$$

$$\tau_{xy} = \frac{K_1}{\sqrt{2\pi r}}\left[\frac{(\alpha-1)}{2} \text{Sin } \tfrac{1}{2}\theta + \frac{(1+\alpha)}{4} \text{Sin } \theta \text{ Cos } \tfrac{3}{2}\theta\right], \quad \text{------(3.2.21)}$$

$$2\mu u = K_1 \sqrt{\frac{r}{2\pi}}\left[\frac{(\kappa+\alpha\kappa-3+\alpha)}{2} \text{Cos } \tfrac{1}{2}\theta + \frac{(1+\alpha)}{2} \text{Sin } \theta \text{Sin } \tfrac{1}{2}\theta\right], \quad \text{-------(3.2.22)}$$

and

$$2\mu v = K_1 \sqrt{\frac{r}{2\pi}} \left[\frac{(\kappa+\alpha\kappa+3-\alpha)}{2} \text{Sin } \tfrac{1}{2}\theta - \frac{(1+\alpha)}{2} \text{Sin } \theta \text{Cos } \tfrac{1}{2}\theta\right], \quad \text{--------(3.2.23)}$$

where $K_1 = \sigma_o \sqrt{\pi a}$, σ_o is the far field applied stress, a is half the crack length, α is the biaxiality coefficient, μ is the shear modulus, $\kappa = 3-4\nu$ for plane strain and $(3-\nu)/(1+\nu)$ for plane stress, ν is the Poisson's ratio and r,θ are polar coordinates at the tip of the crack.

From equations (3.2.19) to (3.2.21), the principal stresses, σ_1 and σ_2 are given as

$$\sigma_1 = \frac{K_1}{\sqrt{2\pi r}}\left[(1+\alpha)\text{Cos } \tfrac{1}{2}\ \theta + \sqrt{(1-\alpha)^2+(1-\alpha^2)\text{Sin}^2\theta + \frac{(1+\alpha)^2}{4}\text{Sin}^2\theta}\right], \text{----(3.2.24)}$$

and

$$\sigma_2 = \frac{K_1}{\sqrt{2\pi r}}\left[(1+\alpha)\text{Cos } \tfrac{1}{2}\ \theta - \sqrt{(1-\alpha)^2+(1-\alpha^2)\text{Sin}^2 + \frac{(1+\alpha)^2}{4}\text{Sin}^2\theta}\right], \text{----(3.2.25)}$$

Fig. 6 shows the plots of the dimensionless principal stresses for some values of α. From the figure, for $\alpha = 1, \sigma_1$ takes a maximum value of $1.3\ K_1/\sqrt{2\pi r}$ at $\theta = 60°$ while for $\alpha = 0$, it takes a maximum of $1.135\ K_1/\sqrt{2\pi r}$ at $\theta = 70°$.

The difference of the maximum and minimum principal stresses, $\sigma_1 - \sigma_2$, is also given as

$$\sigma_1 - \sigma_2 = \frac{K_1}{\sqrt{2\pi r}}\sqrt{4(1-\alpha)^2+(5+2\alpha-3\alpha^2)\text{Sin}^2\theta}, \text{---(3.2.26)}$$

From equations (1.2.1), if the principal stress difference is denoted by $(\sigma_1 - \sigma_2)^*$, one obtains

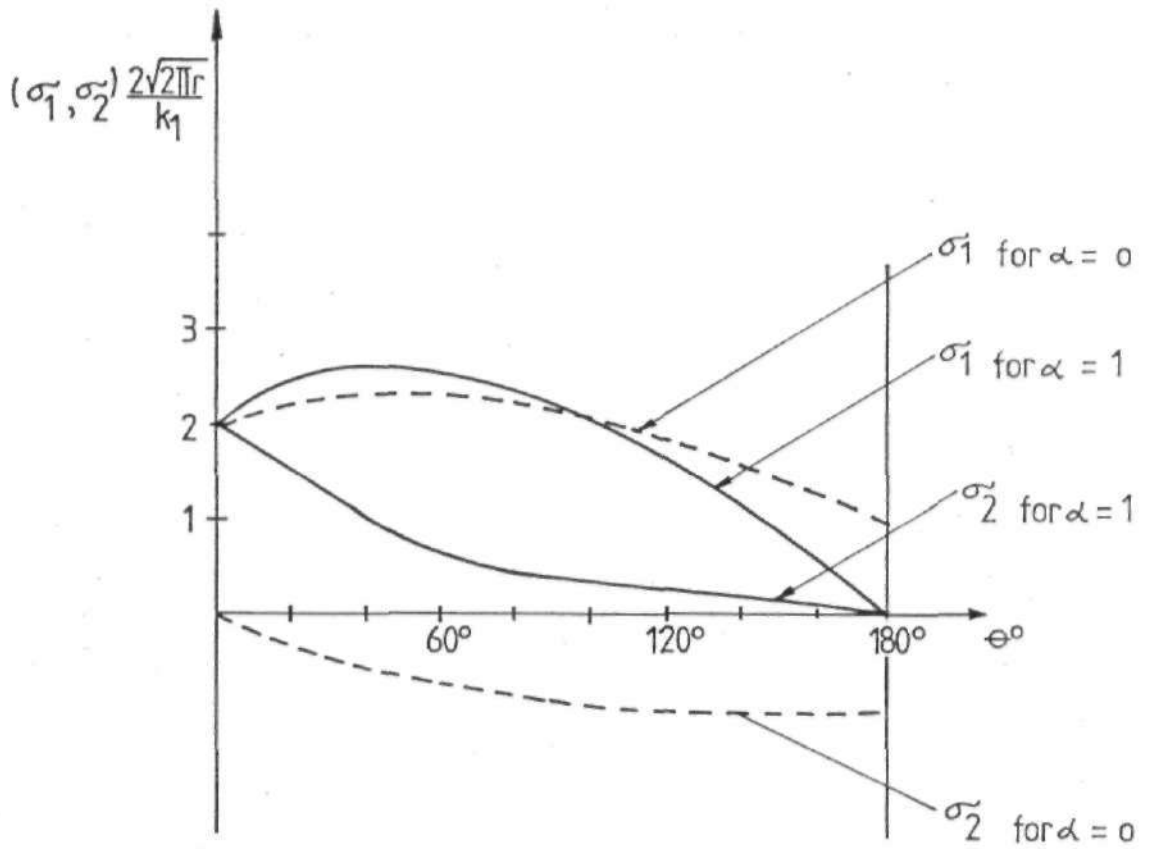


FIG .6: . The plots of $(2\,\sigma_1\sqrt{2\pi r})/k_1$ and $(2\,\sigma_2\sqrt{2\pi r})/k_1$ against angular position θ at the crack – tip .

$$(\sigma_1-\sigma_2)^* = \frac{K_1}{\sqrt{2\pi r}} \sqrt{\text{Sin}^2\theta - 2(1-\alpha)\sigma_o \frac{\sqrt{2\pi r}}{K_1}\text{Sin}\theta\text{Sin}\frac{3\theta}{2} + (1-\alpha)^2\sigma_o^2\frac{(2\pi r)}{K_1^2}},$$

-------(3.2.27)

Note that equation (3.2.26)was obtained via the new formulae while equation (3.2.27) was obtained from the solutions reported in the literature of fracture as discussed in the literature review. These equations, (3.2.26) and (3.2.27) are quite different especially the effect of the biaxial loading, represented by α. As an example, with $\sigma_o = K_1/\sqrt{\pi a}$, and for small distances from the crack-tip, i.e. $\frac{r}{a} \cong 0$, equation (3.2.27) states that the principal stress difference is independent of the biaxial loading, while equation (3.2.26) clearly shows that it is a function of the biaxial loading. Note that even if higher terms of the radius, r, are considered in the Westergaard stress function, equation (3.2.7), the principal stress difference obtained from the new formulae and equation (3.2.27) are never the same.

The strain energy of distortion, W_d, is given by

$$W_d = \frac{1}{6\mu}[\sigma_1^2 - \sigma_1\sigma_2 + \sigma_2^2], \quad \text{----------(3.2.28)}$$

Substituting equations (3.2.24) and (3.2.25) into equation (3.2.28), one arrives at

$$W_d = \frac{K_1^2}{48\pi\mu r}[\frac{(1+\alpha)^2}{2}3(1-\alpha)^2 + \frac{(1+\alpha)^2}{2}\text{Cos}\ \theta$$

$$+3(1-\alpha^2)\text{Sin}^2\theta + 3\frac{(1+\alpha)^2}{4}\text{Sin}^2\theta]. \quad \text{---------(3.2.29)}$$

From equation (3.2.29), it can be proved that the strain energy of distortion, W_d is maximum at a θ, given by

$$\theta = \text{Cos}^{-1}\frac{1+\alpha}{15-9\alpha}, \quad \text{----------(3.2.30)}$$

An important class of the above problem and which we will later be interested in, is for a uniaxially loaded cracked plate. For that case $\alpha = 0$. Then from equations (3.2.19) to (3.2.23), the asymptotic stress and displacement distributions are,

$$\sigma_{yy} = \frac{K_1}{\sqrt{2\pi r}} \left[\text{Cos } \tfrac{1}{2}\theta + \frac{\text{Sin } \theta \text{ Sin } \frac{3}{2}\theta}{4}\right], \text{---(3.2.31)}$$

$$\sigma_{xx} = -\frac{K_1}{\sqrt{2\pi r}} \frac{\text{Sin } \theta \text{ Sin } \frac{3}{2}\theta}{4}, \text{-------(3.2.32)}$$

$$\tau_{xy} = -\frac{K_1}{\sqrt{2\pi r}}\left[\frac{\text{Sin } \theta/2}{2} - \frac{\text{Sin}\theta \text{ Cos } \frac{3}{2}\theta}{4}\right], \text{---(3.2.33)}$$

$$2\mu u = K_1\sqrt{\frac{r}{2\pi}}\left[\frac{(\kappa-3)}{2}\text{Cos } \tfrac{1}{2}\theta + \tfrac{1}{2}\text{ Sin } \theta \text{ Sin } \tfrac{1}{2}\theta\right], \text{-(3.2.34)}$$

and

$$2\mu v = K_1\sqrt{\frac{r}{2\pi}}\left[\frac{(\kappa-3)}{2}\text{Sin } \tfrac{1}{2}\theta - \tfrac{1}{2}\text{ Sin } \theta \text{ Cos } \tfrac{1}{2}\theta\right]. \text{--(3.2.35)}$$

Either from equations (3.2.24) and (3.2.25) with $\alpha = 0$ or from equations (3.2.21) to (3.2.33), the sum and difference of the maximum and minimum principal stresses are then given by

$$\sigma_1+\sigma_2 = \frac{K_1}{\sqrt{2\pi r}}\left[\text{Cos } \tfrac{1}{2}\theta + \tfrac{1}{2}\text{Sin } \theta \text{ Sin } \tfrac{3}{2}\theta\right], \text{---(3.2.36)}$$

and

$$(\sigma_1-\sigma_2) = \frac{K_1}{\sqrt{2\pi r}}\left[1 + \tfrac{5}{4}\text{ Sin}^2\ \theta\right]^{\frac{1}{2}}. \text{-----(3.2.37)}$$

From equation (3.2.27) on the other hand, for the uniaxially loaded plate, one obtains

$$(\sigma_1-\sigma_2)^* = \frac{K_1}{\sqrt{2\pi r}}\left[\text{Sin}^2\theta - 2\sqrt{\frac{2r}{a}}\text{Sin}\theta\text{Sin } \tfrac{3}{2}\theta + \frac{2r}{a}\right]^{\frac{1}{2}}. \text{---(3.2.38)}$$

As was mentioned earlier, equations (3.2.37) and (3.2.38) are not the same. It should be noted that,

accurate and detailed comparison between the two equations is possible only when higher r/a terms are considered in equation (3.2.27) and photoelastic data are available. For the mean time, let us consider the stress distribution along $\theta = 0$. With the stress-optic law

$$\sigma_1 - \sigma_2 = \frac{N_o \, f\sigma}{h} \quad , \text{----------(3.2.39)}$$

where N_o is the fringe order, $f\sigma$ materials fringe value and h is the thickness of material, equations (3.2.37) and (3.2.38), along, $\theta = 0$ give , respectively,

$$\frac{N_o \, f\sigma}{h} = \frac{K_1}{\sqrt{2\pi r}} \quad , \text{----------(3.2.40)}$$

and

$$\frac{N_o \, f\sigma}{h} = \frac{K_1}{\sqrt{\pi a}} . \quad \text{----------(3.2.41)}$$

From Figs. 7, 9, 10 of Irwin et al (1978), Fig. 4 of Sanford (1979), Fig. 9 of Dally (1979) and Fig. 11 of Daniel (1983). Since in all these cases, N_o was never constant along $\theta = 0$, equation (3.2.41) is not representing the stress state. On the other hand, the new equations developed, state that the fringe order N_o, is inversely proportional to the square root of the distance from the crack tip. These seem to agree with the experimental results noted above.

A related problem similar to the uniaxially loaded plate is that shown in Fig.2(i), as shown in Section 3.3.

$$\left.\begin{aligned} \sigma^{\infty}_{xx} &= \sigma_o \quad \text{and} \\ \tau^{\infty}_{xy} &= \sigma^{\infty}_{yy} = 0 \end{aligned}\right\}, \quad \text{----------(3.2.42)}$$

For that problem, the new formulae, equations (2.3.7) to (2.3.11) can be reduced to

$$\sigma_{xx} = \text{Re}\ \phi_1' - \tfrac{1}{2}\, y\ \text{Im}\phi_1'', \quad \text{----------(3.2.43)}$$

$$\sigma_{yy} = \tfrac{1}{2}\, y\ \text{Im}\ \phi_1'', \quad \text{----------(3.2.44)}$$

$$\tau_{xy} = -\tfrac{1}{2}\ \text{Im}\ \phi_1' - \tfrac{1}{2}\, y\ \text{Re}\ \phi_1'', \quad \text{----------(3.2.45)}$$

$$2\mu u = \frac{(\kappa+1)}{4}\ \text{Re}\ \phi_1 - \tfrac{1}{2}\, y\ \text{Im}\ \phi_1', \quad \text{---------(3.2.46}$$

and

$$2\mu v = \frac{(\kappa-1)}{4}\ \text{Im}\ \phi_1 - \tfrac{1}{2}\ \text{Re}\ \phi_1'. \quad \text{----------(3.2.47)}$$

With the same stress function, ϕ_1 considered for the earlier problem, the stress and displacement distributions at the crack tip, become

$$\sigma_{xx} = \frac{K_1}{\sqrt{2\pi r}}\left[\text{Cos}\ \tfrac{1}{2}\theta - \frac{\text{Sin}\ \theta\ \text{Sin}\ \frac{3}{2}\theta}{4}\right], \quad \text{-----(3.2.48)}$$

$$\sigma_{yy} = \frac{K_1}{\sqrt{2\ r}}\ \frac{\text{Sin}\ \theta\ \text{Sin}\ \frac{3}{2}\theta}{4}, \quad \text{----------(3.2.49)}$$

$$\tau_{xy} = \frac{K_1}{\sqrt{2\pi r}}\left[\frac{\text{Sin}\ \frac{1}{2}\ \theta}{2} + \frac{\text{Sin}\ \theta\ \text{Cos}\ \frac{3}{2}\theta}{2}\right], \quad \text{-----(3.2.50)}$$

$$2\mu u = K_1\sqrt{\frac{r}{2\pi}}\left[\frac{(\kappa+1)}{2}\text{Cos}\ \tfrac{1}{2}\theta + \tfrac{1}{2}\text{Sin}\ \theta\ \text{Sin}\ \tfrac{1}{2}\theta\right], \text{--(3.2.51)}$$

and

$$2\mu v = K_1\sqrt{\frac{r}{2\pi}}\left[\frac{(\kappa-1)}{2}\text{Sin}\ \tfrac{1}{2}\theta - \tfrac{1}{2}\text{Sin}\ \theta\ \text{Cos}\ \tfrac{1}{2}\theta\right], \text{--(3.2.52)}$$

where, $K_1 = \sigma_o\sqrt{\pi a}$.

From equations (3.2.48) to (3.2.50), the difference between the maximum and minimum principal stresses is

$$\sigma_1 - \sigma_2 = \frac{K_1}{\sqrt{2\pi r}}\left[1 - \tfrac{3}{4}\ \text{Sin}^2\theta\right]^{\frac{1}{2}} \quad \text{-------(3.2.53)}$$

The stress distributions for the uniaxially loaded plate along the y-axis, equation (3.2.37), and that loaded along the x-axis, equation (3.2.53), are not the same,

as expected. These solutions together with some other problems to be considered, will be utilized for the discussion of crack-tip characterizing parameters in the next chapters.

The next problem considered is again as shown in Fig. 2, with loading as

$$\left.\begin{aligned} \sigma_{yy}(x,o) &= -\sigma_o, \quad |x| \le a \\ \sigma^{\infty}_{yy} &= \sigma^{\infty}_{xx} = \tau^{\infty}_{xy} = 0 \end{aligned}\right\}, \quad \text{--------(3.2.54)}$$

From the new formulae, equations (2.3.7) to (2.3.11), since a free crack surface, $|x| \le a$ cannot carry a normal stress σ_{xx}, then along $y = 0$, σ_{xx} has to be zero. Therefore, equation (2.3.7) gives

$$N = 3, \quad \text{----------(3.2.55)}$$

Substituting equation (3.2.55) into the new formulae, and writing

$$\phi'(z) = \tfrac{1}{4}\,\phi_1'(z),$$

the equations for the stresses and displacements for the problem become,

$$\sigma_{yy} = \text{Re}\,\phi_1'(z) + \tfrac{1}{2}\,y\,\text{Im}\,\phi_1''(z), \quad \text{---------(3.2.56)}$$

$$\sigma_{xx} = -\tfrac{1}{2}\,y\,\text{Im}\,\phi_1''(z), \quad \text{----------(3.2.57)}$$

$$\tau_{xy} = \tfrac{1}{2}\,\text{Im}\,\phi_1'(z) - \tfrac{1}{2}\,y\,\text{Re}\,\phi_1''(z), \quad \text{--------(3.2.58)}$$

$$2\mu u = \frac{(\kappa-3)}{4}\,\text{Re}\,\phi_1(z) - \tfrac{1}{2}\,y\,\text{Im}\,\phi_1'(z), \quad \text{---(3.2.59)}$$

and

$$2\mu v = \frac{(\kappa+3)}{4}\,\text{Im}\,\phi_1(z) - \tfrac{1}{2}\,y\,\text{Re}\,\phi_1'(z), \quad \text{---(3.2.60)}$$

Since the far field boundary conditions on the stresses, stated in equations (3.2.54), must be satisfied, then

let us assume

$$\phi_1(z) = A_o[\sqrt{z^2 - a^2} - z], \quad \text{----------(3.2.61)}$$

Differentiating equation (3.2.61) with respect to z, one obtains

$$\phi_1'(z) = A_o[\frac{z}{\sqrt{z^2-a^2}} - 1], \quad \text{---------(3.2.62)}$$

and

$$\phi_1''(z) = A_o a^2 = \frac{1}{(z^2-a^2)^{\frac{3}{2}}}, \quad \text{---------(3.2.63)}$$

From equations (3.2.54), (3.2.56) and (3.2.62), one obtains the constant A_o as

$$A_o = \sigma_o, \quad \text{----------(3.2.64)}$$

The asymptotic stress distribution in the neighbourhood of the crack-tip is then obtained as

$$\sigma_{yy} = \frac{K_1}{\sqrt{2\pi r}}[\text{Cos } \tfrac{1}{2}\theta + \frac{\text{Sin } \theta \text{ Sin } \frac{3}{2}\theta}{4}] - \sigma_o, \quad \text{--(3.2.65)}$$

$$\sigma_{xx} = -\frac{K_1}{\sqrt{2\pi r}} \frac{\text{Sin } \theta \text{ Sin } \frac{3}{2}\theta}{4}, \quad \text{-------(3.2.66)}$$

and

$$\tau_{xy} = -\frac{K_1}{\sqrt{2\pi r}}[\frac{\text{Sin } \frac{1}{2}\theta}{2} - \frac{\text{Sin } \theta \text{ Cos } \frac{3}{2}\theta}{4}], \quad \text{---(3.2.67)}$$

where $K_1 = \sigma_o\sqrt{\pi a}$ is the stress intensity factor.

Equations (3.2.65) to (3.2.67) are clearly not the same as equations (1.2.16). Equations (3.2.65)to (3.2.67) are obtained via the new formulae while equations (1.2.16) are those commonly reported in the literature of fracture mechanics studies. Some notable differences between the two stress distributions include: The new equations state that a normal stress σ_{xx} cannot act along a free crack surface but a shear stress τ_{xy} is acting on that surface. On the other hand, equations

(1.2.16) state no shear stress along the free crack surface but a normal stress σ_{xx} is acting on the surface. Also as can be seen from equations (1.2.16) and (3.2.65) the σ_{yy} distributions are not the same. Furthermore, the opening of the crack due to the pressure loading when calculated from the new formulae and from equations (1.2.12) differ only by a multiplicative constant but the shapes are identical.

Finally, just like the previous problems solved, the difference between the maximum and minimum principal stresses can be obtained from equations (3.2.65) to (3.2.67) as

$$\sigma_1-\sigma_2 = \frac{K_1}{\sqrt{2\pi r}}\left[1+\tfrac{5}{4}\,\mathrm{Sin}^2\theta+\sqrt{\frac{2r}{a}}\left(1+\mathrm{Sin}\,\tfrac{1}{2}\theta\,\mathrm{Sin}\,\tfrac{3}{2}\theta\right)+\frac{2r}{a}\right]^{\frac{1}{2}}$$

----------(3.2.68)

From equations (3.2.37) and (3.2.68), one can conclude that for negligible r/a ratio, the shape of the isochromatics are the same.

3.3. Some Comments About the New Solutions

In the above section, the new formulae developed were applied to yield new model solutions to the problems shown in Fig. ? In Chapter One of this thesis, it was shown that the reported model solutions to these problems have some limitations. It is intended in this section to investigate the limitations, if any, of the new model solutions.

For the Fig. 2(i) problem, the new model solutions are given by equations (3.2.14) to (3.2.22). From

equations (3.2.17) and (3.2.18), the displacements along the x-axis are obtained as

$$2\mu u = \frac{(\kappa + \alpha\kappa - 3 + \alpha)\sigma_o}{4} \mathrm{Re}[\sqrt{x^2 - a^2}], \text{----(3.3.1)}$$

and

$$2\mu v = \frac{(\kappa + \alpha\kappa + 3 - \alpha)\sigma_o}{4} \mathrm{Im}[\sqrt{x^2 - a^2}], \text{----(3.3.2)}$$

where $0 \leq |x| < \infty$. At the crack tips $x = \pm a$, from equations (3.3.1) and (3.3.2) it could be concluded that both u and v are zero, as expected. Note that the old model gave u some non-zero value.

Also about the displacement, from equation (3.3.2) for $|x| \leq a$, one obtains

$$2\mu v = \frac{(\kappa + \alpha\kappa + 3 - \alpha)\sigma_o}{4} \sqrt{a^2 - x^2}, \text{----(3.3.3)}$$

This equation shows that the vertical displacement of the crack surface is a function of α. Remember that the old model gave v as same constant for all α.

About the resultant traction boundary condition at the free crack surface, given by equation (2.1.11), in the model, it was formulated as

$$[\phi(z) + \bar{\phi}'(z) + \bar{\psi}(z)]_{-a}^{a} = 0, \text{----------(3.3.4)}$$

With $\psi(z)$ defined as $\psi(z) = N\,\phi(z) - z\,\phi'(z)$, equation (3.3.4) becomes

$$[\phi(z) + N\,\bar{\phi}(z) + (z - \bar{z})\bar{\phi}'(z)]_{-a}^{a} = 0, \text{---(3.3.5)}$$

Along the x-axis, $z = \bar{z}$, and with ϕ in equation (3.2.8), one obtains equation (3.3.5) as

$$(1 - N)\sigma_o \sqrt{a^2 - x^2}\,|_{-a}^{a} = 0, \text{----------(3.3.6)}$$

Equation (3.3.6) indicates that the resultant traction on the free crack surface in the new model is zero, as expected.

From the new model, the stress distributions for $y = 0$, $|x| > a$ are

$$\sigma_{xx} = \alpha\sigma_o \frac{x}{\sqrt{x^2 - a^2}}, \quad \text{----------(3.3.7)}$$

$$\sigma_{yy} = \sigma_o \frac{x}{\sqrt{x^2 - a^2}}, \quad \text{----------(3.3.8)}$$

$$\tau_{xy} = 0. \quad \text{----------(3.3.9)}$$

Equations (3.3.7) to (3.3.9) are obtained from equations (3.2.8) and (3.2.14) to (3.2.16). Applying the stress optic law with the equations, one obtains the predicted fringe N as

$$N = \frac{(1 - \alpha)\sigma_o h}{f_\sigma} \frac{x}{\sqrt{x^2 - a^2}}, \quad \text{----------(3.3.10)}$$

Remember that, the old model gave N as independent of x. The prediction in equation (3.3.10) is quite interesting, for it corresponds with what has been observed in many experiments. For example, for the uniaxial loading $\alpha = 0$ then

$$N = \frac{\sigma_o h}{f_\sigma} \frac{x}{\sqrt{x^2 - a^2}}, \quad \text{----------(3.3.11)}$$

These predictions are in good agreement with some reported experimental results in the literature. Some of these are shown in Figs.7, 8, 9 where it could be seen that N is a variable along the x-axis but not constant as predicted by the old model.

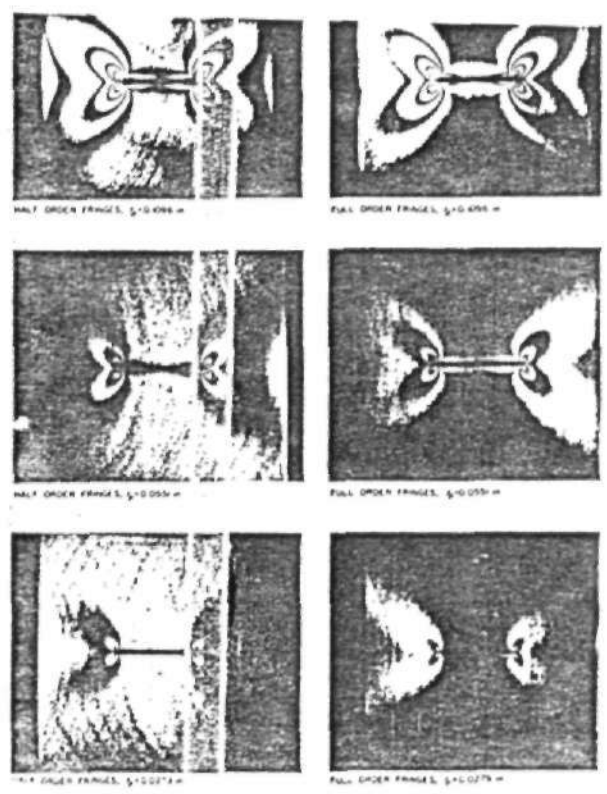


Fig. 7: Some Reported Experimental Fringes, I, for a uniaxially loaded centre crack specimen. [From William Gerberich (1962)]

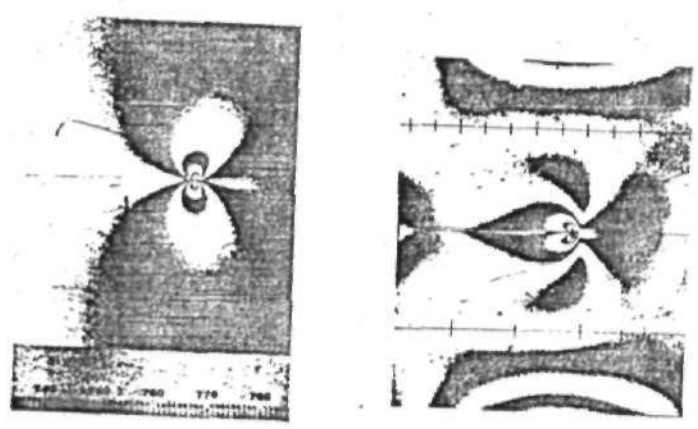


Fig. 8: Some Reported Experimental Fringes, II, for compact tension specimens.

[From Irwin et al (1978)]

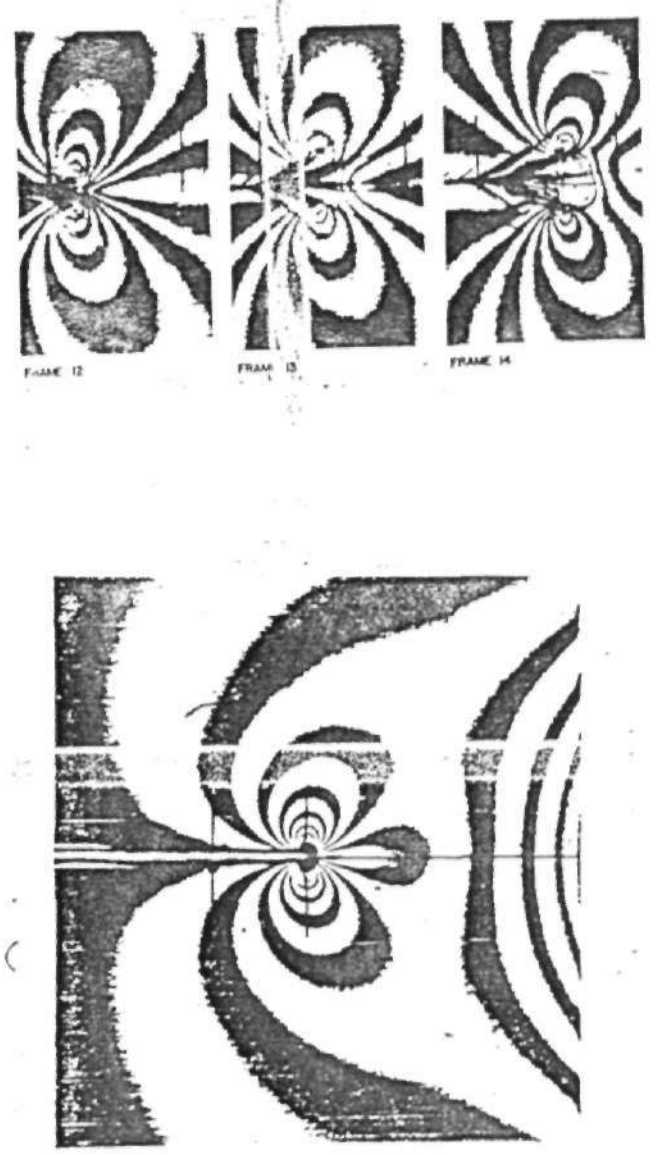


Fig. 9: Some Reported Experimental Fringes, III, for compact tension specimens.

[From Dally (1979) and Sanford (1979)]

Finally, from equation (3.2.15), the σ_{xx} stress has only one value at the crack tip, unlike the old model which predicts dual character of σ_{xx} at the crack tip.

From all the above, it could be concluded that the new model solutions are void of all the limitations of the old model solutions, noted in Chapter One, for the Fig. 2(i) problem.

The next problem is that shown in Fig. 2(ii) and its new model solutions given in equations (3.2.56) to (3.2.61). It should be noted that in the old model solutions to the same problem, two limitations were discussed in Chapter One. These limitations of the old model are unrealistic σ_{xx} distribution along the loading surfaces and some u displacements at the crack tips.

From equations (3.2.57) and (3.2.61), it could be seen that $\sigma_{xx} = 0$, at the loaded surfaces. Secondly at the crack tips from equations (3.2.59) and (3.2.60), the displacements are obtained as

$$2\mu u = \pm \frac{(\kappa - 3)}{4} \sigma_o a, \quad \text{----------(3.3.12)}$$

The old model solution as discussed in Chapter One page 11, gave

$$2\mu u^* = \pm \frac{(\kappa - 1)}{2} \sigma_o a, \quad \text{----------(3.3.13)}$$

For plane stress condition, the ratio of equations (3.3.12) and (3.3.13) is $-\frac{\nu}{1 - 2\nu}$, which is -1 for

$\nu = \frac{1}{3}$ and $-\frac{1}{3}$ for $\nu = .2$.

From the above equations, it could therefore be concluded that the new model solution has one limitation about the u displacement at the crack tips as indicated by equation (3.3.12).

With reference to Fig. 2(ii) problem and the general new model solution derived in Chapter Two, quoted in equations (2.3.1) to (2.3.11), one could show that the displacements u at the crack tips are zero, as expected, by solving the problem as follows:

From equation (2.3.10), since u has to be zero at the crack tips then take

$$N = \kappa. \quad \text{----------(3.3.14)}$$

Then, substitute in equations (2.3.1)to (2.3.11) that,

$$\phi'(z) = \frac{1}{1 + \kappa} \phi_1'(z), \quad \text{----------(3.3.15)}$$

From equations (2.3.1) to (2.3.11), the stress and displacement distributions are then obtained as

$$\sigma_{yy} = \text{Re } \phi_1'(z) + \frac{2}{1 + \kappa} y \text{ Im } \phi_1''(z), \text{---(3.3.16)}$$

$$\sigma_{xx} = \frac{3 - \kappa}{1 + \kappa} \text{Re } \phi_1'(z) - \frac{2}{1 + \kappa} y \text{ Im } \phi_1''(z), \text{--(3.3.17)}$$

$$\tau_{xy} = \frac{\kappa - 1}{\kappa + 1} \text{Im } \phi_1'(z) - \frac{2}{\kappa + 1} y \text{ Re } \phi_1''(z), \text{--(3.3.18)}$$

$$2\mu u = -\frac{2}{\kappa + 1} y \text{ Im } \phi_1'(z), \text{ --------(3.3.19)}$$

and

$$2\mu v = \frac{2\kappa}{\kappa + 1} \text{Im } \phi_1(z) - \frac{2}{\kappa + 1} y \text{ Re } \phi_1'(z), \text{ --(3.3.20)}$$

With $\phi_1(z)$ and $\phi_1'(z)$ as given in equations (3.2.61) and (3.2.62) respectively. From equations (3.2.61) and (3.3.19), it could be seen that at the crack tip u = 0. But the limitation of this solution is that the σ_{xx} along the loaded surface, is obtained as

$$\sigma_{xx}(x,o) = -\frac{3-\kappa}{1+\kappa}\,\sigma_o. \quad \text{----------(3.3.21)}$$

In equation (3.3.21), $x \leq a$ and was obtained from equations (3.2.62) and (3.3.17). One of the unappealing features of equations (3.3.16) to (3.3.21) is that the stress distributions are functions of the Poisson's ratio, ν, which is an elastic constant. This is not expected for this problem.

Finally about this problem, it should be noted that the old model solutions, the first new model solutions given by equations (3.2.57) to (3.2.60) and those derived in this section, given in equations (3.3.16) to (3.3.20), all give the same stress intensity factor as

$$K_1 = \sigma_o\sqrt{\pi a}.$$

The next new model solution to be investigated is that shown in Fig. 2(iv). Following the convension of Muskhelishvili (1953) and Sokolnikoff (1956), the solution of the Fig. 2(iv) problem could be obtained by considering an axial load in the y-direction and a compressive load of same magnitude in the x-direction. Then equations (3.2.14) to (3.2.18) substitute, $\alpha = -1$.

The solution for the Fig. 2(iv) problem is then obtained as

$$\sigma_{yy} = \text{Re } \phi_1'(z), \text{ ------÷ --- ----(3.3.22)}$$

$$\sigma_{xx} = - \text{Re } \phi_1'(z), \text{ ----÷ - ------(3.3.23)}$$

$$\tau_{xy} = \text{Im } \phi_1'(z), \text{----------(3.3.24)}$$

$$2\mu u = - \text{Re } \phi_1(z), \text{----------(3.3.25)}$$

and

$$2\mu v = \text{Im } \phi_1(z), \text{ ----------(3.3.26)}$$

where from equations (3.2.8) and (3.2.12), $\phi_1(z)$ is given by

$$\phi_1(z) = \tau_o\sqrt{z^2 - a^2}, \text{ ----------(3.3.27)}$$

From equations (3.2.26) and (3.2.27) it could be seen that $2\mu v = 0$ for $|x| \geq a$, a property lacked by the old model solution discussed on page 12, Chapter One. Again it should be noted that both the old and new model solutions of the Fig. 2(iv) problem, give the same stress intensity factor.

In the remaining paragraphs of this section, the stress distributions for the uniaxially loaded plate are studied in some detail. Let the old model solution for the uniaxially loaded plate be represented by σ^a_{xx}, σ^a_{yy} and τ^a_{xy}. From equations (1.2.1) to (1.2.3), in the neighbourhood of the crack tip, these are given by

$$\sigma^a_{xx} = \frac{K_1}{\sqrt{2\pi}}[\text{Cos } \tfrac{1}{2}\theta(1-\text{Sin } \tfrac{1}{2}\theta \text{ Sin } \frac{3\theta}{2}) - \sqrt{\frac{r}{a}}], \text{--(3.3.28)}$$

$$\sigma^{a}_{yy} = \frac{K_1}{\sqrt{2\pi r}} \text{Cos } \tfrac{1}{2}\theta(1 + \text{Sin } \tfrac{1}{2}\theta \text{ Sin } \frac{3\theta}{2}), \text{---(3.3.29)}$$

and

$$\tau^{a}_{xy} = \frac{K_1}{\sqrt{2\pi r}} \text{Cos } \tfrac{1}{2}\theta \text{ Sin } \tfrac{1}{2}\theta \text{ Cos } \frac{3\theta}{2}. \text{ ---(3.3.30)}$$

The new model solution denoted by σ^{c}_{xx}, σ^{c}_{yy} and τ^{c}_{xy}, from equations (3.2.31) to (3.2.33) are obtained as

$$\sigma^{c}_{xx} = - \frac{K_1}{\sqrt{2\pi r}} \frac{\text{Cos } \tfrac{1}{2}\theta \text{ Sin } \tfrac{1}{2}\theta \text{ Sin } \frac{3\theta}{2}}{2}, \text{ ---(3.3.31)}$$

$$\sigma^{c}_{yy} = \frac{K_1}{\sqrt{2\pi r}} \text{Cos } \tfrac{1}{2}\theta(1 + \frac{\text{Sin } \tfrac{1}{2}\theta \text{ Sin } \frac{3\theta}{2}}{2}), \text{---(3.3.32)}$$

and

$$\tau^{c}_{xy} = - \frac{K_1}{\sqrt{2\pi r}} \frac{\text{Sin } \tfrac{1}{2}\theta}{2}(1 - \text{Cos } \tfrac{1}{2}\theta \text{ Cos } \frac{3\theta}{2}), \text{--(3.3.33)}$$

From the above equations, one obtains the ratios $\sigma^{c}_{xx}/\sigma^{c}_{xx}$, $\sigma^{c}_{yy}/\sigma^{c}_{yy}$ and $\tau^{c}_{xy}/\tau^{c}_{xy}$ as

$$\frac{\sigma^{c}_{xx}}{\sigma^{a}_{xx}} = - \frac{\text{Cos } \tfrac{1}{2}\theta \text{ Sin } \tfrac{1}{2}\theta \text{ Sin } \frac{3\theta}{2}}{2[\text{Cos } \tfrac{1}{2}\theta(1-\text{Sin } \tfrac{1}{2}\theta \text{ Sin } \frac{3\theta}{2}) - \sqrt{\frac{r}{a}}]}, \text{ ------(3.3.34)}$$

$$\frac{\sigma^{c}_{yy}}{\sigma^{c}_{yy}} = \frac{2 + \text{Sin } \tfrac{1}{2}\theta \text{ Sin } \frac{3\theta}{2}}{2(1 + \text{Sin } \tfrac{1}{2}\theta \text{ Sin } \frac{3\theta}{2})}, \text{ ----(3.3.35)}$$

and

$$\frac{\tau^{c}_{xy}}{\tau^{c}_{xy}} = - \frac{1 - \text{Cos } \tfrac{1}{2}\theta \text{ Cos } \frac{3\theta}{2}}{\text{Cos } \tfrac{1}{2}\theta \text{ Cos } \frac{3\theta}{2}}, \text{-------(3.3.36)}$$

The plots of equations (3.3.34) to (3.3.36), for small values of $\frac{r}{a}$ are shown in Fig. 10.

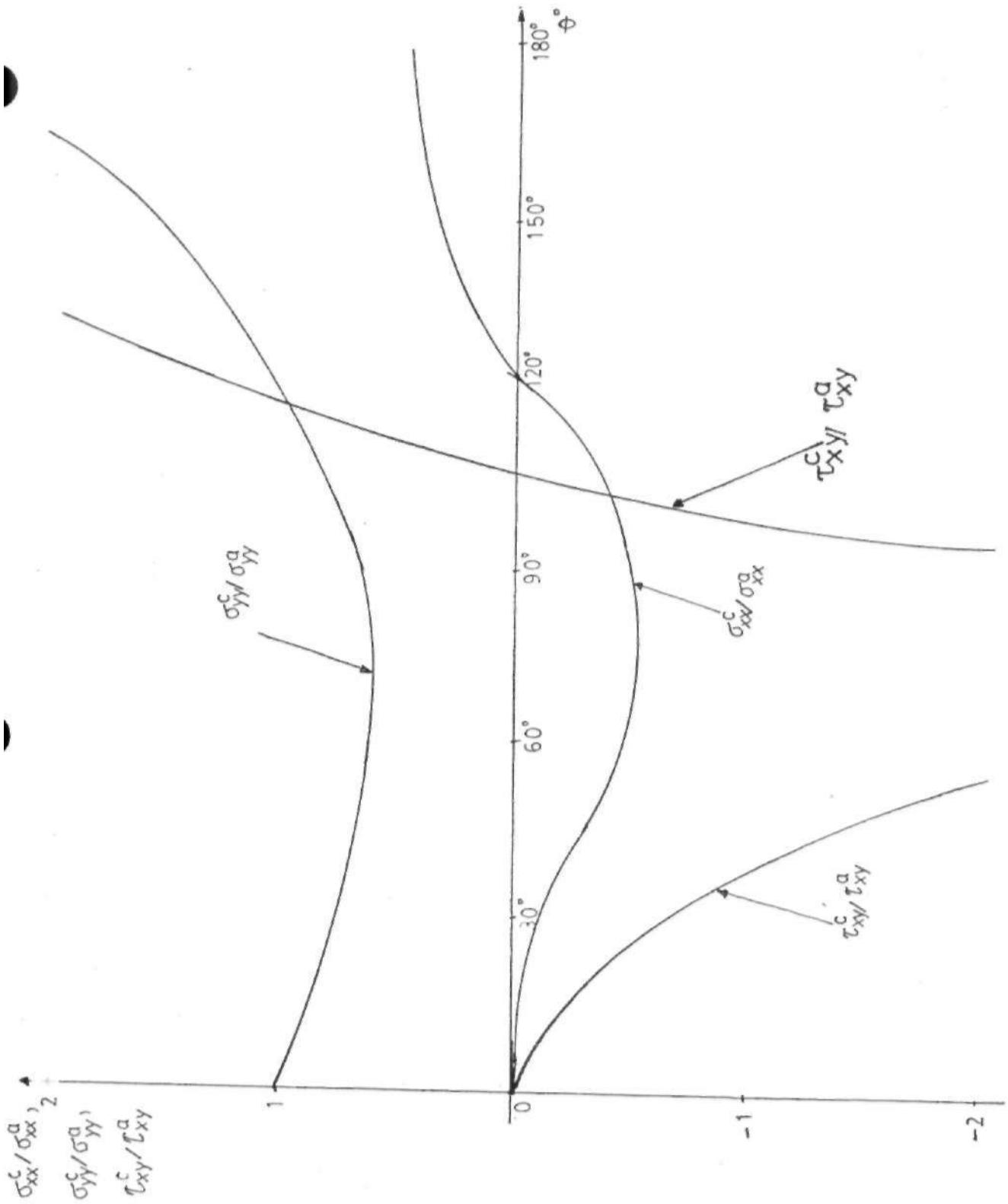


Fig. 10: The Plots of $\frac{\sigma^c_{xx}}{\sigma^a_{xx}}$, $\frac{\sigma^c_{yy}}{\sigma^a_{yy}}$ and $\frac{\tau^c_{xy}}{\tau^a_{xy}}$ for small values of $\frac{r}{a}$

Next, the shape of the fringes developed by the new model is investigated. In the equations to be used, higher orders of $1/\sqrt{r}$ terms would be employed, so that the stresses used are away from crack-tip.

From equations (3.2.14) to (3.2.16) with $\alpha = 0$, the stresses are given by,

$$\sigma_{xx} = -\tfrac{1}{2}\, y\ \mathrm{Im}\ \phi_1''(z), \quad \text{----------(3.3.37)}$$

$$\sigma_{yy} = \mathrm{Re}\ \phi_1'(z) + \tfrac{1}{2}\, y\ \mathrm{Im}\ \phi_1''(z), \quad \text{----(3.3.38)}$$

and

$$\tau_{xy} = \tfrac{1}{2}\ \mathrm{Im}\ \phi_1'(z) - \tfrac{1}{2}\, y\ \mathrm{Re}\ \phi_1''(z), \quad \text{-----(3.3.39)}$$

With $\phi_1'(z)$ given by (3.2.7) the stresses are obtained as,

$$\sigma_{xx} = -\frac{K_1}{\sqrt{2\pi r}}\,\frac{\mathrm{Sin}\ \theta\ \mathrm{Sin}\ \frac{3\theta}{2}}{4}$$

$$+\frac{3K_1}{4a}\sqrt{\frac{r}{2\pi}}\,\frac{\mathrm{Sin}\ \theta\ \mathrm{Sin}\ \frac{1}{2}\theta}{4}, \quad \text{----------(3.3.40)}$$

$$\sigma_{yy} = \frac{K_1}{\sqrt{2\pi r}}\left(\mathrm{Cos}\ \tfrac{1}{2}\theta + \frac{\mathrm{Sin}\ \theta\ \mathrm{Sin}\ \frac{3\theta}{2}}{4}\right.$$

$$\left.+\frac{3K_1}{4a}\sqrt{\frac{r}{2\pi}}\left(\mathrm{Cos}\ \tfrac{1}{2}\theta - \frac{\mathrm{Sin}\ \theta\ \mathrm{Sin}\ \frac{1}{2}\theta}{4}\right), \quad \text{----(3.3.41)}\right.$$

and

$$\tau_{xy} = \frac{K_1}{\sqrt{2\pi r}}\left(\frac{\mathrm{Sin}\ \theta\ \mathrm{Cos}\ \frac{3\theta}{2}}{4} - \frac{\mathrm{Sin}\ \frac{1}{2}\theta}{2}\right)$$

$$+\frac{3K_1}{8a}\sqrt{\frac{r}{2\pi}}\left(\mathrm{Sin}\ \tfrac{1}{2}\theta - \frac{\mathrm{Sin}\ \theta\ \mathrm{Cos}\ \frac{1}{2}\theta}{2}\right). \quad \text{---(3.3.42)}$$

From the above equations, the maximum principal stress difference, $(\sigma_1 - \sigma_2)$ defined as

$$(\sigma_1 - \sigma_2)^2 = (\sigma_{yy} - \sigma_{xx})^2 + 4\tau_{xy}^2, \quad ---(3.3.43)$$

is obtained as,

$$(\sigma_1 - \sigma_2)^2 = \frac{K_1^2}{2\pi r}\left(1 + \frac{5\sin^2\theta}{4}\right) + \frac{3K_1^2}{4\pi a}\cos\theta\left(1 - \frac{3\sin^2\theta}{4}\right)$$

$$+ \frac{9K_1^2\, r}{3^2\pi a^2}\left(1 - \frac{3\sin^2\theta}{4}\right). \quad ----------(3.3.44)$$

From the stress optic law,

$$(\sigma_1 - \sigma_2) = \frac{N_o f_\sigma}{h}, \quad ----------(3.3.45)$$

where N_o is the fringe order, f_σ is the material fringe value and h is the specimen thickness. Therefore, from equations (3.3.44) and (3.3.45), the expected shape of the fringes from the new model solution is obtained as

$$N_o^2 = \frac{K_1^2\, h^2}{2\pi r f_\sigma^2}\left[\left(1 + \frac{5\sin^2\theta}{4}\right) + \frac{3}{2}\left(\frac{r}{a}\right)\cos\theta\left(1 - \frac{3\sin^2\theta}{4}\right)\right.$$

$$\left. + \frac{9}{16}\left(\frac{r}{a}\right)^2\left(1 - \frac{3\sin^2\theta}{4}\right)\right]. \quad ----------(3.3.46$$

The plot of $2\pi r N_o^2 f_\sigma^2 / K_1^2\, h^2$ against θ for some value of $\frac{r}{a}$ is shown in Fig. 11. The theoretical shapes obtained are in agreement with the experimental fringes shown in Figs. 7, 8 and 9.

3.4. Conclusions

The new formulae derived from the Kolosov-Muskhelishvili equations were employed to obtain some

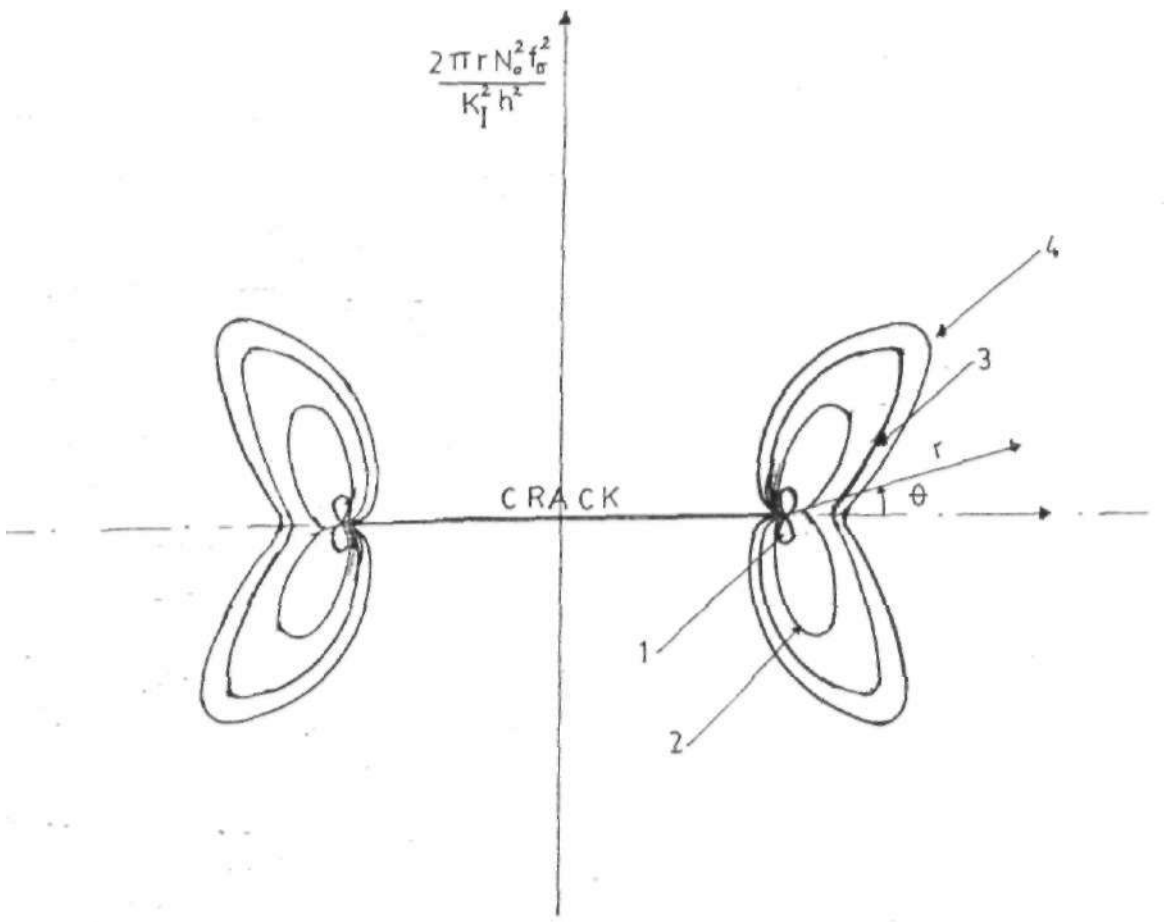


Fig. 11: Theoretical Expected Shape of Fringes from the New Solution for Uniaxial Loading

new asymptotic stress and displacement distributions in the neighbourhood of a crack tip. These stresses are all in the form,

$$\sigma_{ij} = \frac{K_1}{\sqrt{2\pi r}} f_{ij}(\alpha,\theta), \text{ ----------(3.4.1)}$$

and the displacements in the form

$$u_i = K_1\sqrt{\frac{r}{2\pi}}\, h_i(\alpha,\theta), \text{ ----------(3.4.2)}$$

where ij = 1,2, $\sigma_{11} = \sigma_{xx}$, $\sigma_{21} = \sigma_{12} = \tau_{xy}$, $\sigma_{22} = \sigma_{yy}$. $u_1 = u$, $u_2 = v$ and $f_{ij}(\alpha,\theta)$, $h_i(\alpha,\theta)$ are some functions of α and θ, defined in equations (3.2.19) to (3.2.23), (3.2.31) to (3.2.35), (3.2.48) to (3.2.52), and (3.2.65) to (3.2.67). To the author's knowledge, this is the first time these generalized forms of the stress and displacement distributions are reported. The knowledge of these distributions is very important in both the theoretical and experimental studies of fracture mechanics.

What was commonly reported in the literature of fracture mechanics as analogous to equations (3.4.1) and (3.4.2) are equations of the form,

$$\sigma_{ij} = \frac{K}{\sqrt{2\pi r}} f_{ij}(\theta) + A_{ij}(\alpha), \text{ -------(3.4.3)}$$

and

$$u_i = K_1\sqrt{\frac{r}{2\pi}}\, h_i(\theta) + \bar{A}_i(\alpha), \text{ ---------(3.4.4)}$$

for the stresses and displacements, respectively. The functions $f_{ij}(\theta)$, $A_{ij}(\alpha)$, $h_i(\theta)$ and $A_{ij}(\alpha)$ can be

obtained from equations (1.2.1) to (1.2.12). It should be noted that, in Chapter One, it was shown that stress and displacement distributions of the form in equations (3.4.3) and (3.4.4) are possible only if $A_{ij}(\alpha) = 0$ and $\bar{A}_{ij}(\alpha) = 0$.

The new formulae derived in Chapter Two, equations (2.3.7) to (2.3.11) are in terms of a constant number, N. The constant N, $-\infty < N < \infty$, for the particular problems solved was determined from the boundary conditions. For example, in the problem where $\sigma^{\infty}_{yy} = \sigma_o$, $\sigma^{\infty}_{xx} = \alpha\sigma_o$, N is related to the biaxiallity coefficient α by (from equation (3.2.13)),

$$N = \frac{3 - \alpha}{1 + \alpha}, \quad \text{----------(3.4.5)}$$

The plot of N against α is shown in Fig. 12. From the figure, it is seen that unique solutions exist for all N, except when N = -1. It was for the purpose of obtaining a unique solution for the case when N = -1 that the problem defined by equation (3.2.42) was considered. The asymptotic stress and displacement distributions for that problem are given by equations (3.2.48) to (3.2.52) and are also of the form defined in equations (3.4.1) and (3.4.2).

Because of its importance in experimental studies, the problem of a uniaxially loaded plate was reconsidered separately. The new formulae give the stress and

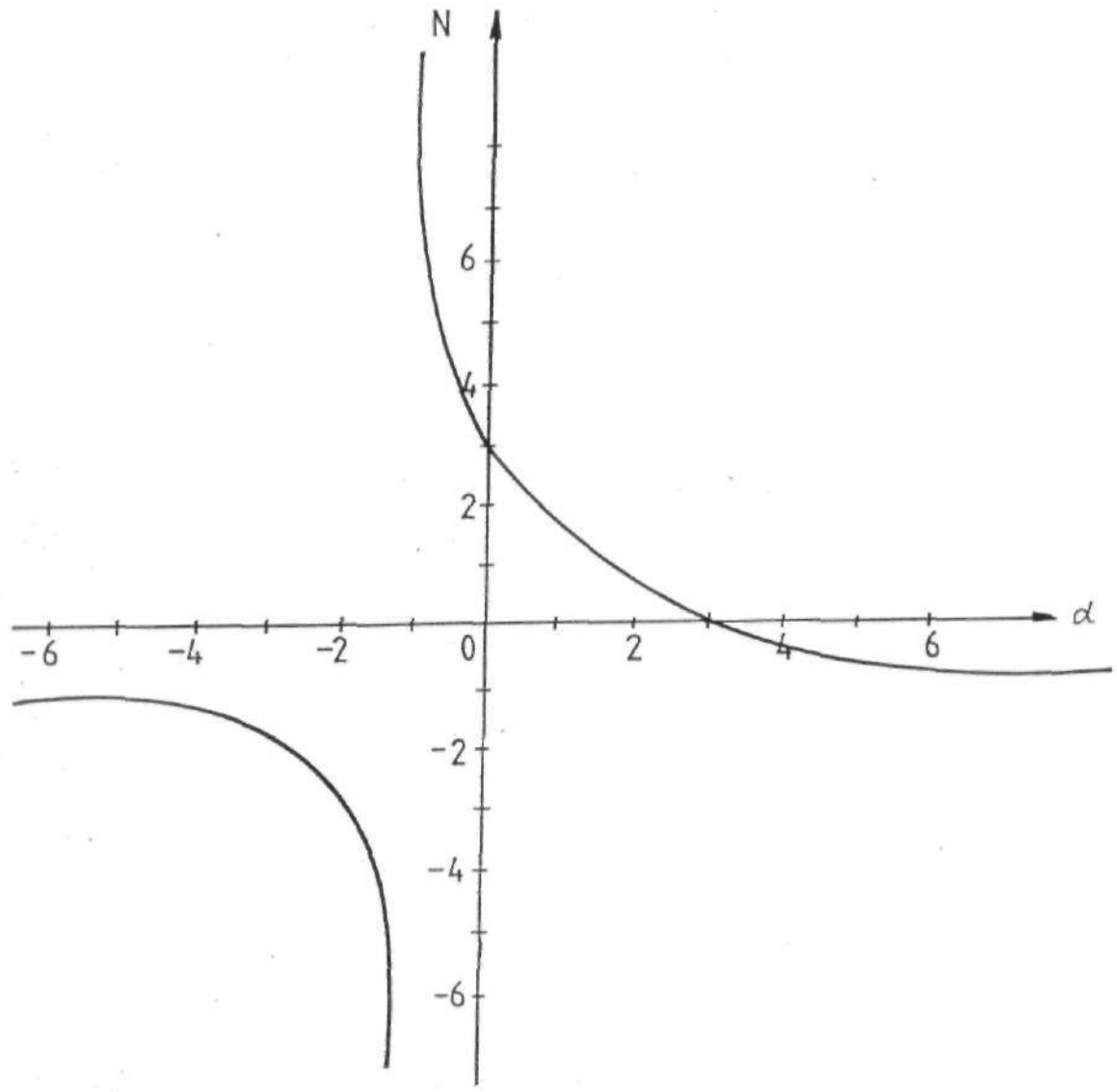


FIG . 12: The plot of the biaxial factor α against N, the constant that appear in the new formulae .

displacement distributions in equations (3.2.31) to (3.2.35) while those reported in the literature are defined in equations (1.2.1) with $2A = \sigma_o$. Although it has already been shown that equations (1.2.1) have limitations when representing the stress state for a uniaxially loaded member, just for comparison purpose, the stress distributions from the old and the new model solutions were compared in Section 3.3. The comparison is shown in Fig. 10.

Of great practical importance in experimental studies are the shapes of isochromatics which was discussed in Section 3.3. The theoretical and experimental shapes were shown to be in good agreement. These shapes could be used to evaluate the stress intensity factor, as discussed in Irwin et (1978). As noted by Irwin et al (1978), in order to accurately evaluate the stress intensity factor from the fringe patterns, higher orders of $\frac{r}{a}$ need to be considered. For that purpose the stress function in equation (3.2.7) can be written as

$$\phi' = \frac{K_1}{\sqrt{2\pi z}}[1 + \tfrac{3}{4}\frac{z}{a} - \tfrac{5}{32}(\frac{z}{a})^2 + ...], \quad ---(3.4.6)$$

where $z = re^{i\theta}$, r, θ are polar coordinates at the crack tip. In equations (3.2.19) to (3.2.23), (3.2.31) to (3.2.35) and (3.2.48) to (3.2.52), only the first term of equation (3.4.6) was considered. For experimental applications, therefore, at least the second term of equation (3.4.6) should be considered.

Finally, in the appendix some few other problems were solved via the new formulae. From these solutions the strain energy-release rate and the J-integral are evaluated in the next chapters. Some studies on the strain energy-release rate and the J-integral as crack-tip characterizing parameters are then made.

CHAPTER IV

THE STRAIN ENERGY-RELEASE RATE

4.1. Introduction

Griffith (1920), introduced the concept of the strain energy balance approach in the studies of crack propagation. The modified version of the Griffith criterion introduced by Irwin (1957, 1960) is extensively used in the studies of fracture. Some account of that can be found in Hayes (1975) and Erdogan (1983), where the origin of the strain energy-release rate and the stress intensity factors were discussed; Clausing (1969) where the strain energy-release rate concept was discussed and applied in analysing crack growth instability phenomenon; Heyer (1973) in which the experimental determination of the strain energy-release rate was reviewed and Sanders (1960) who relates the strain energy-release rate to a path independent integral.

In all the reported studies of the Griffith criterion, it was inferred or assumed that the final fracture criterion is independent of loading. This was accepted simply because the stress intensity factor say, K_1, is not effected by an applied stress parallel to the crack. Although the above inference concerning the effect of loading on the Griffith criterion seems to be well established, in this chapter, it is shown that it is not necessarily so.

Before making some detailed calculations of the strain energy-release rate, G_1, let the strain energy

density, W_s, be computed for some of the problems discussed in Chapter III. For a large plate with a central crack of length 2a, loaded by $\sigma^{\infty}_{yy} = \sigma_o$, and $\sigma^{\infty}_{xx} = \alpha\sigma_o$, from equations (3.2.19) to (3.2.21), if it is assumed that the direction of crack propagation is along the x-axis, then

$$W_{sp} = \frac{K_1^2}{4\pi Er}[1 + \alpha^2 - 2\nu\alpha], \text{ ----------(4.1.1)}$$

where W_{sp} is the strain energy-density along the direction of crack propagation. Similarly, if the plate was subjected to pressure loading only and the direction of crack propagation assumed to be along the x-axis, then from equations (3.2.65) to (3.2.67), the strain energy density is obtained as

$$W_{sp} = \frac{(K_1^p)^2}{4\pi Er}\left[1 - \sqrt{\frac{2r}{a}}\right]^2, \text{ ----------(4.1.2)}$$

where $K_1^p = \sigma_o{}^p\sqrt{\pi a}$ is the stress intensity factor due to the applied pressure, $\sigma_o{}^p$.

Now, if tensile and pressure loadings are combined, from equations (3.2.19) to (3.2.21) and (3.2.65) to (3.2.67), the combined strain energy density along the direction of crack propagation is given by

$$W_{sp} = \frac{K_1^2}{4\pi Er}\left[\alpha^2 + \left(1 + \frac{K_1^p}{K_1} - \frac{K_1^p}{K_1}\sqrt{\frac{2r}{a}}\right)^2 - 2\nu\alpha\left(1 + \frac{K_1^p}{K_1} - \frac{K_1^p}{K_1}\sqrt{\frac{2r}{a}}\right)\right].$$

--------(4.1.3)

From the above three equations, (4.1.1) to (4.1.3), one may strongly suspect that any criterion based on the strain energy may depend on the distribution of the applied stresses because equation (4.1.3) cannot easily be obtained by simply adding equations (4.1.1) and (4.1.2).

In what follows, the strain energy criterion or the Irwin crack extension force is proved to behave in a manner similar to equations (4.1.1) to (4.1.3).

4.2. Evaluation of the Strain Energy-Release Rate

For a body with a central crack of length 2a, as shown in Fig. 2, the strain energy-release rate, G_1, is defined as, Hayes (1975), Sneddon and Lowengrub (1969),

$$G = \tfrac{1}{2} \frac{\partial W}{\partial a} , \text{----------(4.2.1)}$$

where W is the strain energy required to form the crack. If the body is subjected to opening mode forces, σ_{yy} and σ_{xx}, W is denoted by W_1 and the strain energy-release rate by G_1.

With U as the surface energy of the body, the Griffith criterion states that a crack of length 2a in a body will begin to spread when

$$\frac{\partial}{\partial a} [W - U] = 0 , \text{----------(4.2.2)}$$

Griffith (1920) gave the surface energy U in terms of the 'surface tension force' T for the material as

$$U = 4a\ T, \text{----------(4.2.3)}$$

From equations (4.2.1) to (4.2.3) one obtains

$$G = 2\ T, \text{----------(4.2.4)}$$

The major aim in this section is to find mathematical expressions for the strain energy-release rate, defined by equation (4.2.1), for a number of loading conditions. In most of the problems, the opening mode loadings are considered. In that case, G_1, can be

evaluated from equation (4.2.1) with W_1 calculated from, Hayes (1975),

$$W_1 = -\int_{-a}^{a} \sigma_o \, v(x,o)dx, \quad \text{----------(4.2.5)}$$

and therefore,

$$G_1 = \frac{\partial}{\partial a} \int_{o}^{a} \sigma_o \, v(x,o)dx, \quad \text{----------(4.2.6)}$$

where σ_o is a postulated applied stress and $v(x,o)$ is the crack opening due to the applied stresses. Alternatively, the strain energy-release rate, G_1, can be calculated from Irwin crack extension force theory, Irwin (1957), defined in equation (1.3.3). For the problems to be considered here, there are always two crack tips, then n = 2. Thus,

$$G_1 = \lim_{\Delta a \to o} \frac{1}{\Delta a} \int_{0}^{\Delta a} (\sigma_{yy}|_{r=r;\ \theta=o})(v|_{r=\Delta a-r',\theta=\pi})dr' \quad \text{--------(4.2.7)}$$

For a large plate with a central crack of length 2a, loaded by $\sigma^{\infty}_{yy} = \sigma_o$ and $\sigma^{\infty}_{xx} = \alpha\sigma_o$, from equations (3.2.7), (3.2.8) and (3.2.18), one obtains

$$v(x,o) = \frac{(\kappa+\alpha\kappa+3-\alpha)}{8\mu} \sigma_o \sqrt{a^2 - x^2}, \quad \text{-----(4.2.8)}$$

Equation (4.2.6) gives the strain energy, W_1 as

$$W_1 = \frac{(\kappa+\alpha\kappa+3-\alpha)}{16\mu} \sigma_o^2 \pi a^2, \quad \text{--------(4.2.9)}$$

From equations (4.2.6) and (4.2.8), the strain energy-release rate, G_1, is calculated as

$$G_1 = \frac{(\kappa+\alpha\kappa+3-\alpha)}{16\mu} K_1^2, \quad \text{----------(4.2.10)}$$

where $K_1 = \sigma_o\sqrt{\pi a}$. Alternatively, from equations (3.2.19) and (3.2.23), we obtain

$$\sigma_{yy}(r = r',\ \theta = 0) = \frac{K_1}{\sqrt{2\pi r'}}\ ,\text{---------}\quad (4.2.11)$$

and

$$v\,(r=\Delta a-r',\theta=\pi) = \frac{(\kappa+\alpha\kappa+3-\alpha)}{4\mu} K_1\sqrt{\frac{\Delta a-r'}{2\pi}},\ \text{---}(4.2.12)$$

Then with equations (4.2.12), (4.2.11) and (4.2.7), equation (4.2.10) is obtained. These are shown in Appendix B.

Consider next a second problem in which the strain energy-release rate is to be evaluated. Consider a large plate with a central crack of length 2a, loaded by $\sigma^{\infty}_{xx} = \sigma_o$ and $\sigma^{\infty}_{yy} = 0$. From equations (3.2.47) and (3.2.8) the crack opening, v(x,o) is obtained as

$$v(x,o) = \frac{(\kappa-1)}{8\mu}\ \sigma_o\ \sqrt{a^2 - x^2},\ \text{----------}(4.2.13)$$

Then equations (4.2.13) and (4.2.6) give the strain energy-release rate, G_1, as,

$$G_1 = \frac{\kappa-1}{8\mu}\ K_1^2,\ \text{----------}(4.2.14)$$

The third problem is that of a large plate with a central crack of length 2a, subjected to a uniform pressure loading, σ_o^p on the crack faces. From equations (3.2.56), (3.2.60) and (3.2.61), one arrives at

$$\sigma_{yy}(r=r',\theta=0) = \frac{K_1^p}{\sqrt{2\pi r'}} - \frac{K_1^p}{\sqrt{\pi a}}\ ,\ \text{---------}(4.2.15)$$

and

$$v\,(r=\Delta a-r',\theta=\pi) = \frac{\kappa+3}{4\mu}\ K_1^p\ \sqrt{\frac{\Delta a-r'}{2\mu}}\ ,\ \text{-------}(4.2.16)$$

where $K_1^p = \sigma_o^p\sqrt{\pi a}$ is the stress intensity factor due to the pressure loading. Then from equation (4.2.7), the strain energy-release rate, G_1 is obtained as

$$G_1 = \frac{\kappa+3}{16\mu}\ (K_1^p)^2,\ \text{----------}(4.2.17)$$

Finally, consider the problem of a large plate with a central crack of length 2a, subjected to combined far field tensile loading, $\sigma^{\infty}_{yy} = \sigma_o$, $\sigma^{\infty}_{xx} = \alpha\sigma_o$ and some uniform pressure loading, $\sigma_o{}^P$ at the crack faces. Then from equations (3.2.19), (3.2.23), (3.2.56), (3.2.60), and (3.2.61), one obtains the stress σ_{yy} and the crack-tip opening, v, as

$$\sigma_{yy}(r=r',\theta=0) = \frac{K_1}{\sqrt{2\pi r'}} + \frac{K_1^P}{\sqrt{2\pi r'}} - \frac{K_1^P}{\sqrt{\pi a}}, \text{-----(4.2.18)}$$

and

$$v(r=\Delta a-r',\theta=\pi) = \frac{(\kappa+\alpha\kappa+3-\alpha)}{4\mu} K_1\sqrt{\frac{\Delta a-r'}{2\pi}} + \frac{+3}{4\mu}K_1^P\sqrt{\frac{\Delta a-r'}{2\pi}},$$

----------(4.2.19)

Then the strain energy-release rate, G_1, from equations (4.2.19), (4.2.18 and (4.2.7) is obtained as

$$G_1 = \frac{(\kappa+\alpha\kappa+3-\alpha)}{16\mu}[K_1{}^2+K_1K_p]+\frac{(\kappa+3)}{16\mu}[(K_1^P)^2+K_1K_1^P], \text{--(4.2.20)}$$

where $K_1 = \sigma_o\sqrt{\pi a}$ and $K_1^P = \sigma_o{}^P\sqrt{\pi a}$. Refer to Appendix B.

From equations (4.2.10) (4.2.14), (4.2.17) and (4.2.20), since all these expressions are different, then the strain energy-release rate expression is always a function of loading. Also from equations (4.2.10), (4.2.17) and (4.2.20), one can conclude that the strain energy-release rate for a combined loading cannot be obtained by simply adding the strain energy-release rate for the individual loadings. In the sections that follow, some applications and implications of the derived equations are discussed.

4.3. Some Applications of the Concept of the Strain Energy-Release Rate

Griffith (1920) reported some experimental results he conducted on large tubes and spheres made of

hard glass. He obtained the specific surface tension force per unit area, T, for hard glass at room temperature by extrapolating results obtained at higher temperatures. The major aim of Griffith's experiments with the hard glass was to compare the measured and the predicted failure loads. From the results he obtained, an almost constant value of the product of the failure load and the square root of half the crack length, i.e. $\sigma_o\sqrt{a}$, for a range of crack lengths was observed. Also he experimentally proved that $\sigma_o\sqrt{a}$ is not influenced by an applied stress parallel to the crack plane. Finally, he found that the conditions of failure from his criterion, (Griffith (1920), as

$$\sigma_o = \sqrt{\frac{2ET}{\pi a}}\ , \qquad \text{----------(4.3.1)}$$

for plane stress and

$$\sigma_o = \sqrt{\frac{2ET}{\pi a(1-\nu^2)}}\ , \qquad \text{----------(4.3.2)}$$

for plane strain were not satisfied. Where σ_o was the applied stress at failure, a half crack length, E, is the Young's modulus, ν is the Poisson's ratio and T is the specific surface tension force per unit area.

A number of researchers, such as Irwin (1957, 1960) made some attempt to modify the Griffith equations; equations (4.3.1) and (4.3.2), so as to satisfy some experimental results. One noticable and acceptable improvement is to write the surface tension force per unit area, which appears in equations (4.3.1) and (4.3.2) as

$$2T = 2T_{el} + 2T_{pl}, \qquad \text{----------(4.3.3)}$$

where T_{el} and T_{pl} are respectively the elastic component and the plastic component of the surface tension force per unit area. Griffith (1920) considered the elastic component only. Based on experimental observations that, Irwin (1957, 1960),

$$T_{pl} >> T_{el}, \text{ ----------(4.3.4)}$$

Irwin proposed that

$$G = 2T_{pl}, \text{ ----------(4.3.5.)}$$

where G is termed the strain energy-release rate, with the G after Griffith. There are now well established procedures of experimentally evaluating, G, Irwin(1960), Hayes (1973).

Then with equations (4.3.3) to (4.3.5), equations (4.3.1) to (4.3.2) become,

$$\sigma_o = \sqrt{\frac{EG}{\pi a}}, \text{ ----------(4.3.6)}$$

for plane stress and

$$\sigma_o = \sqrt{\frac{EG}{\pi a(1-\nu^2)}}, \text{ ----------(4.3.7)}$$

for plane strain. Equations (4.3.6) and (4.3.7) give the failure load from the modified Griffith criterion, introduced by Irwin. Note that equations (4.3.6) and (4.3.7) can be obtained from equation (4.2.10) with $\alpha = 1$.

The above modifications of Irwin to the Griffith theory, though of much importance, are still not sufficient to handle many other fracture problems. The modified equations, equations (4.3.6) and (4.3.7) can only handle the problem of a large plate subjected to equal biaxial tension. Applying these equations to any other problem must result in errors.

Apart from experimental errors, the Griffith criterion was not satisfied by his experimental results, Griffith (1920), because the equations he derived and used, equations (4.3.1) and (4.3.2), and their Irwin modifications, equations (4.3.6) and (4.3.7), were derived with inference that the final condition of fracture was independent of the loading conditions. It simply implies that the final fracture condition was not effected by the biaxiallity of the loading. These cannot be possible, as can be seen from equations (4.2.10), (4.2.17) and (4.2.20). If the inference or the assumption was correct, then all these equations for the strain energy-release rate could have been the same.

Equations (4.2.10), 4.2.14), (4.2.17) and (4.2.20) will now be used to derive the expected failure load, $(\sigma_o)\alpha$, as a function of the material property, G_1.

For a large plate with a central crack of length 2a, loaded by some far field stresses as $\sigma^{\infty}_{yy} = \sigma_o$ and $\sigma^{\infty}_{xx} = \alpha\sigma_o$, the stress at failure denoted by $(\sigma_o)\alpha$, can be obtained from equation (4.2.10) as

$$(\sigma_o)\alpha = \sqrt{\frac{16\ G_1}{\pi a(\kappa+\alpha\kappa+3-\alpha)}}, \text{----------(4.3.8)}$$

Writing $\kappa = 3 - 4\nu$ for plane strain, $(3-\nu)/(1+\nu)$ for plane stress and $\mu = E/2(1+\nu)$, equation (4.3.8) can be reduced to

$$(\sigma_o)\alpha = \sqrt{\frac{4E\ G_1}{\pi a(3+\alpha+\nu-\alpha\nu)}}, \text{----------(4.3.9)}$$

for plane stress and

$$(\sigma_o)\alpha = \sqrt{\frac{4E\ G_1}{\pi a(1+\nu)(3+\alpha-2\nu-2\nu\alpha)}}, \text{------(4.3.10)}$$

for plane strain. It should be noted that in equations (4.3.1) to (4.3.7), we used $(\sigma_o)_\alpha = 1 = \sigma_o$ at failure.

Taking the ratios of equations (4.3.9) and (4.3.6), (4.3.10) and (4.3.7), one obtains,

$$\frac{(\sigma_o)_\alpha}{\sigma_o} = \frac{2}{\sqrt{3+\alpha+\nu-\alpha\nu}}, \text{----------(4.3.11)}$$

for plane stress and

$$\frac{(\sigma_o)_\alpha}{\sigma_o} = 2\sqrt{\frac{(1-\nu)}{3+\alpha-2\nu-2\nu\alpha}}, \text{----------(4.3.12)}$$

for plane strain. The plots of equations (4.3.11) and (4.3.12) with $\nu = .3$ are shown in Fig.13. The important implication of equations (4.3.11) and (4.3.12) as can be seen from Fig.13, is that for biaxial loading with $\alpha > 1$, we expect the failure load to be slightly lower than the failure load for $\alpha = 1$ while for $\alpha < 1$, the failure load is higher.

If the large plate with a straight central crack of length 2a, was subjected to some pressure loading, then the applied pressure at failure, $\sigma_o{}^p$ can be obtained from equation (4.2.17), as

$$\sigma_o{}^p = \sqrt{\frac{16\mu\ G_1}{\pi a(\kappa+3)}}, \text{----------(4.3.13)}$$

If on the other hand the large plate with a straight central crack of length 2a, was subjected to known pressure loading and unknown far field tensile loadings, then from equation (4.2.20) one can obtain the far field applied stress at failure, σ_o as

$$\sigma_o = \frac{K_1^p}{2\sqrt{\pi a}}\sqrt{[1+\frac{\kappa+3}{\kappa+\alpha\kappa+3-\alpha}]^2+4[\frac{16\mu\ G_1}{(K_1^p)^2(\kappa+\alpha\kappa+3-\alpha)}-\frac{\kappa+3}{\kappa+\alpha\kappa+3-\alpha}]}$$

$$-\frac{K_1^p}{2\sqrt{\pi a}}[1+\frac{\kappa+3}{\kappa+\alpha\kappa+3-\alpha}], \text{----------(4.3.14)}$$

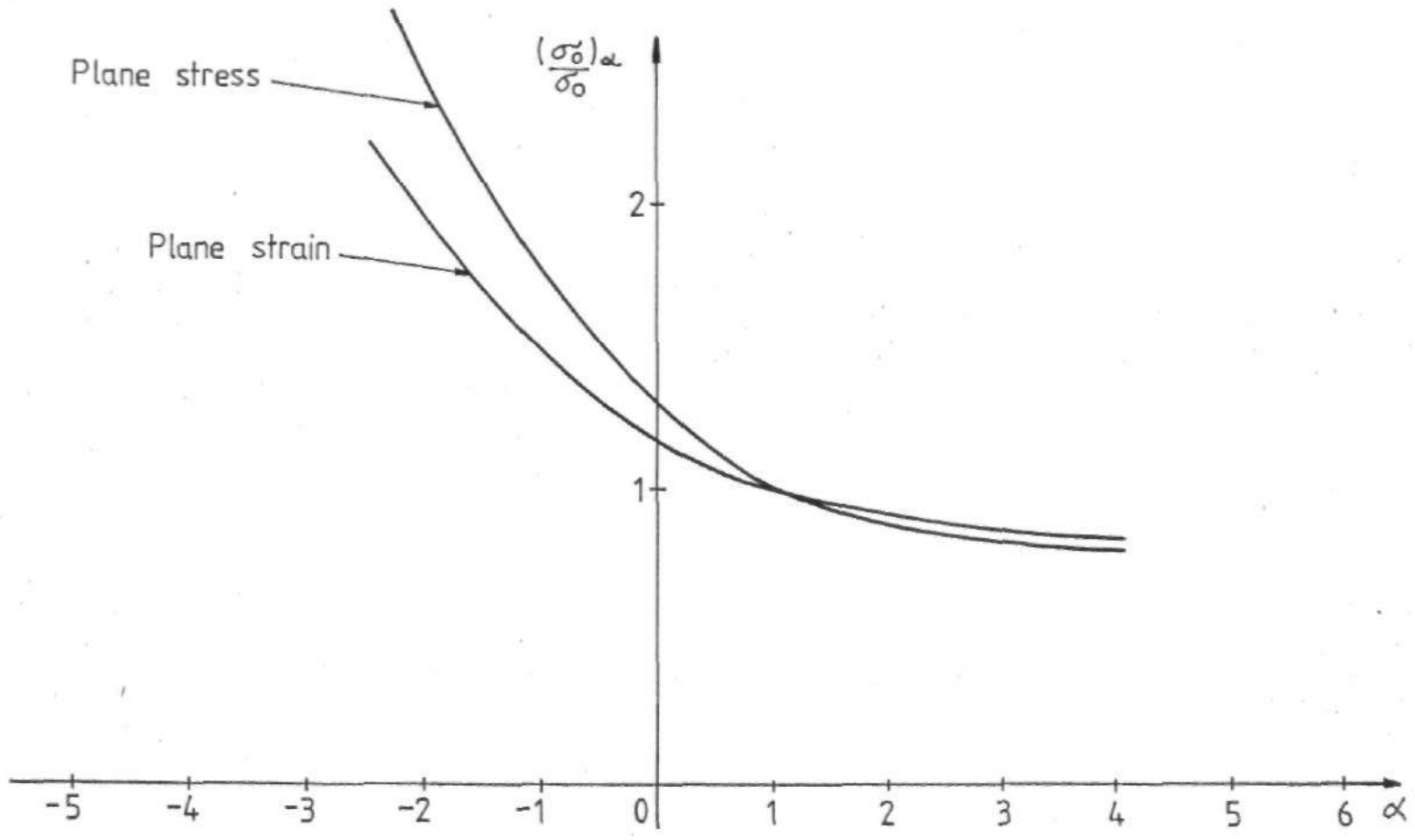


FIG .13. The plot of $(\sigma_\theta)_\alpha/\sigma_0$ against α for $\nu = .3$

where K_1^p is the stress intensity factor due to the pressure loading.

It should be noted that in all the above equations for the failure stress, equations (4.3.6) to (4.3.14), a constant $G = G_1$ appears. The constant G_1 or G is the strain energy-release rate and is a material property similar to Young's modulus, Poisson's ratio, etc. Some detailed discussions about how it can be determined experimentally, can be obtained in Heyer (1973), and Wheeler et al (1982).

From the above equations, therefore, one can conclude that when the Griffith criterion is applied correctly, the failure load for a cracked member can be predicted. The prediction is in terms of a material property, the strain energy-release rate. These predicted failure loads are functions or depend on the nature of loading.

In the next section a new crack-tip parameter which is also a material property is introduced. It is called the Irwin crack-tip parameter because of its similarity to Irwin's G.

4.4. The New Irwin Crack-Tip Characterizing Parameter

In the discussions above, the material property or the crack-tip ch acterizing parameter introduced is the strain energy-release rate, G or G_1. For all the stress states derived in Chapter III, these stresses are in terms of the stress intensity factor K_1. But from equations (4.3.8) to (4.3.13), all the stresses in equations (3.2.19) to (3.2.67) can be written as

$$\sigma_{ij} = \left[\frac{16\mu\, G_1}{\kappa+\alpha\kappa+3-\alpha}\right]^2 \frac{f_{ij}(\alpha,\theta)}{\sqrt{2\pi r}}, \quad \text{----------(4.4.1)}$$

where i,j = 1,2, r,θ are polar coordinates at the crack-tip, α is the biaxiallity coefficient and $f_{ij}(\alpha,\theta)$ are some functions of α,θ which can be obtained from equations (3.2.19) to (3.2.67) for a particular problem under consideration. From equation (4.4.1), since the stresses must at all times be real quantities then μ, G_1 and $(\kappa+\alpha\kappa+3-\alpha)$ must be real and positive. These conditions are satisfied by all those parameters. It should be noted that there are some values of α for which

$$\kappa+\alpha\kappa+3-\alpha \leq 0, \quad \text{----------(4.4.2)}$$

That is quite meaningful,for it refers to the cases where the crack cannot propagate but will tend to 'close'. It has its own different analysis which is not the subject of the present discussions.

It is a common practice to characterize the stress state by what Irwin (1957) termed the stress intensity factor instead of the energy-base parameter. He defined the parameters by equations (1.3.1) and (1.3.2). It was accepted by many researchers that crack-tip characterization via the strain energy-release rate is equivalent to crack-tip characterization via the stress intensity factor approach. As it was showr in Section 4.2 that any stress state has its own unique expression of the strain energy-release rate and that the stress intensity factor is not effected by a far field applied stress parallel to the crack, then one can easily conclude that crack-tip characterization via the strain energy-release rate is not equivalent to

crack-tip characterization via the stress intensity factor approach.

For the purpose of introducing a new crack-tip parameter, which is equivalent to the strain energy-release rate characterization, the solutions for some problems discussed in Chapter III will be employed, in addition to the Griffith criterion.

The new parameter, termed Irwin crack-tip characterizing parameter , denoted by I (after Irwin) can also be classified into the three different modes of failure. Similar to the stress intensity factor, Irwin (1957), the Irwin crack-tip parameter for mode I, denoted by I_1 is associated with opening at the crack-tip associated to opening mode loadings, σ_{xx}, σ_{yy}. The mode II Irwin parameter, denoted by I_{11} is associated with opening at the crack-tip due to in-plane shear loading, τ_{xy}. And the mode III Irwin parameter, denoted by I_{111} is associated with out of plane shear loading, τ_{yz}. See Fig. 1.

In mathematical form, these parameters are defined as

$$I_1 = \lim_{\substack{r\to o \\ \theta=\pi}} 2\mu v(r,\theta)\sqrt{\frac{2\pi}{r}}, \quad \text{----------(4.4.3)}$$

for the opening mode problems,

$$I_{11} = \lim_{\substack{r\to o \\ \theta=\pi}} 2\mu u(r,\theta)\sqrt{\frac{2\pi}{r}}, \quad \text{----------(4.4.4)}$$

for the in-plane shear problems and

$$I_{111} = \lim_{\substack{r\to o \\ \theta=\pi}} 2\mu w(r,\theta)\sqrt{\frac{2\pi}{r}}, \quad \text{----------(4.4.5)}$$

for the out of plane shear problems.

As examples, the definition above, equation (4.4.3) is applied to some of the problems discussed in Chapter III, and the following expressions for the Irwin parameter I_1 are obtained: For a large plate with a central crack of length 2a, loaded by $\sigma^{\infty}_{yy} = \sigma_o$ and $\sigma^{\infty}_{xx} = \alpha\sigma_o$, the Irwin parameter, I_1 from equations (4.4.3) and (3.2.23) is obtained as

$$I_1 = \frac{(\kappa+\alpha\kappa+3-\alpha)}{2} K_1, \quad \text{----------(4.4.6)}$$

For the same plate as above but loaded by $\sigma^{\infty}_{yy} = 0$, $\sigma^{\infty}_{xx} = \sigma_o$, from equations (4.4.3) and (3.2.47) one obtains

$$I_1 = \frac{(\kappa-1)}{2} K_1, \quad \text{----------(4.4.7)}$$

Similarly, if the plate is loaded by pressure loading, $\sigma_o{}^p$ along the crack faces, then from equations (4.4.3) and (3.2.64) one obtains

$$I_1 = \frac{(\kappa+3)}{2} K_1^p, \quad \text{----------(4.4.8)}$$

From equations (4.2.10), (4.2.14), (4.2.17) and (4.4.6) to (4.4.8), one can observe that

$$G_1 = \frac{K_1 I_1}{c\mu}, \quad \text{----------(4.4.9)}$$

where c is a numerical constant, μ is the shear modulus, K_1 is the model stress intensity factor, I_1 is the model Irwin parameter and G or G_1 is the strain energy-release rate. Furthermore, all the stress and displacement distributions in Chapter III can be written as

$$\sigma_{ij} = \left[\frac{I_1}{\kappa+\alpha\kappa+3-\alpha}\right] \frac{f_{ij}(\alpha,\theta)}{\sqrt{2\pi r}}, \quad \text{---------(4.4.10)}$$

and

$$u_i = I_1 \sqrt{\frac{r}{2\pi}}\ h_i(\alpha,\theta), \text{ ----------(4.4.11)}$$

where ij = 1,2, $\sigma_{11} = \sigma_{xx}$, $\sigma_{21} = \sigma_{12} = \tau_{xy}$, $\sigma_{22} = \sigma_{yy}$, $u_1 = u$, $u_2 = v$, $f_{ij}(\alpha,\theta)$ and $h_i(\alpha,\theta)$ are some functions of α,θ which can be found from Chapter III.

For all cases, the new Irwin crack-tip parameter, I is a function of the biaxial loading, the crack length, the applied stress and an elastic constant. For example,

$$I = I(\alpha, a, \sigma_o, \nu), \text{ ----------(4.4.12)}$$

It has the unit of Newtons/metre$^{\frac{1}{2}}$

with the new Irwin parameter, I and the Griffith criterion of failure, one can easily obtain

$$I_{applied} = I_{critical}, \text{ ----------(4.4.13)}$$

at crack propagation, where $I_{critical}$ is a material property.

For the mode I problems, one can write equation (4.4.13) as

$$I_{1_{applied}} = I_{1_{critical}}, \text{ ---------(4.4.14)}$$

where again $I_{1_{critical}}$ is a material property which can be determined experimentally. Since the material properties are commonly found from uniaxial tests, equations (4.4.6) and (4.4.14), one can obtain $I_{1_{critical}}$ in terms of K_{1c} as

$$I_{1_{critical}} = \frac{(\kappa+3)}{2} K_{1c}, \text{ ----------(4.4.15)}$$

where $\kappa = 3-4\nu$ for plane strain and $(3-\nu)/(1+\nu)$ for plane strain and K_{1c} is the critical stress intensity

factor to be determined by experimenting on a uni-axially loaded cracked member, as discussed in Heyer (1973) and Wheel et al (1982).

Then the Griffith criterion based on the I-concept, reads

$$2I_{applied} = (\kappa+3)\, K_{1c}, \quad \text{----------(4.4.16)}$$

where $K_{1c} = \sigma_o\sqrt{\pi a}$ from uniaxial tests only.

Just for the sake of having a non-dimensional crack-tip characterizing parameter, another parameter, denoted by $\bar{I}$ is defined as

$$\bar{I} = I/\sigma_f\sqrt{\sigma_f/\rho g}, \quad \text{----------(4.4.17)}$$

where σ_f is the yield stress of the material, ρ is its density and g is the acceleration due to gravity. For linear elastic (brittle) materials $\sigma_f = \sigma_y$, the yield strength of the material.

The dimensionless Irwin parameter, $\bar{I}$ can be obtained for the cases considered above as follows: For a large plate with a central crack of length 2a, loaded by $\sigma^{\infty}_{yy} = \sigma_o, \sigma^{\infty}_{xx} = \alpha\sigma_o$, from equations (4.4.17) and (4.4.6) one obtains

$$\bar{I}_1 = \frac{(\kappa+\alpha\kappa+3-\alpha)}{2}\left(\frac{\sigma_o}{\sigma_y}\right)\left[\frac{\pi\rho g a}{\sigma_y}\right]^{\frac{1}{2}}, \quad \text{--------(4.4.18)}$$

When the plate is loaded by $\sigma^{\infty}_{xx} = \sigma_o$ and $\sigma^{\infty}_{yy} = 0$, then equations (4.4.17) and (4.4.7), give

$$\bar{I}_1 = \frac{(\kappa-1)}{2}\left(\frac{\sigma_o}{\sigma_y}\right)\left[\frac{\pi\rho g a}{\sigma_y}\right]^{\frac{1}{2}}, \quad \text{----------(4.4.19)}$$

But when the crack faces are loaded by constant pressure only, then equations (4.4.17) and (4.4.8) give

$$\bar{I}_1 = \frac{\kappa+3}{2}\left(\frac{\sigma_o}{\sigma_y}\right)\left[\frac{\pi\rho g a}{\sigma_y}\right]^{\frac{1}{2}}, \quad \text{----------(4.4.20)}$$

And finally, the Griffith criterion of failure in terms of the non-dimensional Irwin crack-tip parameter, equations (4.4.13) and (4.4.17) give

$$\bar{I}_{applied} = \bar{I}_{critical}, \quad \text{----------(4.4.21)}$$

when the crack propagates, where $\bar{I}_{critical}$ is a dimensionless material property.

4.5. Conclusions

The expressions for the strain energy-release rate, G_1, for a number of loading conditions, were derived. From those expressions, it was observed that crack-tip characterization via the strain energy-release rate concept is not equivalent to crack-tip characterization via the stress intensity factor approach. It has also been observed that the stress intensity factor is not affected by an applied stress parallel to the direction of crack propagation. More importantly, it was proved that a final fracture criterion obtained from the Griffith criterion of failure is a function of loading conditions.

A new crack-tip characterizing parameter, denoted by I with the units of Newtons/metre$^{\frac{1}{2}}$ was introduced. A non-dimensional counterpart of the new Irwin crack-tip parameter was also introduced. A simple relationship between the strain energy-release rate, the stress intensity factor and the new Irwin crack-tip parameter equation (4.4.9), was also derived. With the relationship, it was shown that crack-tip characterization via the new Irwin crack-tip parameter is equivalent to crack-tip characterization via the strain energy-release rate concept.

CHAPTER V

THE J-INTEGRAL

5.1. Introduction

The J-integral is the most recent fracture model used for fracture mechanics problems. In fact, it has been applied not only to linear elastic fracture but also to non-linear elastic and elastic-plastic fracture. Some detailed discussions on the subject can be found in Rice (1968), Atkinson and Eshelby (1968) where the concept was introduced, Begley and Landes (1972) where the J-integral concept was applied to some fracture tests, Budiansky and Rice (1973), Hermans (1981) and Paris (1977) where the concept was interpreted as a crack-tip parameter, Turner (1975), Paris et al (1979) where the J-integral concept was used for developing fracture resistance curves for some metals and Aoki et al (1981) where the J-concept was employed to describe elastic-plastic fracture.

As mentioned earlier, the J-integral was first introduced by Rice (1968) and has been shown to be path-independent around the crack-tip, as follows:

The J-integral around a curve Γ, defined by equation (1.3.5) can also be written as

$$J = \int_{\Gamma} [W\, dy - T_i u_{i,x}\, ds], \quad \text{----------(5.1.1)}$$

where W is the strain energy density, defined as

$$W = \int_{o}^{e} \sigma_{ij}\, de_{ij}, \quad \text{----------(5.1.2)}$$

T_i is the traction vector defined as

$$T_i = \sigma_{ij}\, n_j, \quad \text{----------(5.1.3)}$$

$i,j = 1,2$, $n_1 = n_x$, $n_y = n_2$ are components of a unit vector on the curve Γ. Also, $x = x_1$, $y = x_2$, $u_1 = u$ and $u_2 = v$.

Consider the crack-tip shown in Fig. 14. A closed path is $\Gamma + C_2C_3 + \Gamma_1 + C_4C_1$. Denote the J-integral evaluated around the closed path by J*, i.e.

$$J^* = \int_{\Gamma+S_1+\Gamma_1+S_2} [W\, dy - T_i\, U_{i,x}\, ds], \quad \text{-------(5.1.4)}$$

where S_1 = curve C_2C_3 and S_2 = curve C_4C_1.

But along the crack faces, $dy = 0$ and $T_i = 0$. Therefore the integral along S_1 and S_2 is zero. Equation (5.1.4) then reduces to

$$J^* = \int_{\Gamma+\Gamma_1} [W\, dy - T_i\, u_{i,x}\, ds], \quad \text{---------(5.1.5)}$$

The length integral in equation (5.1.5) can be converted into an area integral by employing Green's formula, as

$$\int_{\Gamma+\Gamma_1} [P\, dx + Q\, dy] = \int_{Ar} [\frac{\partial Q}{\partial x} - \frac{\partial P}{\partial y}] dx\, dy, \quad \text{---(5.1.6)}$$

where Ar is the area enclosed by the curve $\Gamma+\Gamma_1$.

Then with equations (5.1.3) and (5.1.6), equation (5.1.5.) can be written as

$$J^* = \int_{Ar} [\frac{\partial W}{\partial x} - \frac{\partial}{\partial x_j}(\sigma_{ij}\, \frac{\partial u_i}{\partial x}] dx\, dy, \quad \text{-----(5.1.7)}$$

Differentiating equation (5.1.2), one obtains

$$\frac{\partial W}{\partial x} = \frac{\partial W}{\partial e_{ij}}\, \frac{\partial e_{ij}}{\partial x} = \sigma_{ij}\, \frac{\partial e_{ij}}{\partial x}. \quad \text{----------(5.1.8)}$$

But

$$e_{ij} = \tfrac{1}{2}[u_{i,j} + u_{j,i}], \quad \text{----------(5.1.9)}$$

From equations (5.1.8) and (5.1.9) one obtains

$$\frac{\partial W}{\partial x} = \sigma_{ij}\, \frac{\partial}{\partial x_j}(\frac{\partial u_i}{\partial x}), \quad \text{----------(5.1.10)}$$

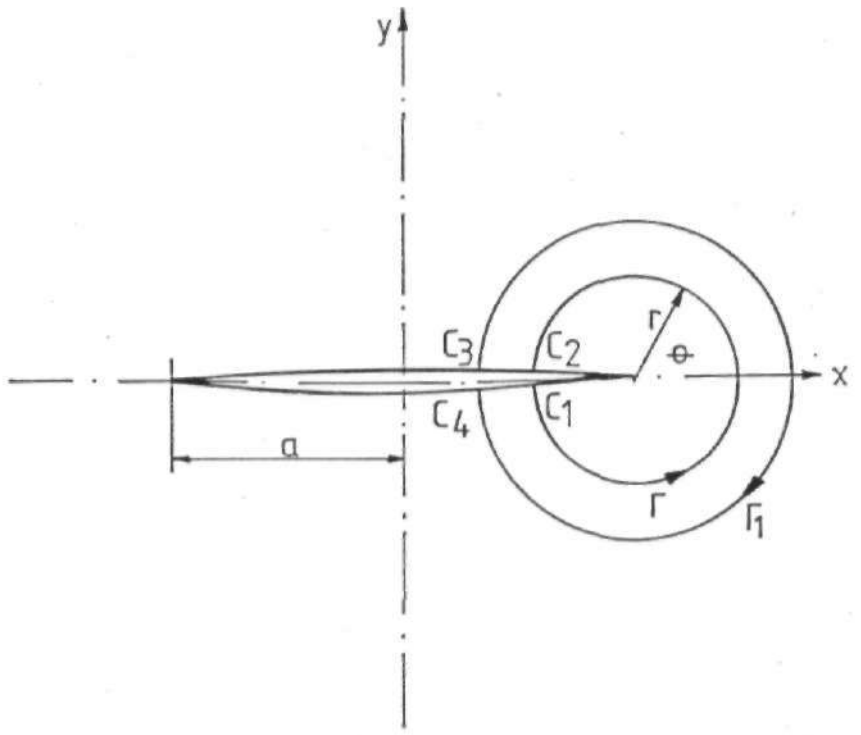


FIG 14: The J-integral evaluation for a crack in a large plate .

The equilibrium condition states

$$\frac{\partial \sigma_{ij}}{\partial X_j} = 0, \quad \text{----------(5.1.11)}$$

Therefore, equation (5.1.10) can also be written as

$$\frac{\partial W}{\partial x} = \frac{\partial}{\partial x_j}(\sigma_{ij} \frac{\partial u_j}{\partial x}), \quad \text{----------(5.1.12)}$$

Then from equation (5.1.7), we get

$$J^* = 0 \text{ .----------(5.1.13)}$$

Therefore, equation (5.1.5) implies that

$$\int_{\Gamma}[W\, dy - T_i\, u_{i,x}\, ds] = -\int_{\Gamma_1}[W\, dy - T_i\, u_{i,x}\, ds], \text{--(5.1.14)}$$

which means that, the J-integral can be evaluated around any curve around the crack-tip and the result will be independent of the choice of the path.

For the linear elastic case that we are interested in, in this report, equation (5.1.2) reduces to

$$W = \frac{1}{2E}[\sigma_{xx}^2+\sigma_{yy}^2-2\nu\sigma_{xx}\sigma_{yy}+2(1+\nu)\tau_{xy}^2], \quad \text{-----(5.1.15)}$$

Equation (5.1.15) is for the case of plane stress.

Based on the fact that the J-integral evaluated around a crack-tip is path independent, many researchers accepted it as a crack-tip characterizing parameter and that equal J- means equal intensities of the surrounding deformatio· fields of identical form for a given material. In fact, it has been interpreted by Begley and Landes (1972), Budiansky and Rice (1973), Hermans (1981), Paris (1977) and Rice (1968) as the rate of charge of the potential energy at the crack-tip. Furthermore, these authors, interpreted the J-integral method of crack-tip characterization as a universal concept that can be used to describe cracking behaviour for linear

elastic (brittle) materials, non-linear elastic materials and elastic-plastic materials, etc.

Begley and Landes (1972) were the first researchers to report some experimental results based on the J-integral analysis of Rice (1968). They introduced interesting techniques for the determination of the material property $J_{critical}$. To date, many researchers use the J-model not only for $J_{critical}$ determination but also for obtaining complete J-R resistance curves and instability analyses. These can be found in Turner (1975) and Paris et al (1979) and some of the references appended to these papers.

This thesis, as already mentioned earlier, deals with linear elastic (brittle) fracture; a class of fracture which the J-model has to satisfy before it can be applied to any other class of fracture. We intend to make some detailed studies on the J-integral by viewing the new stress and displacement fields at a crack-tip with some appropriate rationale, similar to what we did for the strain energy-release rate model, Chapter IV. Some discussions will then follow on the relationship between the J- and the G- models. In general, we will be interested to find whether the J-model is equal to the G-model discussed in Chapter IV.

It should be noted that the J-integral was evaluated in Section 1.3 for a case where the correct solution was known even before the new formulae (Chapters II and III) were derived. These solutions are given by equations (1.2.1) with A = 0 which are

equivalent to equations (3.2.19) to (3.2.23) with $\alpha = 1$. It represents the problem of a large plate with a central crack of length 2a, loaded by far field equal biaxial tension. In Section 1.3, after evaluating the J-integral and the strain energy-release rate, it was found that they are not equal. The author would like to consider some other problems for the purpose of arriving to a general conclusion.

5.2. Evaluation of the J-Integral

The J-integral, as mentioned earlier, has been interpreted by many researchers as the potential energy-release rate for an advancing crack. Here, it is not assumed to be that, until it has been proved to be so. It is intended to evaluate the J-integral defined by equation (5.1.1) for a number of problems. Just for comparison purpose, the J-integral will be evaluated for the problems for which the strain energy-release rate, G_1, was evaluated in Chapter IV.

First, consider the problem solved in Chapter III, in which a large plate with a central crack of length 2a, is subjected to $\sigma^{\infty}_{yy} = \sigma_o$, $\sigma^{\infty}_{xx} = \alpha\sigma_o$, where $-\infty < \alpha < \infty$. The stresses and displacements in the neighbourhood of the crack-tip $x = +a$, are given by equations (3.2.19) to (3.2.23). These equations can be written as

$$\sigma_{yy} = \frac{K_1}{\sqrt{2\pi r}}\left[\cos\tfrac{1}{2}\theta + \frac{1+\alpha}{4}\sin\theta\sin\tfrac{3}{2}\theta\right],$$

$$\sigma_{xx} = \frac{K_1}{\sqrt{2\pi r}}\left[\alpha\cos\tfrac{1}{2}\theta - \frac{1+\alpha}{4}\sin\theta\sin\tfrac{3}{2}\theta\right],\}\text{---(5.2.1)}$$

$$\tau_{xy} = \frac{K_1}{\sqrt{2\pi r}}\left[\frac{1+\alpha}{4}\sin\theta\cos\tfrac{3}{2}\theta - \frac{(1-\alpha)}{2}\sin\tfrac{1}{2}\theta\right],$$

and

$$u = \frac{K_1}{8\mu}\sqrt{\frac{r}{2\pi}}[(2\kappa+2\alpha\kappa-5+3\alpha)\text{Cos}\ \tfrac{1}{2}\theta-(1+\alpha)\text{Cos}\ \tfrac{3}{2}\theta],$$

$$v = \frac{K_1}{8\mu}\sqrt{\frac{r}{2\pi}}[(2\kappa+2\alpha\kappa+5-3\alpha)\text{Cos}\ \tfrac{1}{2}\theta-(1+\alpha)\text{Sin}\ \tfrac{3}{2}\theta] \quad \}\text{---(5.2.2)}$$

Furthermore, from Fig.14, by considering the circular path Γ, one can write

$$x = a + r\ \text{Cos}\ \theta, \quad \text{----------(5.2.3)}$$

$$y = r\ \text{Sin}\ \theta, \quad \text{----------(5.2.4)}$$

$$n_x = \text{Cos}\ \theta, \quad \text{----------(5.2.5)}$$

and $$n_y = \text{Sin}\ \theta. \quad \text{----------(5.2.6)}$$

Equation (5.1.3) gives the fraction vectors as

$$T_1 = \sigma_{xx}\, n_x + \tau_{xy}\, n_y, \quad \text{----------(5.2.7)}$$

and

$$T_2 = \sigma_{yy}\, n_y + \tau_{xy}\, n_x, \quad \text{----------(5.2.8)}$$

With equations (5.2.1), the strain energy-density, W, defined in equation (5.1.15) becomes

$$W = \frac{K_1^2}{4\pi Er}[1+\alpha^2-2\nu\alpha)\text{Cos}^2\ \tfrac{1}{2}\theta+\frac{(1+\alpha)^2(1+\nu)}{8}\text{Sin}^2\theta$$

$$+\frac{(1-\alpha^2)(1+\nu)}{2}\text{Sin}^2\theta+\frac{(1-\alpha)^2(1+\nu)}{2}\text{Sin}^2\ \tfrac{1}{2}\theta], \quad \text{---(5.2.9)}$$

From equations (5.2.5) and (5.2.9), one can get

$$W\, n_x = \frac{K_1^2}{4\pi Er}[(1+\alpha^2-2\nu\alpha)(2\ \text{Cos}^4\ \tfrac{1}{2}\theta-\text{Cos}^2\ \tfrac{1}{2}\theta)$$

$$+\frac{(1+\alpha)^2(1+\nu)}{8}\text{Sin}^2\theta\ \text{Cos}\ \theta+\frac{(1-\alpha^2)(1+\nu)}{2}\text{Sin}^2\theta\ \text{Cos}\ \theta$$

$$+\frac{(1-\alpha)^2(1+\nu)}{2}(\text{Sin}^2\ \tfrac{1}{2}\theta-2\ \text{Sin}^4\ \tfrac{1}{2}\theta)], \quad \text{--------(5.2.10)}$$

Also, substituting equations (5.2.1), (5.2.5) and (5.2.6), the traction vectors are obtained as (equations (5.2.7) and (5.2.8)),

$$T_1 = \frac{K_1}{\sqrt{2\pi r}}[\alpha\ \text{Cos}\ \tfrac{1}{2}\theta\ \text{Cos}\ \theta-\frac{(3-\alpha)}{4}\text{Sin}\ \tfrac{1}{2}\theta\ \text{Sin}\ \theta], \text{-(5.2.11)}$$

and

$$T_2 = \frac{K_1}{\sqrt{2\pi r}}[\frac{5+\alpha}{4}\ \text{Cos}\ \tfrac{1}{2}\theta\ \text{Sin}\ \theta-\frac{(1-\alpha)}{4}\text{Sin}\ \tfrac{1}{2}\theta\ \text{Cos}\ \theta], \text{-(5.2.12)}$$

The rate of change with respect to x of the displacements u and v, from equations (5.2.2) are obtained as

$$u_{,x} = \frac{K_1}{8\mu\sqrt{2\pi r}}[(\kappa+\alpha\kappa-3+\alpha)\cos\tfrac{1}{2}\theta-(1+\alpha)\sin\theta\sin\tfrac{3}{2}\theta], \text{---(5.2.13)}$$

and

$$v_{,x} = -\frac{K_1}{8\mu\sqrt{2\pi r}}[(\kappa+\alpha\kappa+3-\alpha)\sin\tfrac{1}{2}\theta-(1+\alpha)\sin\tfrac{3}{2}\theta]. \text{---(5.2.14)}$$

From equations (5.2.11) to (5.2.14), one obtains the sum of $T_1 u_{,x}$ and $T_2 v_{,x}$ as

$$T_1 u_{,x}+T_2 v_{,x} = \frac{+K_1^2}{32\pi\mu r}[\alpha(\kappa+\alpha\kappa-3+\alpha)(\cos^2\theta+\cos\theta)$$

$$+(1-\alpha)(\kappa+\alpha\kappa+3-\alpha)(\sin^2\tfrac{1}{2}\theta-2\sin^4\tfrac{1}{2}\theta)-\frac{(4\kappa+4\alpha\kappa+3-2\alpha-\alpha^2)}{2}\sin^2\theta$$

$$-\frac{\alpha(1+\alpha)}{2}(\cos^2\tfrac{1}{2}\theta-\cos\tfrac{1}{2}\theta\cos\tfrac{7}{2}\theta)-\frac{(1-\alpha)(1+\alpha)}{4}(\sin^2\tfrac{1}{2}\theta+\sin\tfrac{1}{2}\theta\sin\tfrac{7}{2}\theta)$$

$$+\frac{(3-\alpha)(1+\alpha)}{8}(\cos^2\tfrac{1}{2}\theta-\cos\tfrac{1}{2}\theta\cos\tfrac{5}{2}\theta-\cos\tfrac{1}{2}\theta\cos\tfrac{3}{2}\theta+\cos\tfrac{3}{2}\theta\cos\tfrac{5}{2}\theta)$$

$$+\frac{(5+\alpha)(1+\alpha)}{8}(\sin\tfrac{1}{2}\theta\sin\tfrac{5}{2}\theta-\sin^2\tfrac{1}{2}\theta-\sin\tfrac{1}{2}\theta\sin\tfrac{3}{2}\theta+\sin\tfrac{3}{2}\theta\sin\tfrac{5}{2}\theta)],$$

--------(5.2.15)

Finally, with equation (5.1.1) written as

$$J = \int_{-\pi}^{\pi}[W n_x - (T_1 u_{,x} + T_2 v_{,x})]\, r\, d\theta, \text{---(5.2.16)}$$

and substituting equations (5.2.10) and (5.2.15) into equation (5.2.16), one obtains, after the integration,

$$J = \frac{(3+2\alpha-\alpha^2)}{4}\frac{K_1^2}{E}, \text{----------(5.2.17)}$$

It should be noted that all the above derivations are for plane stress. The J-integral around the crack-tip x = +a, for the plane strain, can be obtained by replacing E by $E/(1-\nu^2)$. Refer to Appendix B for the algebra.

So far, all the above lengthy calculations were on the circular curve Γ, Fig.14, not including the crack-

faces, y = ±0. Let us investigate what value the J-integral could take when evaluated along the crack faces. Still as shown in Fig.14, a curve of radius r is considered. The J-integral in equation (5.1.1) can also be written as

$$J = \int_{S_1+S_2} [(W - \sigma_{xx} u_{,x} - \tau_{xy} v_{,x})dy - (\tau_{xy} u_{,x} + \sigma_{yy} v_{,x})dx], \quad \text{---------(5.2.18)}$$

On the crack faces,

$$dy = 0, \quad \text{----------(5.2.19)}$$

and from equation (5.2.3)

$$x = a - r, \quad \text{----------(5.2.20)}$$

which means,

$$dx = - dr, \quad \text{----------(5.2.21)}$$

then equation (5.2.18) simplifies to

$$J = \int_{S_1+S_2} [\tau_{xy} u_{,x} + \sigma_{yy} v_{,x}]dn, \quad \text{----(5.2.22)}$$

From the problem defined by equation (3.2.1), along the crack faces and for - a ≤ x ≤ a, we obtained

$$\sigma_{yy} = 0, \quad \text{----------(5.2.23)}$$

and from the new formulae, equation (2.3.10), gives the displacement u, along the crack faces as,

$$2\mu u = (\kappa - N) \text{ Re } \phi. \quad \text{---------(5.2.24)}$$

Differentiating equation (5.2.24) with respect to x, one obtains

$$2\mu u_{,x} = (\kappa - N) \text{ Re } \phi', \quad \text{------(5.2.25)}$$

Then from equations (3.2.7) and 5.2.25), along the crack faces, y = ±0, - a ≤ x ≤ a, one obtains

$$2\mu u_{,x} = 0. \quad \text{----------(5.2.26)}$$

Therefore, from equations(5.2.26) and (5.2.23), one concludes that equation (5.2.22) gives nothing after integration, This implies that the J-integral is always zero along the crack faces, for which a general proof was derived in Section 5.1.

The derivation of the J-integral from the first principle, as shown above, seems to be very lengthy. Fortunately, Budiansky and Rice (1973) have developed a complex representation of the J-integral. They developed it in terms of the two complex functions $\phi(z)$ and $\chi(z)$ which appear in the Kolosov-Muskhelishvili equations. Budiansky and Rice (1973) reduced equation (5.1.1) to

$$J = \frac{2}{E} \operatorname{Im}\{ \int_{C_1}^{C_2} [(\phi')^2 + 2\phi'\chi']dz + [\bar{z}(\phi')^2]_{C_1}^{C_2} \}, \quad --(5.2.27)$$

Equation (5.2.27) is for plane stress. Now, similar to the new formulae, Chapter II, the J-integral, can also be written in terms of one complex function, $\phi(z) = \phi$, as

$$J = \frac{2}{E} \operatorname{Im}\{ \int_{C_1}^{C_2} [(2N-1)(\phi')^2 - 2z\,\phi'\phi'']dz + [\bar{z}(\phi')^2]_{C_1}^{C_2} \}, \quad -(5.2.28)$$

where $N = (3-\alpha)/(1+\alpha)$ with α as the biaxiality factor to be determined from the far field boundary conditions of a particular problem. The points C_1 and C_2 are as shown in Fig.14.

For all further evaluation of the J-integral, equation (5.2.28) is used instead of equation (5.2.1). Let us first of all reconsider the problem discussed above. The problem is that of an infinite plate with

a central crack of length 2a, loaded by $\sigma^{\infty}_{yy} = \sigma_o$ and $\sigma^{\infty}_{xx} = \alpha\sigma_o$. From Chapter III, for the problem, we have

$$\phi_1 = \frac{\sigma_o}{1+N}\sqrt{z^2 - a^2}\,, \text{----------(5.2.29)}$$

Then equation (5.2.28) and Fig. 6 give

$$J = \frac{2}{E}\,\mathrm{Im}\left[\frac{(2N-1)}{(1+N)^2}\ \frac{\sigma_o^2\, a}{2}\ln\frac{z-a}{z+a} + \frac{\sigma_o^2\, a}{2(1+N)^2}\ln\frac{z-a}{z+a}\right]_{C_1}^{C_2}, \text{---(5.2.30)}$$

or

$$J = \frac{4N}{(1+N)^2}\ \frac{K_1^2}{E}\,, \text{----------(5.2.31)}$$

With $N = (3-\alpha)/(1+\alpha)$, equations (5.2.31) and (5.2.17) are the same.

Next, let us consider evaluating the J-integral for a large plate with a central crack of length 2a, loaded by $\sigma^{\infty}_{xx} = \sigma_o$ and $\sigma^{\infty}_{yy} = 0$. The problem was discussed in Chapter III, equations (3.2.42) to (3.2.52). From equation (5.2.28), the solutions of the problem in Chapter III and Fig.14, one arrives at a J value of

$$J = -\tfrac{1}{2}\,\frac{K_1^2}{E}\,, \text{----------(5.2.32)}$$

Finally, consider the problem of a large plate, subjected to some pressure loading, $\sigma_o{}^P$. The problem was again solved in Chapter III, equations (3.2.54) to (3.2.67). Then from equation (5.2.28), solutions of the problem solved in Chapter III and Fig.14, one obtains

$$J = \frac{2}{E}\,\mathrm{Im}\left[\tfrac{5}{32}(\sigma_o{}^P)^2 a\ln\frac{z-a}{z+a} + \frac{(\sigma_o{}^P)^2 a}{32}\ln\frac{z-a}{z+a}\right]_{C_1}^{C_2}, \text{---(5.2.33)}$$

or

$$J = \tfrac{1}{4}\ \frac{(K_1^P)^2}{E}\,, \text{----------(5.2.34)}$$

where $K_1^P = \sigma_o{}^P\sqrt{\pi a}$, is the stress intensity factor due to pressure loading.

The results of the evaluations above will, in the next section, be studied very critically. In particular, an attempt to use the J-integral as a crack-tip parameter will be presented and the equality of the J-integral and the strain energy-release rate will also be tested.

5.3. Some Discussion On the J-Integral

Let the discussions begin with comparing the expressions of the J-integral and the strain energy-release rate. For a large plate with a central crack of length 2a, loaded by $\sigma^{\infty}_{yy} = \sigma_o$ and $\sigma^{\infty}_{xx} = \alpha\sigma_o$, at the crack-tip x = a, from equations (5.2.17) and (4.2.10), for plane stress, one obtains

$$J = \frac{K_1^2}{4E}\,[3 + 2\alpha - \alpha^2],$$

and

$$G_1 = \frac{K_1^2}{4E}\,[\frac{3+\nu+(1-\nu)\alpha}{2}]\,\}, \text{--------} \text{---(5.3.1)}$$

The plot of the dimensionless J and G_1 for $\nu = .3$ are shown in Fig.15. Clearly from equations (5.3.1) and Fig.15, the J-integral equivalent to the first of equation (5.3.1) and the strain energy-release rate represented by G_1, are not equal. From Fig.15, only for $\alpha = -.7$ and $\alpha = 2.3$ that the J and the G_1 are equal but for these cases, one obtains, at the crack-tip x = -a, $J = -\ G_1$ and therefore the J and the G_1 are not equal.

Secondly, consider the problem of a large plate with a central crack of length 2a, loaded by $\sigma^{\infty}_{xx} = \sigma_o$ and $\sigma^{\infty}_{yy} = 0$. Then from equations (5.2.32) and (4.2.14), one obtains, at the crack-tip x = +a,

$$J = -\ \tfrac{1}{2}\,\frac{K_1^2}{E} \quad \text{and} \quad G_1 = \frac{(1-\nu)}{4}\,\frac{K_1^2}{E} \qquad \text{----(5.3.2)}$$

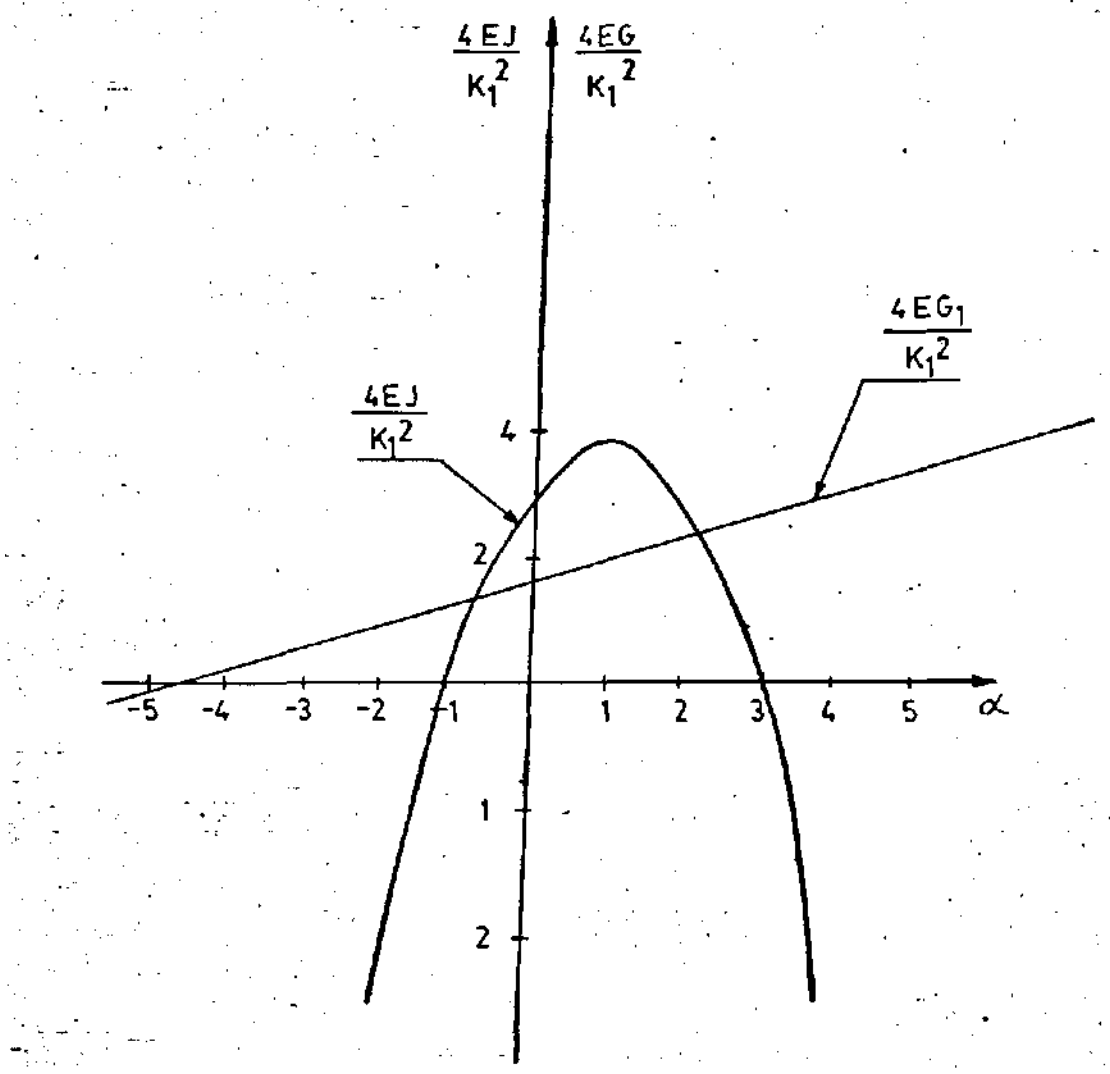


FIG .15: The plots of $\frac{4EJ}{K_1^2}$ and $\frac{4EG1}{K_1^2}$ against α for plane stress, $\nu = .3$.

Equations (5.3.2) are for plane stress. Again, for the same stress intensity factor, the J-integral represented by J and the strain energy-release rate, represented by G_1 are not equal for this problem.

Next, we consider the problem of a large plate with a central crack of length 2a, loaded by constant pressure loading. From equations (5.2.34) and (4.2.17), for the case of plane stress, one obtains

$$J = \frac{3}{4} \frac{(K_1^p)^2}{E},$$

and } ----------(5.3.3)

$$G_1 = \frac{3+\nu}{8} \frac{(K_1^p)^2}{E}$$

Again, equations (5.3.3) indicate that the J-integral is not equal to the strain energy-release rate, G_1.

The three problems considered above, with $-\infty < \alpha < \infty$, represent an infinite number of different problems. It has been shown for all these problems that the J-integral and the strain energy-release rate are not equal. Since for the linear elastic case, the strain energy-release rate and the J-integral are supposed to be the same and equal to the potential energy-release rate for the system, then one of them does not represent the potential energy rate at the crack tip.

In the next paragraphs, the possibility of the J-integral to be another crack-tip parameter (different from the strain energy-release rate) is investigated.

Consider again the problem of infinite plate with a central crack of length 2a, loaded by $\sigma_{yy}^{\infty} = \sigma_o$ and $\sigma_{xx}^{\infty} = \alpha\sigma_o$. If it is assumed that the J is a crack-tip

parameter, then with equation (5,2.17), the stress distribution in the neighbourhood of the crack-tip $x = +a$, from equations (3.2.17) to (3.2.19), can be written as

$$\sigma_{yy} = \left[\frac{4EJ}{3+2\alpha-\alpha^2}\right]^{\frac{1}{2}} \frac{1}{\sqrt{2\pi r}} \left[\text{Cos } \tfrac{1}{2}\theta + \frac{(1+\alpha)}{4} \text{Sin } \theta \text{ Sin } \tfrac{3}{2}\theta\right], \quad \text{---(5.3.4)}$$

$$\sigma_{xx} = \left[\frac{4EJ}{3+2\alpha-\alpha^2}\right]^{\frac{1}{2}} \frac{1}{\sqrt{2\pi r}} \left[\alpha \text{Cos } \tfrac{1}{2}\theta - \frac{(1+\alpha)}{4} \text{Sin } \theta \text{ Sin } \tfrac{3}{2}\theta\right], \text{--(5.3.5)}$$

and

$$\tau_{xy} = \left[\frac{4EJ}{3+2\alpha-\alpha^2}\right]^{\frac{1}{2}} \frac{1}{\sqrt{2\pi r}} \left[\frac{(1+\alpha)}{4} \text{Sin } \theta \text{ Cos } \tfrac{3}{2}\theta - \frac{(1-\alpha)}{2} \text{Sin } \tfrac{1}{2}\theta\right], \quad \text{---(5.3.6)}$$

Similarly, for a large plate with a central crack of length 2a, loaded by $\sigma^{\infty}_{xx} = \sigma_o$ and $\sigma^{\infty}_{yy} = 0$, from equations (5.2.32) and (3.2.48) to (3.2.50), one can write the stress distribution as

$$\sigma_{yy} = \left[-\frac{EJ}{\pi r}\right]^{\frac{1}{2}} \left[\frac{\text{Sin } \theta \text{ Sin } \frac{3}{2}\theta}{4}\right], \quad \text{--------(5.3.7)}$$

$$\sigma_{xx} = \left[-\frac{EJ}{\pi r}\right]^{\frac{1}{2}} \left[\text{Cos } \tfrac{1}{2}\theta - \frac{\text{Sin } \theta \text{ Sin } \frac{3}{2}\theta}{4}\right], \quad \text{-----(5.3.8)}$$

and

$$\tau_{xy} = \left[-\frac{EJ}{\pi r}\right]^{\frac{1}{2}} \left[\frac{\text{Sin } \frac{1}{2}\theta}{2} + \frac{\text{Sin } \theta \text{ Cos } \frac{3}{2}\theta}{2}\right], \quad \text{----(5.3.9)}$$

Now, since J is assumed to be a crack-tip parameter, then assume it to be positive and a material property, similar to the strain energy-release rate, G_1. Then from equations (5.3.4) to (5.3.6) for all $\alpha < 1$ and $\alpha > 3$, and equations (5.3.7) to (5.3.9) the stresses are all complex functions which naturally cannot be possible.

Secondly for $\alpha = -1$ and $\alpha = 3$, the stress distributions in equations (5.3.4) to (5.3.6) are undefined for all J. By considering the physical nature of these problems,

one simply concludes that the J-integral cannot have these values, which may be an indication of limitation of the new model.

Finally, we expect a crack-tip parameter to describe the stress state of a number of different problems uniquely. By considering equations (5.3.4) to (5.3.6), one can easily note that for a constant J value, theere are at least two different values of α which can give the same value of $4EJ/(3+2\alpha-\alpha^2)$. This means that the J-concept does not yield unique stress distributions. These also disprove the assertion that equal J means equal intensity of the surrounding deformation field as far as the new solutions are concerned.

5.4. Conclusions

The J-integral around a crack-tip was shown to be path independent. With the Budiansky and Rice (1973) formulation of the J-integral in terms of two complex functions, the new fornulae introduced in Chapter II and Chapter III were employed, and the J-integral was derived in terms of only one complex potential. The J-integral formulation in terms of only one complex potential was used in the evaluation of J for a number of problems.

After some evaluations and comparisons, it has been shown that the J-integral is not equal to the strain energy-release rate. Since for the linear elastic case, the strain energy rate and the J-integral are supposed to be equal to the total potential energy rate, then one of them is not equal to the potential energy-release rate at the tip of the stationary or moving crack.

By viewing some stress states with the appropriate rationale, the J-integral was shown not to be a possible crack tip parameter, because it does not give unique stress distributions for a number of different problems. Furthermore, the assertion that the crack tip acts as a singularity point and the J is equal to the crack extension force on the singular point seems to be very doubtful because equation (5.2.17) and some other equations in the appendix imply that there are some loading conditions ($\alpha = -1$ and $\alpha = 3$ for example) in which the crack extension force is zero. The conclusions about the J-integral are only based on the new solutions developed and it should be noted that for the αs that yielded non unique J, the solutions used have certain limitations which hopefully would be eliminated in future research works. But the conclusion that the J-integral is not equal to the Irwin's G stands for all α.

CHAPTER VI

EXPERIMENTAL PROGRAMME

6.1. Introduction

This chapter is mainly devoted to experimental results on the centre cracked specimen. The specimens are uniaxially loaded in simple tension with $\sigma^{\infty}_{yy} = \sigma_o$ and $\sigma^{\infty}_{xx} = 0$. Each is of length 2L (in the y direction) width $2b_o$ (in the x-direction) and thickness, t, with a straight central crack of length 2a along the x-axis. See Fig. 16. In these experiments, 2L = 150 mm, 80 mm $\leq 2\,b_o \leq$ 100 mm and 10 mm $\leq 2a \leq$ 20 mm.

The objectives of the experiments are to evaluate some fracture characterizing parameters, such as the critical strain energy-release rate, G_{1c}, the critical Irwin crack tip parameter and the non-dimensional Irwin crack tip parameter for an engineering material. These fracture characterizing parameters are very useful properties in selection and quality assurance of materials. In addition to the fracture characterizing parameters determination, the material was statically characterized.

Before fracture toughness measurements, the analytical expressions of these parameters in terms of the dimensions of the specimen were derived. Then the dimensions of the specimen were recorded and fracture strength, density, loading rate and testing temperature were recorded.

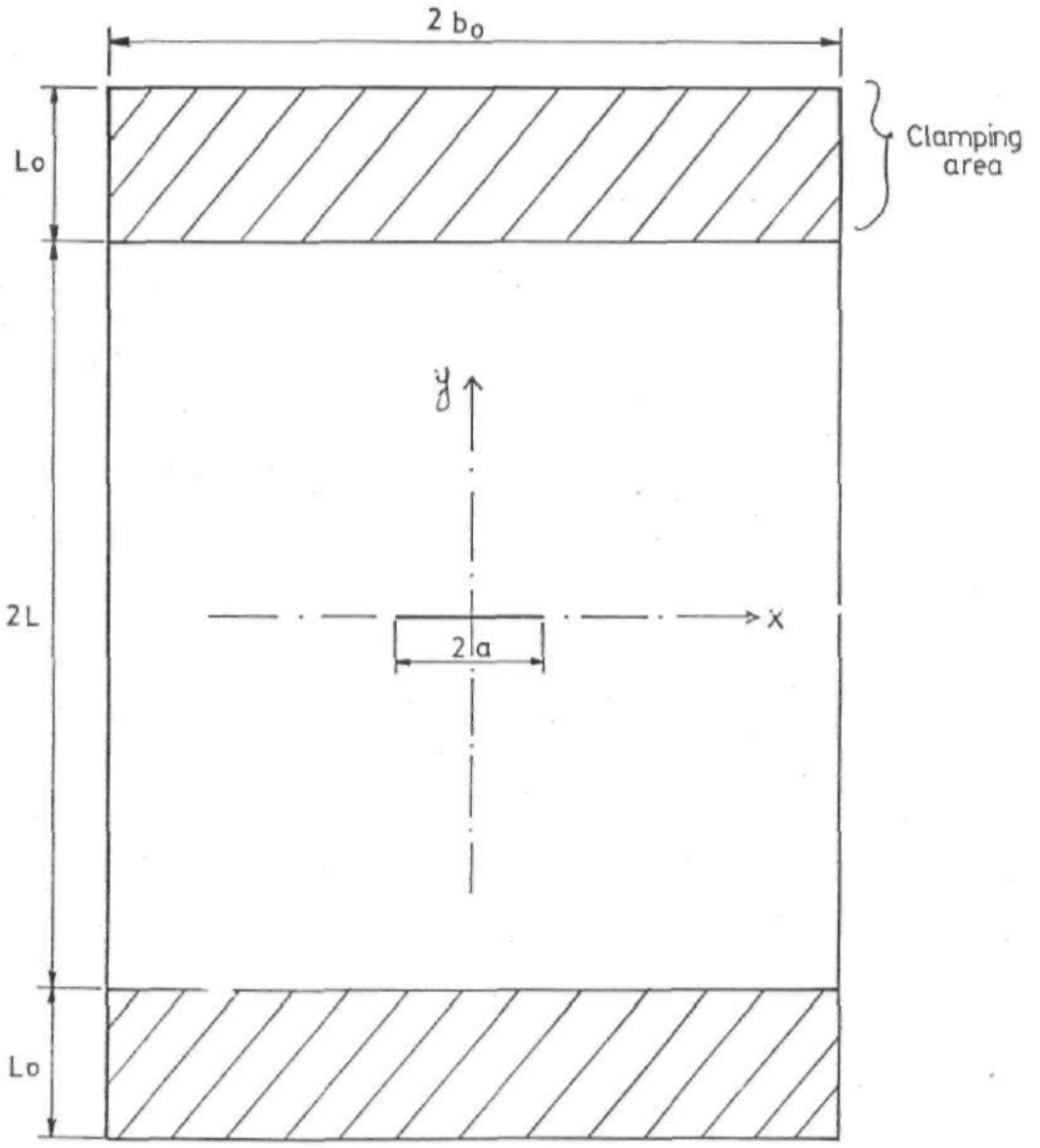


FIG 16: A sketch of the centre cracked specimen .

The sketch of the specimen for the fracture toughness measurements is shown in Fig.16. The formulae derived in Chapter III were used, assuming $\alpha = 0$ and

$$2b \cong \infty$$

$$2b_o \cong \infty$$

Modifications in the analysis are introduced such as to take into account the effect of the finite width of the specimen, on the parameters to be determined.

Considering our initial assumptions for the specimen, from Chapters III and IV, the critical stress intensity factor, K_{1c}, the critical strain energy-release rate, G_{1c}, and the critical Irwin parameter, I_{1c}, can be obtained.

The critical stress intensity factor, K_{1c}, is given by

$$K_{1c} = (\sigma_o)_{max} \sqrt{\pi a} . \quad \text{---(6.1.1)}$$

The critical strain energy-release rate, G_{1c}, from equation (4.2.17), for plane strain is obtained as

$$G_{1c} = \frac{(3-2\nu)(1+\nu)}{4E} K_{1c}^2 . \quad \text{---(6.1.2)}$$

The critical Irwin crack-tip parameter, I_{1c}, from equation (4.4.6) is given by

$$I_{1c} = \frac{(3-2\nu)}{2} K_{1c} , \quad \text{---(6.1.3)}$$

for plane strain. Similarly, from equation (4.4.19), the non-dimensional Irwin parameters $\bar{I}_{1c}$ is obtained as

$$I_{1c} = \frac{(3-2\nu)}{2} \frac{K_{1c}}{K_g} , \quad \text{---(6.1.4)}$$

where K_g is defined as

$$K_g = \sigma_y \sqrt{\sigma_y/\rho g}, \quad \text{----------(6.1.5)}$$

with σ_y as the yield strength of the material, ρ its density and g is the acceleration due to gravity.

As mentioned earlier, equations (6.1.1) to (6.1.4) are for a large plate of infinite extent in all directions.

That condition is not satisfied in the x-direction. Therefore modifications for the finite width of the specimen were introduced. That process is termed 'finite width correction', and the factor introduced is called 'finite width correction factor'. Usually the boundary collacation method is used for finite width corrections.

In this work, a new parameter, employing the complex potentials is introduced. The derivation of the finite width correction factor, Y, by employing the complex potentials and the new formulae, Chapters II and III, is shown below.

For the specimen, from Chapter III, the new formulae can be reduced to,

$$\sigma_{yy} = \text{Re } Z_1 + \tfrac{1}{2} y \text{ Im } Z_1', \quad \text{----------(6.1.6)}$$

$$\sigma_{xx} = -\tfrac{1}{2} \text{ Im } Z_1', \quad \text{----------(6.1.7)}$$

$$\tau_{xy} = \tfrac{1}{2} \text{ Im } Z_1 - y \text{ Re } Z_1', \quad \text{----------(6.1.8)}$$

$$2\mu u = \frac{(\kappa-3)}{4} \text{Re} \int Z_1 dz - \tfrac{1}{2} y \text{ Im } Z_1, \quad \text{-----(6.1.9)}$$

and

$$2\mu v = \frac{(\kappa+3)}{r} \text{Im} \int Z_1 dz - \tfrac{1}{2} y \text{ Re } Z_1, \quad \text{-----(6.1.10)}$$

303013

The complex stress function in equations (6.1.6) to (6.1.10) is assumed as

$$Z_1 = \sigma_o \frac{z}{\sqrt{z^2-a^2}} + \frac{C_m}{z^m\sqrt{z^2-a^2}} \quad \text{----------(6.1.11)}$$

where $\sigma_o = \sigma^{\infty}_{yy}$ the applied stress, C_m are some real constants and m = 0, 1, 2, -----. The stress function in equation (6.1.11) differs from the Westergaard stress function, equation (2.26) by the function

$$\frac{C_m}{z^m\sqrt{z^2-a^2}}.$$

It has the property that, as $z \to \infty$, it goes to zero which implies that for any integer m, it does not add any additional far field stress. Also, along the free crack surfaces, $-a \leq x \leq a$, $y = \pm 0$, it does not introduced any 'normal' stress.

The stress function in equation (6.1.11), similar to the derivation of the new formulae in Chapters Two and Three, was again obtained by employing the Saint-Venant semi-inverse method. Ideally, the method involves the application of trial functions.

For any integer m, the added function, along the x-axis, $y = 0$, $|x| \leq a$ becomes

$$\frac{-iC_m}{x^m\sqrt{a^2-x^2}}$$

since from the new formulae, the normal stresses σ_{yy} and σ_{xx} along the x-axis are of the form

$$\sigma_{xx} - \mathrm{Re}\left[\frac{i\,C_m}{x^m\sqrt{a^2-x^2}}\right], \quad \sigma_{yy} - \mathrm{Re}\left[\frac{i\,C_m}{x^m\sqrt{a^2-x^2}}\right],$$

then these normal stresses are both zero for $|x| \leq a$ for any integer m, as noted above.

Similarly for any integer m, as $z \to \infty$ the added stress function is of the form

$$\frac{C_m}{z^{m+1}} .$$

That means, even for m = 0 and for any other values >0, the added function goes to zero when z goes to infinity. This implies that when $z \to \infty$, the added stress function introduced no stress as again mentioned above.

The constants C_m in equation (6.1.11) are to be obtained by considering the equilibrium of forces along the uncrack ligaments of the specimen. Then from equations (6.1.6), (6.1.11) and the equilibrium of the plate, one obtains

$$\sigma_o b_o = \int_a^{b_o} [\sigma_o \frac{x}{\sqrt{x^2-a^2}} + \frac{C_m}{x^m\sqrt{x^2-a^2}}] dx, \quad \text{----(6.1.12)}$$

Theoretically, any integer m = 0, 1, 2, ----- in equation (6.1.12) can be used to obtain the corresponding correction coefficient C_m.

When C_m is obtained from equation (6.1.12) the stress intensity factor K_1 can then be obtained from equation (6.1.11) as

$$K_1 = \sigma_o\sqrt{\pi a}\ [1 + \frac{C_m}{a^{(m+1)}\sigma_o}], \quad \text{---------(6.1.13)}$$

Let Y represent the finite width correction factor, i.e.

$$Y = 1 + \frac{C_m}{a^{(m+1)}\sigma_o} , \text{----------(6.1.14)}$$

then equation (6.1.13) can be written as

$$K_1 = Y \sigma_o \sqrt{\pi a} , \text{----------(6.1.15)}$$

Similarly, with equations (6.1.6) to (6.1.11) the stress and displacement distributions in the neighbourhood of the crack-tip, can be obtained as

$$\sigma_{yy} = \frac{Y\sigma_o\sqrt{\pi a}}{\sqrt{2\pi r}}[\text{Cos } \tfrac{1}{2}\theta + \frac{\text{Sin } \theta \text{ Sin } \frac{3}{2}\theta}{4}], \text{---(6.1.16)}$$

$$\sigma_{xx} = -\frac{Y\sigma_o\sqrt{\pi a}}{\sqrt{2\pi r}} \frac{\text{Sin } \theta \text{ Sin } \frac{3}{2}\theta}{4}, \text{-------(6.1.17)}$$

$$\tau_{xy} = \frac{Y\sigma_o\sqrt{\pi a}}{\sqrt{2\pi r}}[\frac{\text{Sin } \theta \text{ Cos } \frac{3}{2}\theta}{4} - \frac{\text{Sin } \frac{1}{2}\theta}{2}], \text{---(6.1.18)}$$

$$2\mu u = Y\sigma_o\sqrt{\pi a} \sqrt{\frac{r}{2\pi}}[\frac{(\kappa-3)}{2}\text{Cos } \tfrac{1}{2}\theta + \frac{\text{Sin } \theta \text{ Sin } \frac{1}{2}\theta}{2}],$$

------(6.1.19)

and

$$2\mu v = Y\sigma_o\sqrt{\pi a} \sqrt{\frac{r}{2\pi}}[\frac{(\kappa+3)}{2}\text{Sin } \tfrac{1}{2}\theta - \frac{\text{Sin } \theta \text{ Cos } \frac{1}{2}\theta}{2}],$$

------(6.1.20)

where Y is defined by equation (6.1.14).

Therefore, the modified critical stress intensity factor becomes,

$$K_{1c} = Y (\sigma_o)_{max} \sqrt{\pi a}, \text{----------(6.1.21)}$$

where Y is given by equation (6.1.14). The modified critical strain energy-release rate, G_{1c}, the Irwin parameter, I_{1c} and the dimensionless Irwin parameter, $\bar{I}_{1c}$, are respectively given by equations (6.1.2), (6.1.3) and (6.1.4) with K_{1c} represented by equation (6.1.21).

As mentioned earlier, one could choose any value of m to evaluate C_m and hence Y in equation (6.1.14). Fig.17 shows the plots of y for m = 0,1,2 and the ASTM standard curve, Brown and Strawley (1967), Heyer (1973). In this thesis, m = 0 is chosen because it gives Y close to that of ASTM standard. With m = 0 then, the finite width correction factor, Y, in equation (6.1.14) becomes

$$Y = 1 + \frac{C_o}{a\ \sigma_o}, \quad \text{----------} \quad \text{---(6.1.22)}$$

From equation (6.1.12) with m = 0, one can obtain C_o, and equation (6.1.22) becomes, (use positive of square root term),

$$Y = 1 + \frac{b_o}{a}\frac{1 - \sqrt{1 - a^2/b_o^2}}{\text{Cosh}^{-1}\ \frac{b_o}{a}}, \quad \text{----------(6.1.23)}$$

Therefore, for our purpose, the critical stress intensity factor, K_{1c}, the strain energy-release rate, G_{1c}, the Irwin parameter and the dimensionless Irwin parameter, $\bar{I}_{1c}$, are respectively given by equations (6.1.21), (6.1.2) to (6.1.4) with the factor Y defined by equation (6.1.23).

Therefore, all the necessary equations required for the evaluation of the crack-tip characterizing parameters are derived in terms of some measurable quantities such as dimensions of the specimen, maximum load carried by the specimen and elastic constants of the material. The important task left is to determine these measurable quantities. In the next section, specimen preparation is discussed.

6.2. Specimens Preparation

The material for the tests is glass. Glass was specifically chosen because of its brittle nature,

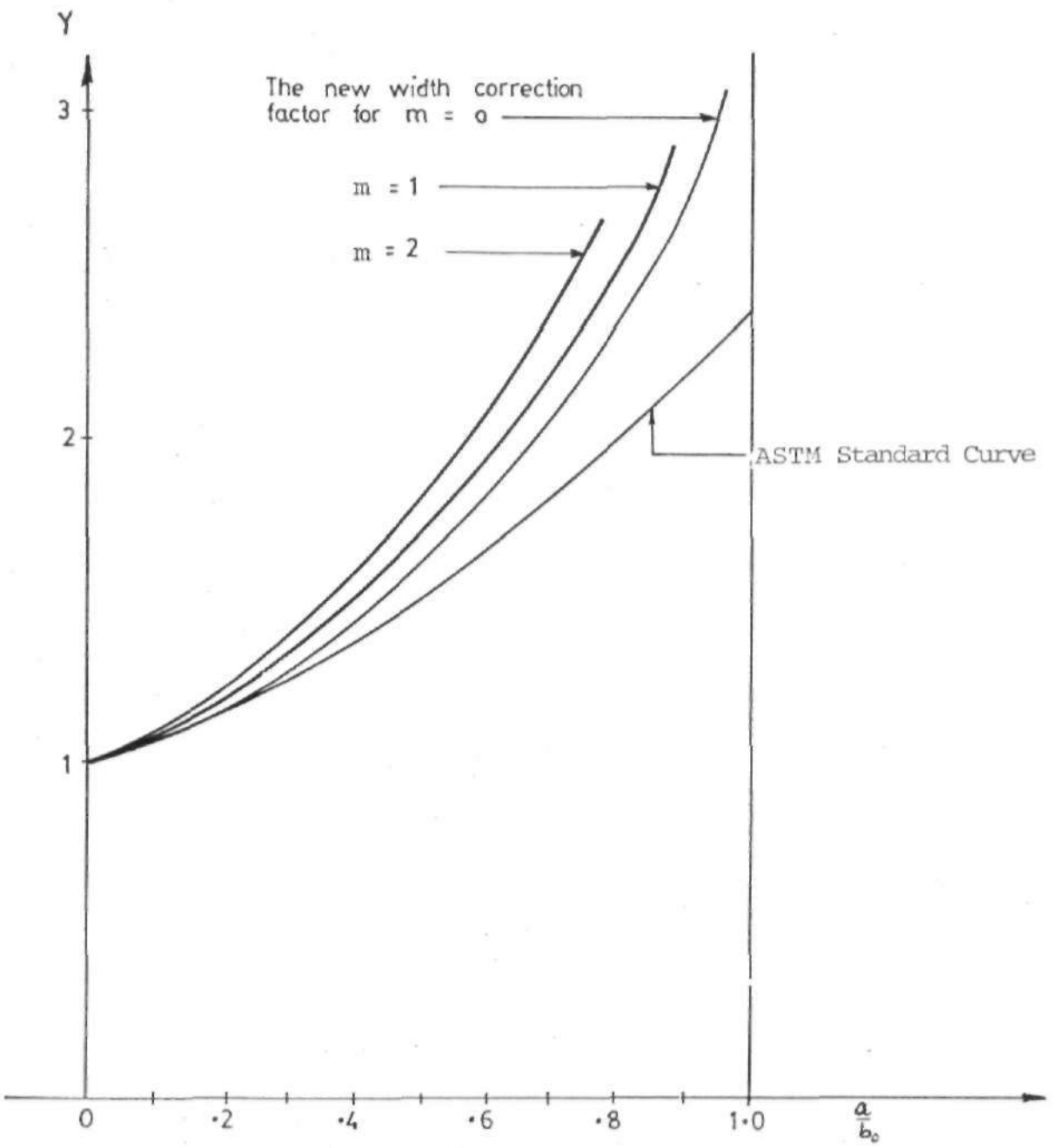


FIG . 17. The plots of the width correction factors y against a/b_o

so that there may be negligible deviation from the assumptions of linear elastic fracturing, assumed in the theory presented. Also from what the author saw in the markets, the material can easily be obtained in abundant quantity.

For the determination of the fracture strength, σ_f, a simple tensile test specimen, measuring 300 mm x 25 mm x 3 mm was used. These specimens were cut by employing a steel rule and a hand glass cutter. For the determination of Young's modulus, E, and Poisson's ratio, ν, the same simple tension test specimen, used for fracture strength determination, was employed. In this case a two-element rosette strain gauge was mounted at the centre of the 300 mm x 25 mm faces of the specimen. The purpose of the gauges on both sides was to indicate any bending stress on the specimen.

At the clamping ends of all the simple tension specimen, with the aid of evostick, cudboard measuring 75 mm x 25 mm, were attached as cushion for the grip jaws.

For the determination of the density, ρ, simple measurements of mass and volume were conducted. The glass cutter was used to cut some specimens from which simple measurements of length, width and thickness were made from which the volume was obtained. An Avery weighing machine with an accuracy of 2.5 g was used to determine the mass of the specimen.

For the determination of the fracture toughness the centre cracked specimen, Fig.18, was employed. A diamond glass cutter was used to cut the 300 mm x 25 mm x 3 mm specimen. Some other instruments used on the

centre notched specimen include, the drilling machine, diamond saw cutter, diamond wire and a hand saw. They were employed as follows:

A special spindle which carries the circular diamond saw cutter of 25 mm diameter and 0.15 mm thickness was designed and produced at the Mechanical Engineering workshop. The spindle was then attached to the drilling machine whose speed was set at 3,000 r.p.m. As the cutter rotates, the specimen, supported from both sides, was moved slowly and automatically towards the cutter. After the cutter and the specimen are fully engaged and coolant applied, an initial through-the-thickness crack was obtained. After the initial crack, its edges were made more uniform by employing the hand saw and the diamond wires of 0.15 mm diameter. Similar to the simple tension specimen, the clamping edges of the centre notched specimen had cudboard measuring 75 mm x $2b_o$ attached as cushions to the grip jaws.

6.3. Tests Procedure

All the tests were conducted at room temperature. The Denison testing machine, which is a constant load rate testing machine, was used for the tensile tests. Three different tests were conducted on the Denison testing machine. In all the experiments, the cross-head speed was set at 2 cm/min.

The first set of experiments on the Denison testing machine was on the simple tension specimen without any attachment. For this, siz specimens were successfully tested. In this report, a successful test means a specimen loaded that failed or fractured at almost the

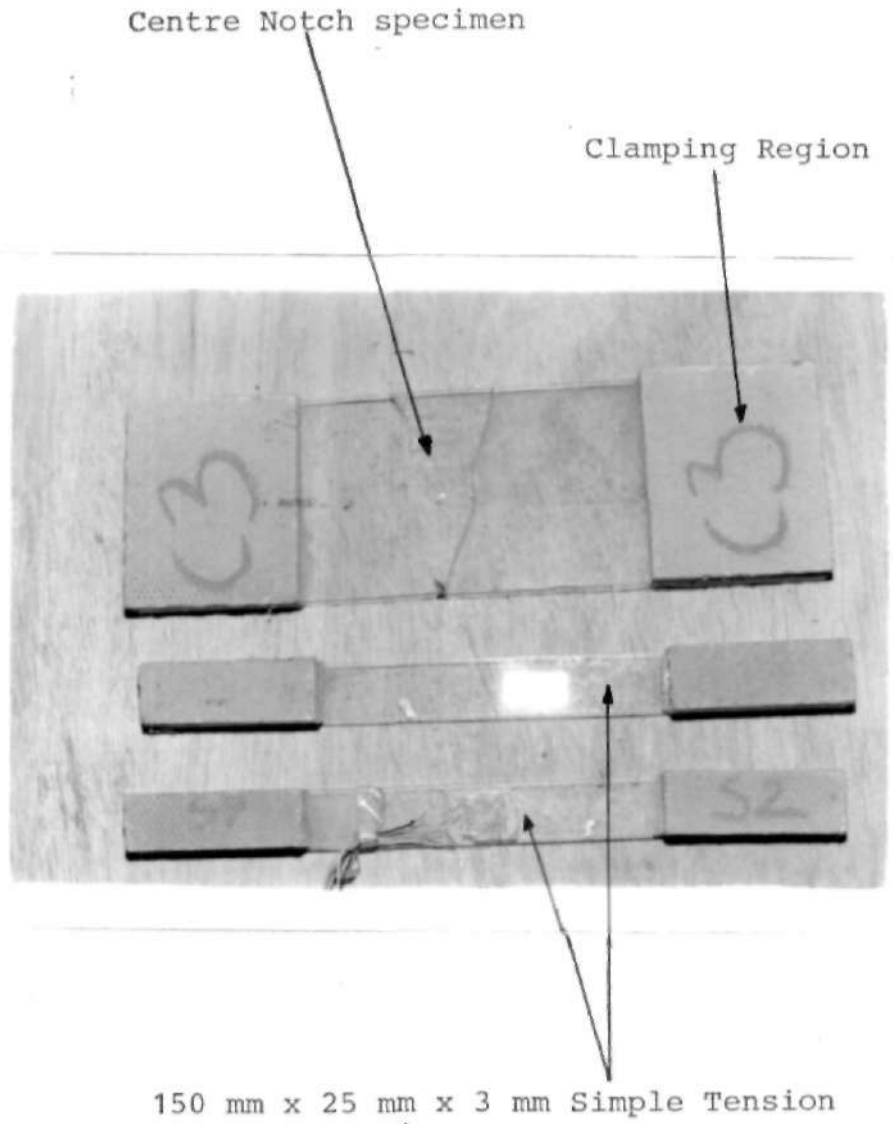


Fig. 18 : Simple Tension Tests Specimens for Statically Characterizing Glass

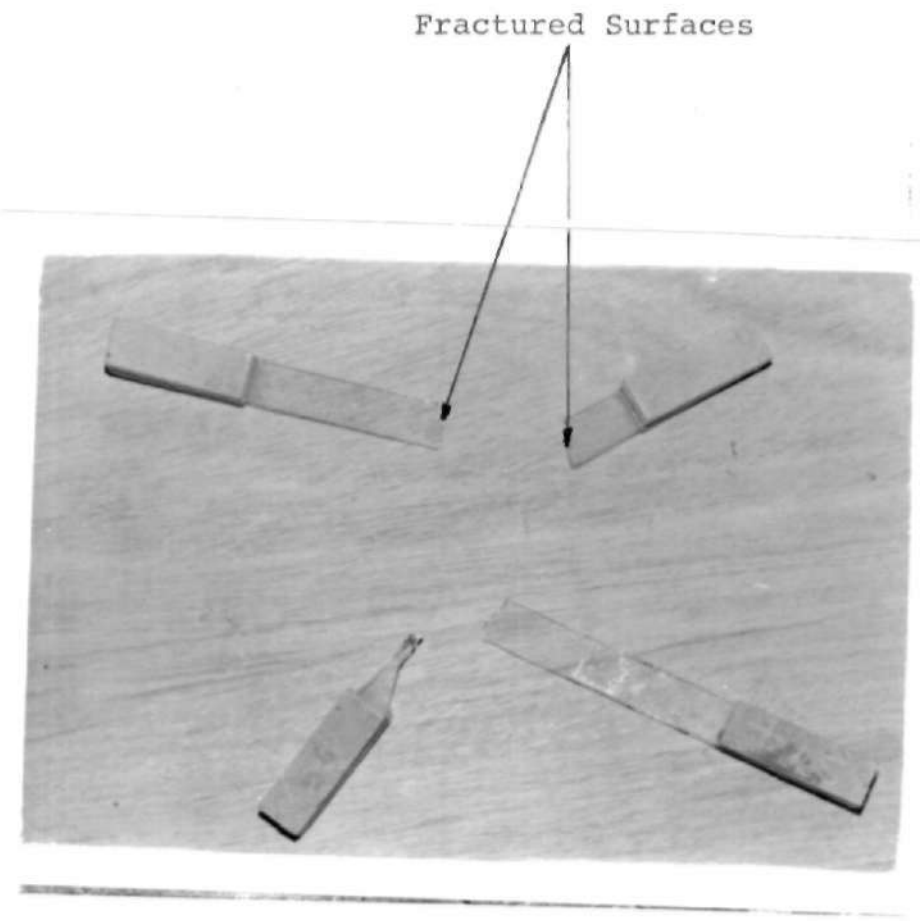


Fig. 19.: Some Unsuccessful Broken Specimens

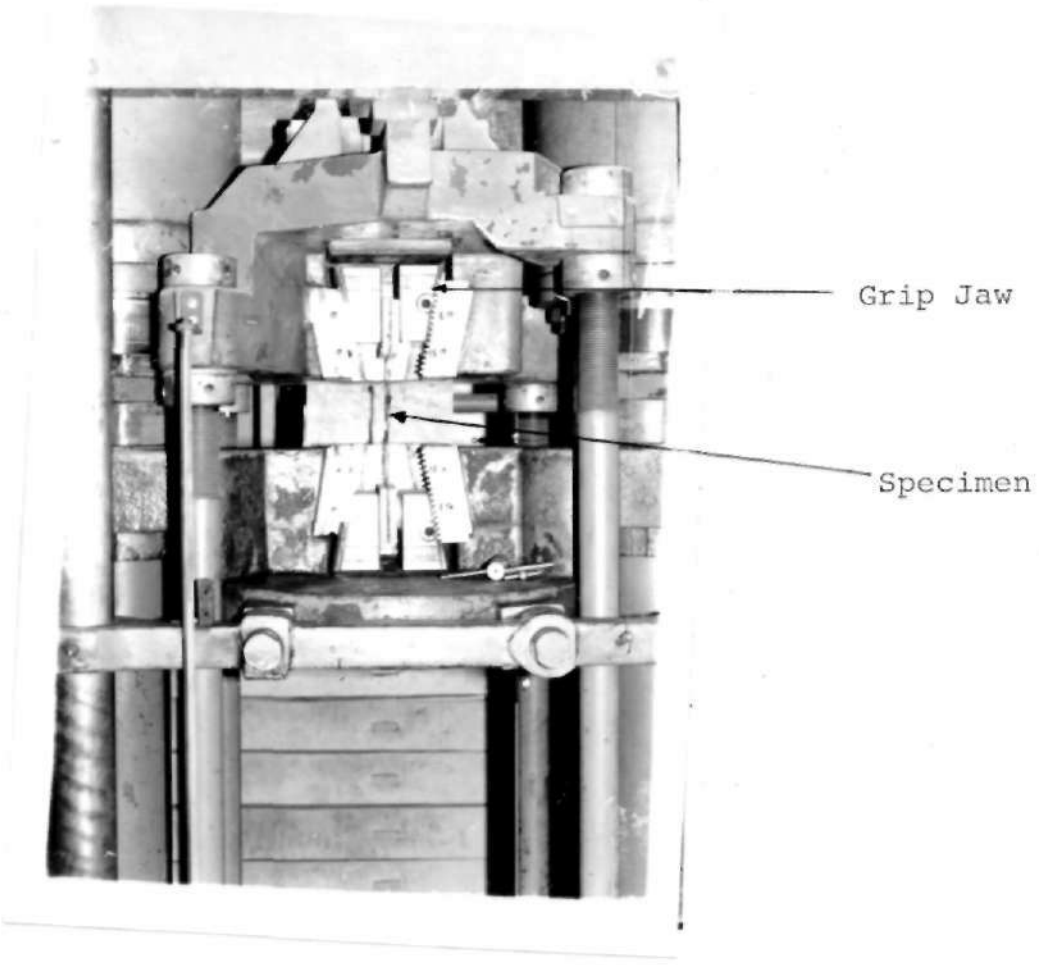
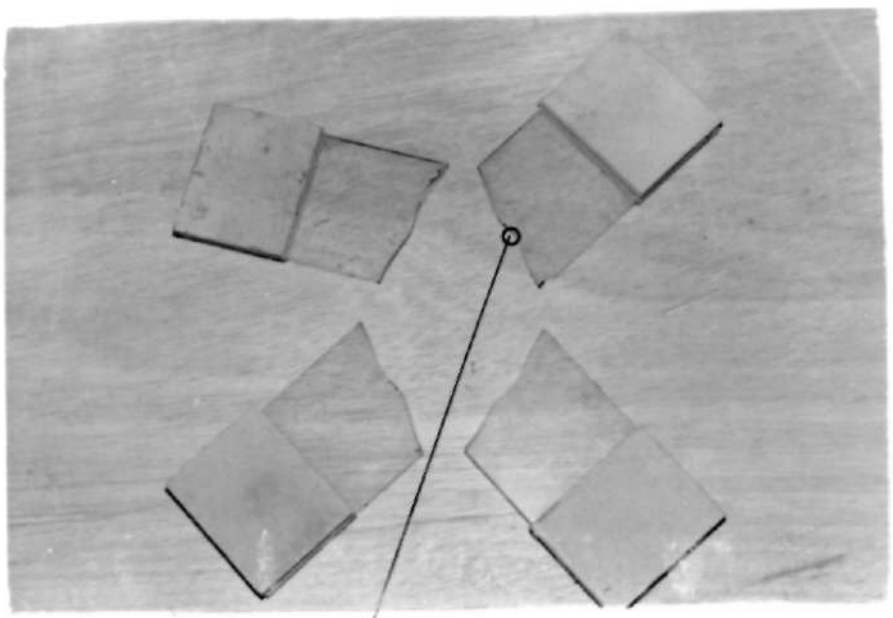
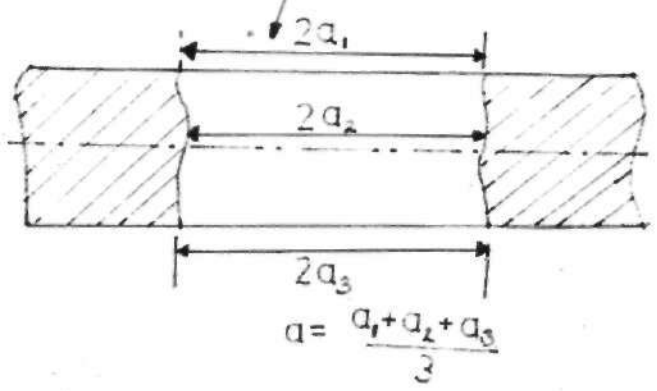


Fig. 20 : Set up of the Specimen on the Denison Testing Machine



i



ii

Fig. 21: Some Broken Specimens for Fracture Toughness Measurements, (i) and Cross-Sectional Area of a Broken Specimen, showing initial crack length a, (ii)

[redacted]

TABLE 1: The Maximum Load Recorded For Some Simple Tension Sperimen

Specimen No.	Width (mm)	Thickness (mm)	Max. Load (kN)	Fracture Stress (kN/m^2)
S13	25	3	1,85	24,667
S15	25	3	1.85	24,667
S16	25	3	1.90	25,333
S17	25	3	1.80	24,000
S20	25	3	1.85	24,667
S24	25	3	1.80	24,000

in Table 2. From Table 2, Figs. 22, 23, 24, were plotted. From Fig. 22, Young's modulus is obtained as $E = 66.7\ GN/m^2$. From Fig. 24, Poisson's ratio is obtained as $\nu = 0.235$. Then from the well-known relationship between E, ν, and the shear modulus, μ, u is obtainted as $\mu = 27.0\ GN/m^2$. Two other similar calculations were carried out for specimen numbers 57 and 59 and the results are shown in Table 3.

From Table 3, average values of Young's modulus and Poisson's ratio were obtained. The average values of some mechanical properties of glass are shown in Table 4. Also included in Table 4 is an average value of the density obtained for the glass.

For the determination of the fracture strength parameters, sixe of the results are shown in Table 5. From Table 5, the critical stress intensity factor, the strain energy-release rate, and the Irwin crack-tip parameter were calculated from equations (6.1.2), (6.1.3) and (6.1.4), respectively. The results are shown in Table 6.

To be more accurate, the modified theory of width correction discussed in Section 6.1 was employed for the calculations of the crack-tip characterizing parameters. The results of these calculations are shown in Table 7. The average critical strain energy-release rate for the glass is then obtained as $G_{1c} = 6.93\ N/m$, the Irwin crack-tip characterizing parameter s $I_{1c} = 997.6\ MN/m^{\frac{3}{2}}$ and the non-dimensional critical Irwin parameter as $\bar{I}_{1c} = 1.169 \times 10^{-3}$.

TABLE 2: The Load and Strains Recorded From An S6 Specimen

Load (kN)	Axial Strain, e_{xx} (μ Strain)	Transverse Strain, e_{yy} (μ Strain)
0	0	0
.2	30	- 10
.3	60	- 20
.4	80	- 25
.5	100	- 30
.6	110	- 25
.7	150	- 30
.8	160	- 38
.9	190	- 40
1.0	200	- 40
1.1	227	- 48
1.2	240	- 57
1.3	260	- 60
1.4	280	- 66
1.5	310	- 70
1.6	320	- 72
1.7	330	- 80
1.8	360	- 80

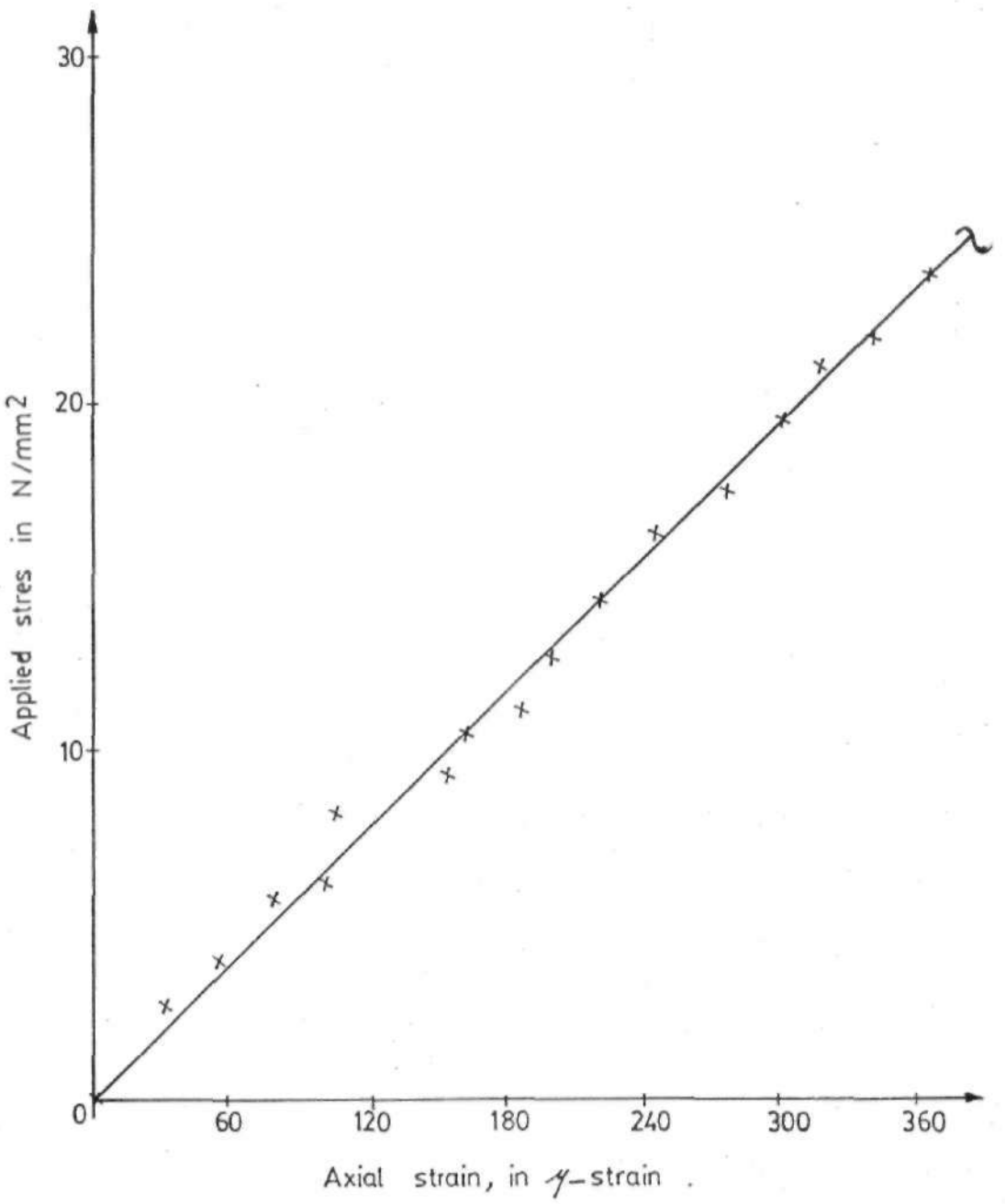


FIG.22: The plot of the applied stress against the axial strain.

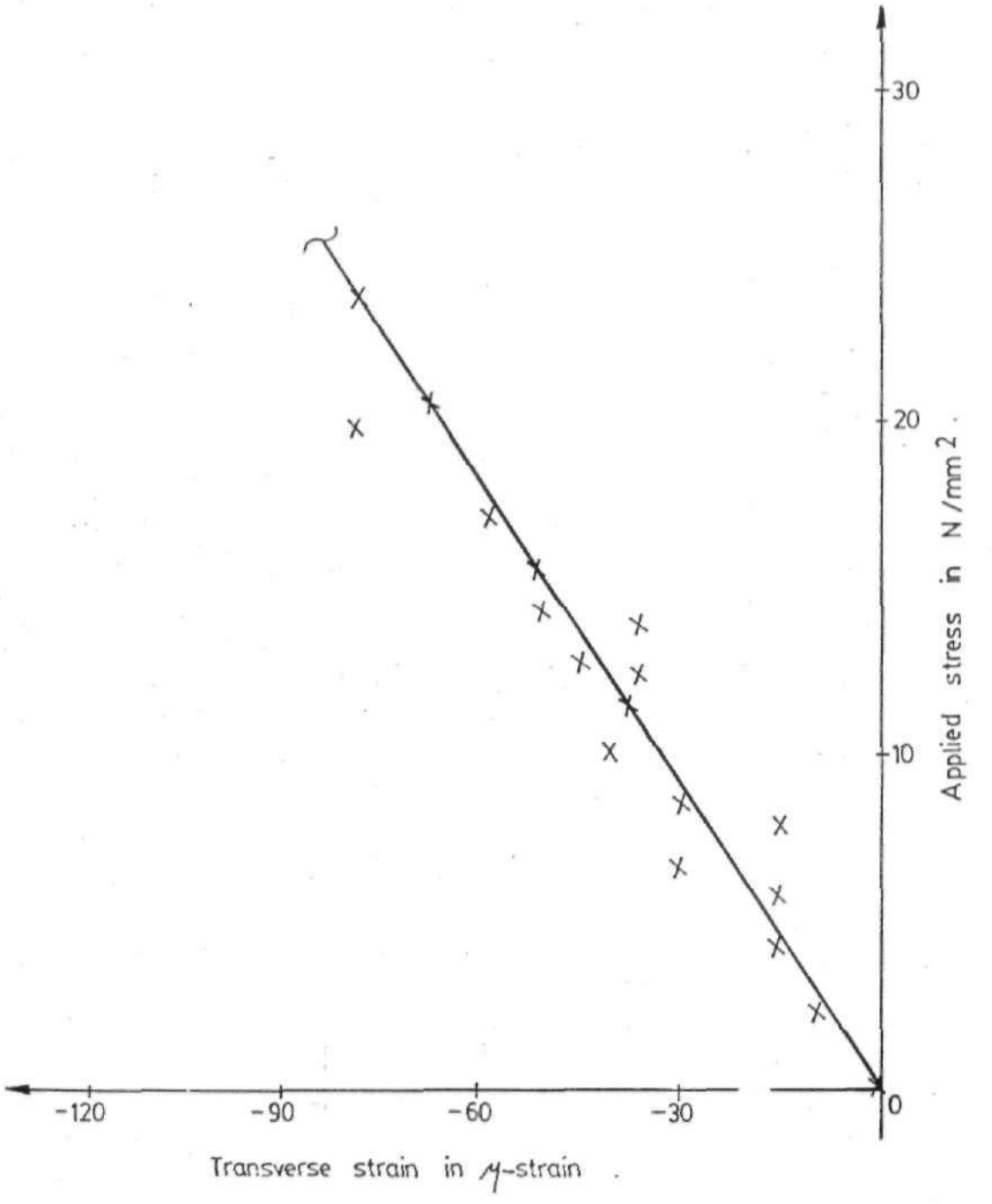


FIG. 23: The plot of the applied stress against the transverse strain .

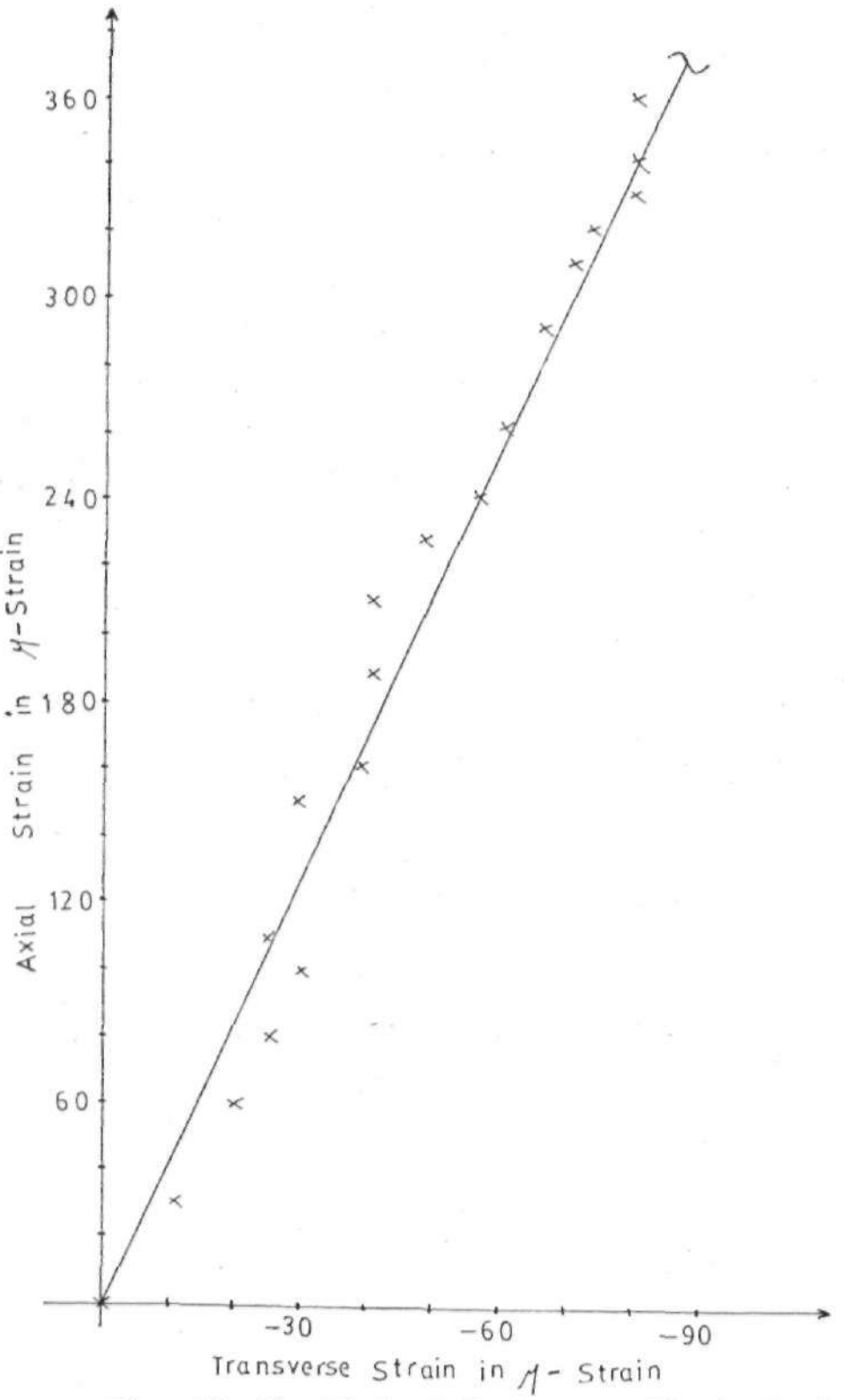


Fig. 24: The Plot of Transverse Strain Against Axial Strain

TABLE 3: Values of Young's Modulus and Poisson's Ratio From Specimens S6, S7 and S9

Specimen No.	Young's Modulus (GN/m^2)	Poisson's Ratio
S6	66.7	.235
S7	60.5	.200
S9	67.7	.195

TABLE 4: The Average Values of Some Mechanical Properties of Glass

Young's modulus, (GN/m^2)	65.0
Shear modulus (GN/m^2)	26.9
Poisson's ratio	.21
Ultimate Strength, σ_f (MN/m^2)	24.6
Density, ρ (kg/m^3)	2083.0

TABLE 5: Maximum Load and Initial Crack Length for Six Centre Notched Specimens

Specimen No.	Width of Specimen (mm)	Average Initial Length Of Crack (mm)	Maximum Load (kN)
C1	92	15.6	1.30
C2	92	16.3	1.30
C3	92	15.8	1.35
C4	93	16.0	1.30
C5	93	17.8	1.25
C6	93	16.0	1.30

TABLE 6: Some Crack-Tip Characterizing Parameters For Glass Evaluated Without Width Corrections

Specimen No.	Critical Stress Intensity Factor, K_{1c}, ($kN/m^{\frac{3}{2}}$)	Critical Strain Energy-Release Rate, G_{1c} (N/m)	Critical Irwin Parameters	
			I_{1c} $kN/m^{\frac{3}{2}}$	$\bar{I}_{1c}$
C1	736.8	6.51	950.5	1.114×10^{-3}
C2	746.3	6.68	962.7	1.128×10^{-3}
C3	762.1	6.97	983.1	1.152×10^{-3}
C4	740.0	6.57	954.6	1.118×10^{-3}
C5	749.4	6.74	966.7	1.133×10^{-3}
C6	740.0	6.57	954.6	1.118×10^{-3}

TABLE 7: Some Crack-Tip Characterizing Parameters for Glass Evaluated with Width Corrections

Specimen No.	Correc-tion Factor Y	Critical Strain Energy Release Rate G_{1c} (N/m)	Critical Irwin Crack-TipeParameters	
			I_{1c} ($kN/m^{\frac{3}{2}}$)	$\bar{I}_{1c}$
C1	1.0350	6.97	983.8	1.15×10^{-3}
C2	1.0380	6.93	999.3	1.171×10^{-3}
C3	1.0350	6.21	1017.5	1.192×10^{-3}
C4	1.0350	6.80	988.3	1.151×10^{-3}
C5	1.0410	7.02	1006.3	1.179×10^{-3}
C6	1.0353	6.80	988.3	1.151×10^{-3}
Average	-	6.93	997.6	1.169×10^{-3}

The values of these characterizing parameters, say the critical strain energy-release rate, G_{1c}, is very low. For AS-4/3501-6, graphite/epoxy, Aliyu and Daniel (1985) reported a G_{1c} of 210 N/m and for F185-7300 composite, Aliyu et al (1985) reported a G_{1c} value of 1890 N/m, at the same loading rate for which the G_{1c} = 6.93 N/m for glass was obtained. The low G_{1c} value for glass or any low value of a crack-tip parameter, implies that small loads can very easily cause propagation of an existing crack.

The crack-tip parameters are measures of toughness of a material. From the results reported above, it is therefore obtained that Graphite/epoxy composite is almost thirty times tougher and the thorium/epoxy F185-7300 composite is two hundred and seventy times tougher than glass. These conclusions cannot be revealed by the elastic constants of the materials alone.

In addition to the crack-tip parameters evaluated above, another simple characterizing parameter, commonly used for material selection, is call the 'strength ratio'. It is defined as the ratio of the maximum stress carried by the flawed member and the fracture strength, σ_f, for the material, or

$$R_{sc} = \frac{\sigma_o}{\sigma_f} \qquad \text{----------(6.4.1)}$$

where R_{sc} is the 'strength ratio'. From Table 5, the strength ratios are obtained as follows: For C1 specimen, $R_{sc} = .191\text{x}10^{-3}$; C2 specimen, $R_{sc} = .191\text{x}10^{-3}$; C3 specimen, $R_{sc} = .199\text{x}\ 10^{-3}$; C4 specimen, $R_{sc} = .191\text{x}10^{-3}$; C5

specimen, R_{sc} = .182 x 10^{-3} and for C6 specimen, R_{sc} = .189 x 10^{-3}. The major drawback of the strength ratio concept is that it does not have a strong analytical basis and the parameter does not provide any useful information at the crack-tip.

6.5. Conclusions

The results presented in Chapter III were applied to the centre notched specimen for the determination of the fracture strength parameters for glass. A new width correction factor was introduced and used with the experimental results obtained.

As mentioned earlier, the smallest value of the new width correction factor, Y, was used so as to get the new width correction factor, Y, close to that of the ASTM. It can also be seen from Fig. 24 that width correction factors (6.5.1) and form = 0 are almost the same for small a/b_o ratio.

The material employed for the test, glass, was statically characterized. The dimensions of the specimen were taken as suggested by Wheeler et al (1982). The following values of some of its properties were obtained: E = 65.0 GN/m², μ = 26.9 GN/m², ν = 0.21, σ_f = 24.6 MN/m², and ρ = 2083.0 kg.m³. All these properties were determined at room temperature.

Furthermore, fracture toughness parameters were evaluated. The critical strain energy-release rate, G_{1c} was obtained as 6.93 N/m and the Irwin crack-tip parameter was obtained as I_{1c} = 997.6 kN/$m^{\frac{3}{2}}$. These properties

of glass were compared with those of some other materials. Glass, as expected, was concluded as not a tough material.

Finally, it should be noted that these fracture toughness parameters are very useful in determining the effects of metallurgical variables on the toughness of engineering materials. The parameters can also be used in research, design and development when the flaw size is known before hand. The characterizing parameters can also be used to determine the suitability of a material for a particular purpose for which the stress conditions are known. The parameters can, furthermore, be used by industries for acceptance and or quality control.

CHAPTER VII

SUMMARY, CONCLUSIONS AND SUGGESTIONS FOR FUTURE WORK

7.1. Summary

In Chapter I, some elementary crack propagation problems were re-examined and some of their solutions were shown to have limitations. Some of the problems include that of a large plate with a straight central crack loaded by some generalized modes I and II loadings and the same crack problem as above but loaded with some pressure loading along the crack faces. These problems, although very elementary, can be used to develope and check the validity of some crack tip characterizing parameters, when their correct solutions are known. But due to the limitations of the reported solutions of these problems, the applications and interpretations of the introduced crack tip parameters have to be questionable. By employing the solutions with limitations the strain energy-release rate and the J-integral concepts were shown to violate some elementary principles of fracture.

With the aim of developing new solutions for the crack propagation problems, the plane elasticity problem was reconsidered. The complex potential technique was employed for the analysis. The analysis began with the Kolosov-Muskhelishvili formulae. These equations were modified and the formulae for the stresses and displacements were made to depend on only one complex potential. These new equations were shown to satisfy

the equilibrium conditions, the compatability conditions and the boundary conditions of many problems. They were also shown to be the generalized Westergaard formulae.

In Chapter III and Appendix A, the new formulae were applied to some crack problems. Asymptotic stress and displacement distributions for a number of problems were derived. In all cases, the stresses were of the form $\sim r^{-\frac{1}{2}}$ and the displacements $\sim r^{\frac{1}{2}}$ and unlike in the older solutions both σ_{ij} and u_i in the new solutions were shown to be functions of the loading conditions.

By employing the new solutions derived in Chapter III and Appendix A, the following conclusions on the strain energy-release rate and the J-integral as crack-tip parameters were reached:

(i) The strain energy-release rate concept introduced by Griffith (1920) and modified by Irwin (1957) as the crack extension force was shown to be possible crack tip characterizing parameter.

(ii) The strain energy-release rate is a function of loading condition, which is similar to the yield strength concept of non-flawed members.

(iii) A strain energy-release rate material property, G_{1c}, similar to yield strength σ_y in simple tension (material property) was also introduced.

(iv) A new crack-tip characterizing parameter, the Irwin crack-tip parameter, denoted by I was introduced.

(v) A simple relationship between the strain energy-release rate and the Irwin crack-tip parameter was derived.

(vi) It was shown that crack-tip characterization via the strain energy-release rate concept is equivalent to crack-tip characterization via the Irwin crack-tip parameter concept.

(vii) The crack-tip parameters, the strain energy-release rate and the Irwin crack-tip parameter were modified to take into account the finite width of the specimen employed for fracture toughness tests.

(viii) The new width correction factor introduced for the strain energy-release rate and the Irwin parameter was shown to be in good agreement with another reported width correction factor. (ASTM standard).

(ix) Comprehensive experiment was conducted on glass and the properties shown in Table 8 were obtained.

(x) The crack-tip parameters of the glass were compared with the crack-tip parameters of some other materials reported by the author and it was shown that glass is not a tough material.

(xi) The J-integral was shown not to be equal to the Irwin crack extension force, G, or the strain energy-release rate.

(xii) The J-integral was shown to be path independent, but behaves abnormally for some values of α, for the new model solutions.

TABLE 8: Some Properties of Glass

Young's Modulus, E(GN/m^2)	65.0
Shear Modulus, μ (GN/m^2)	26.9
Poisson's ratio, ν	0.21
Yield Strength, σ_y (MN/m^2)	24.6
Density, ρ (kg/m^3)	2083.0
Critical Strain Energy-Release Rate, G_{1c} (N/m)	6.9
Critical Irwin Crack-Tip Parameter, I_{1c} ($kN/m^{3/2}$)	997.6
Critical non-dimensional Irwin parameter, $\bar{I}_{1c}$	1.17×10^{-3}

7.2. Conclusions

1. The solutions of some elementary crack problems including a centre-notch plate, are shown to have certain limitations. The limitations are due to some imposed unrealistic stress and displacement distributions around the crack, by those model solutions.

2. The reported model solutions are not in good agreement with reported experimental stress distributions, while the new solution is shown to confirm much more reported experimental results.

3. The strain energy-release rate and the J-integral concepts based on the reported (old) solutions are shown to violate some elementary principles of fracture.

4. A generalized solution for plane crack problems was developed. The new generalized solution is in terms of only one complex stress function.

5. The new solution is shown to satisfy equations of equilibrium, compatibility and stress strain relations and the boundary conditions of a number of crack problems. Furthermore, the new equations are shown to be in the generalized Westergaard equations.

7. By employing the new developed solution, the original Griffith strain energy-release rate criterion was modified. It was concluded that biaxial loading affect the criterion.

8. A new crack tip characterizing parameter, the Irwin crack tip parameter, was also developed. It was shown that crack tip characterization via the strain energy release rate concept is equivalent to crack tip characterization via the new Irwin parameter concept.

9. A new procedure of taking into account the effect of finite width of the cracked plate was developed. The new width correction factor developed was shown to be in good agreement with another reported factor.

10. The J-integral was shown to be path independent but is not equal to the strain energy release rate, G, or its equivalent, the Irwin crack extension force. From the values of the J-integral, it was concluded that the new solutions need some further studies for some $\alpha < 0$.

11. The crack-tip parameter, the critical strain energy release rate and the critical Irwin parameter, interpretted as material property, were experimentally evaluated by employing the centre-notch specimen, loaded at a cross head speed of 2 cm/min. The procedure employed was found to yield consistent results.

7.3. Discussions and Suggestions for Future Work

1. Based on the new analysis of some crack problems

presented in Chapter III and the appendix, the expressions of the strain energy-release rate, G and the new Irwin crack-tip parameter, were derived. For example, for a large plate with a straight central through-the-thickness crack of length 2a, loaded by $\sigma^{\infty}_{xx} = \alpha\sigma_o$ and $\sigma^{\infty}_{yy} = \sigma_o$, in Chapter IV the strain energy release rate and the Irwin crack-tip parameter were obtained.

$$G_1 = \frac{(\kappa + \alpha\kappa + 3 - \alpha)}{16\mu} K_1^2$$

and

$$I_1 = \frac{(\kappa + \alpha\kappa + 3 - \alpha)}{2} \Big\}, \quad \text{----------(7.2.1)}$$

where $K_1 = \sigma_o \sqrt{\pi a}$. It is a well known theory, Sokolnikoff (1956), that a pure shear loading is equivalent to a tension in the yy-direction and a compression in the xx-direction. That means a pure shear loading can also be defined by $\sigma^{\infty}_{xx} = -\sigma_o$ and $\sigma^{\infty}_{yy} = \sigma_o$. Therefore, with $\alpha = -1$, from equations (7.2.1), one can obtain the strain energy-release rate and the Irwin parameter for shear loading as

$$G_{11} = \frac{1}{4\mu} K_{11}^2 , \quad \text{----------(7.2.2)}$$

and

$$I_{11} = 2 K_{11}, \quad \text{----------(7.2.3)}$$

where $K_{11} = \tau_o \sqrt{\pi a}$. The stress and displacement distributions

2. In deriving the expressions for the strain energy-release rates G_1 and G_{11} and the Irwin parameter I_1 and I_{11}, because of the symmetrical nature of the problem, it was assumed that the direction of the crack propagation is known. If it is not known, one can still employ the strain energy-release rate concept or the Irwin parameter concept for its determination. Thus, if $G = G(K_1, K_{11})$ and $I = I(K_1, K_{11})$, the Griffith theory states, Irwin (1960),

$$G(K_1, K_{11}) = G_{critical}, \text{----------(7.2.11)}$$

or

$$I(K_1, L_{11}) = I_{critical}, \text{----------(7.2.12)}$$

for crack propagation. The direction of crack propagation, θ^*, can be obtained from

$$\left.\frac{\partial G}{\partial \theta}\right|_{\theta=\theta^*} = 0, \text{----------(7.2.13)}$$

or

$$\left.\frac{\partial I}{\partial \theta}\right|_{\theta=\theta^*} = 0. \text{----------(7.2.14)}$$

Let us, for the moment, consider formulating the new Irwin parameter for a mixed mode problem. For the strain energy-release rate, one is referred to Ichikawa and Tanaka (1982).

The problem is that of a large plate with a central crack, loaded by a uniaxial opening mode stress intensity factor, K_1, and an inplane shear mode stress intensity factor, K_{11}. From equations (3.2.22), (3.2.23), (7.2.7)and (7.2.8), and with the modified definitions,

$$I_u = 2\mu/u_r/\sqrt{\frac{2\pi}{r}}, \text{----------(7.2.15)}$$

and

$$I_v = 2\mu/v_r/\sqrt{\frac{2\pi}{r}}, \text{----------(7.2.16)}$$

where

$$u_r + iv_r = e^{i\theta}(u + iv), \quad \text{----------(7.2.17)}$$

one obtains

$$I_u = /K_1(\kappa \cos \tfrac{3}{2}\theta - 3 \cos \tfrac{1}{2}\theta + \sin \theta \sin \tfrac{3}{2}\theta)$$

$$-4 K_{11} \cos \tfrac{1}{2}\theta/, \quad \text{----------(7.2.18)}$$

and

$$I_v = /K_1(\kappa \sin \tfrac{3}{2}\theta - 3 \sin \tfrac{1}{2}\theta - \sin \theta \cos \tfrac{3}{2}\theta)$$

$$-4 K_{11} \sin \tfrac{1}{2}\theta/. \quad \text{----------(7.2.19)}$$

Then the Irwin parameter for a mixed mode problem is defined as

$$I = \text{Max}[I_u, I_v]. \quad \text{----------(7.2.20)}$$

With equations (7.2.18) to (7.2.20), equation (7.2.14) can be used to predict the direction of crack propagation while equation (7.2.12) can be used to predict the stresses at failure when the material property is known. The above formulations are only introductory. It is therefore suggested that detailed studies be done on the new Irwin crack-tip parameter especially with regards to mixed mode loading.

3. In all the reported stress and displacement distributions only the first term of the asymptotic expansion of the complex stress function was employed. That is, the stress and displacement distributions of Chapter III and the appendix can be obtained with

$$\phi_1' = \frac{K_1}{\sqrt{2\pi z}}, \quad \text{----------(7.2.21)}$$

where $z = re^{i\theta}$. Especially for the purpose of experimental studies where the fringe patterns can be used for the evaluation of the stress intensity factor(s), Irwin et al (1978), higher terms in the asymptotic expansion of the

stress function, should be considered.

It is therefore suggested that the new formulae introduced in Chapters II, III and the appendix, should be used with the stress function

$$\phi_1' = \frac{K_1}{\sqrt{2\pi z}}[1+\alpha_3 \frac{z}{a} +\alpha_4 (\frac{z}{a})^2 +.....], \text{-------(7.2.22)}$$

where $z = re^{i\theta}$, r,θ are polar coordinates at the crack-tip and α_3 α_4 are some constants. These stress distributions can be investigated with some photoelastic experimental results.

It should be noted that even if the higher terms of expansion of the complex stress function are employed the expressions of the strain energy-release rate, G_1 and the Irwin crack-tip parameter, I, discussed in Chapter IV, will not change.

4. In the experimental studies reported, the material properties, G_{1c} and I_{1c} for glass were determined by employing the centre-notch specimen. It is suggested that these fracture toughness material properties discussed in Chapter IV be determined by employing some other specimens such as the edge-notch, compact tension and the double-cantilever beam specimens. It should be noted that for any other specimen, di erent from the centre cracked specimen employed in this report, the analysis must be modified.

Another new alternative procedure for the determination of the material property, G_{1c}, which seems promising is from the knowledge of the average grain size for the material. This will involve some chemical

analysis. If the elastic constants, the Poisson's ratio, ν, the shear modulus, μ, and the yield strength in simple tension, σ_y, are known, then from equation (4.2.10), the strain energy-release rate, G_{1c} can be expressed as

$$G_{1c} = \frac{\pi d_g (\kappa+3)}{32\mu} \sigma_y^2, \quad \text{----------(7.2.23)}$$

where d_g is the grain size. It should be noted that equation (7.2.23) was obtained by assuming that the grain forms a through-the-thickness crack, which is not true physically. Before the new approach for the determination of G_{1c} by the chemical analysis, the theory presented here must be modified to take into account, the fact that the grain is an internal flaw.

5. It is also suggested that the theory presented and the experimental methods discussed be extended to cover non-linear elastic, elastic-plastic fracturing. For the small scale yielding, the Irwin (1960) procedure where the crack size a is replaced by some fictitious crack size $a+\Delta a$, may still hold. It is suggested that these be investigated in some detail.

6. Apart from the strain energy-release rate concept presented in this thesis there are some other viable concepts which can also be used for the prediction of the direction of crack propagation and the load which can cause the crack to propagate. All these theories start with the asymptotic stress and displacement distributions at the crack-tip. Therefore, with the newly introduced formulae for the stresses and displacements, Chapter II, these theories would have some face

lift similar to the strain energy-release rate theory. It seems desirable therefore to investigate in some detail, some other fracture theories by employing the new fcrmulae.

For structural members without any flaw, some standard strength theories include, the maximum principal stress theory, the maximum principal strain theory, the maximum shear theory, the total strain energy theory, and the distortion energy theory. With the newly developed equations for the stresses around the crack-tip it seems to the author that the above theories, can all be extended to be applicable to members with flaws. Let the new theories be referred as the maximum principal stress density theory, maximum principal strain density theory, maximum shear stress density factor theory, maximum strain energy density factor throry, and the maximum distortion energy density factor theory. These factors in terms of the principal stresses $\sigma_1 > \sigma_2$ can be defined as:

Maximum principal stress density factor, P

$$P = \lim_{r \to o} \sigma_1 \sqrt{2\pi r}, \quad \text{----------(7.2.24)}$$

Maximum principal strain density factor, Q,

$$Q = \lim_{r \to o} (\sigma_1 - \nu\sigma_2) \sqrt{2\pi r}, \quad \text{----------(7.2.25)}$$

Maximum shear stress density factor, R,

$$R = \lim_{r \to o} \frac{\sigma_1 - \sigma_2}{2} \sqrt{2\pi r}, \quad \text{----------(7.2.26)}$$

Maximum strain energy density factor, S

$$S = \lim_{r \to o} W\, 2\pi r, \quad \text{----------(7.2.27)}$$

and the maximum distortion energy density factor, T

$$T = \lim_{r \to o} W_d \, 2\pi r \, , \text{----------(7.2.28)}$$

where W is the strain energy density and W_d is the distortion energy density.

With the factors defined by equations (7.2.24) to (7.2.28), crack propagation criteria can be stated as

$$\text{Max}[P] = P_{critical}, \text{----------(7.2.29)}$$

$$\text{Max}[Q] = Q_{critical}, \text{----------(7.2.30)}$$

$$\text{Max}[R] = R_{critical}, \text{----------(7.2.31)}$$

$$\text{Max}[S] = S_{critical}, \text{----------(7.2.32)}$$

and

$$\text{Max}[T] = T_{critical}, \text{----------(7.2.33)}$$

for the respective theories stated earlier. Where $P_{critical}$, $Q_{critical}$, $R_{critical}$, $S_{critical}$ and $T_{critical}$ are some material properties. Except for the criterion stated in equation (7.2.32), Sih (1974), to the author's knowledge none of the other criteria, equations (7.2.29) (7.2.30), (7.2.31) and (7.2.33) was ever investigated. It is therefore suggested that all these criteria be investigated in detail by employing the new formulae discussed in Chapters I, II and the appendix. Furthermore, the predicted load which can cause crack propagation from these criteria should be compared with those obtained from the strain energy-release rate theory.

7. In this investigation as mentioned earlier, we only concentrated on finding whether the strain energy-release rate and the J-integral are equal. It was shown that the strain energy-release rate and the J-integral are not

equal. Especially because of its property of being path independent, the J-integral and some other path independent integrals, discussed by Budiansky and Rice (1973) should be fully investigated so as to find their real physical meanings.

8. Finally, the analyses were restricted to isotropic, plane and quasi-static problems. It is suggested that the three-dimensional version of the crack problems be investigated.

9. Also because rapid crack propagations are very common in real problems, an attempt should also be made to incorporate the dynamic effects into the analyses.

7.4. New and Major Contributions to Knowledge

1. To the author's knowledge, this is the first time that the limitations of some solutions of fracture mechanics models are re-examined.

2. New stress and displacement distributions for some elementary but important fracture mechanics problems, for infinite regions, were derived through the reduction of the Kolo. v-Muskhelishvili potential functions $\phi(z)$ and $\psi(z)$ to only one unknown function. These new solutions were shown to be void of most of the limitations in previous solutions.

3. In order to account for the finiteness of cracked bodies employed in real engineering applications, a new mathematical analysis was attempted. The new finite width correction factor was compared with that of the ASTM standard and were found to be predicting almost the same results especially for smaller rates of crack length to width of the plate ratio.

4. A new crack tip characterizing parameter denoted by I, which physically represents a measure of critical displacement, was proposed.

APPENDIX A: SOLUTIONS OF SOME OTHER PROBLEMS

In Chapter III, a few problems were solved by employing the new formulae derived in Chapter II. In this appendix, a few additional elementary problems are reconsidered and the stress and displacement distributions around the crack-tip are derived by employing the new formulae. Based on the new solutions, the strain energy-release rate, the new Irwin crack-tip parameter and the J-integral, will be evaluated.

First consider an infinite plate with a straight central crack of length 2a. It is subjected to some equilibrating point forces at x = b, as shown in Fig. 25. As discussed in Chapter III, the new formulae for the stresses in terms of only one complex potential, $\phi_1(z)$ can be written as

$$\left.\begin{aligned} \sigma_{yy} &= \text{Re } \phi_1' + \frac{2}{1+N}\, y\, \text{Im } \phi_1'', \\ \sigma_{xx} &= \frac{3-N}{1+N}\,\text{Re } \phi_1' - \frac{2}{1+N}\, y\, \text{Im } \phi_1'' \\ \tau_{xy} &= \frac{N-1}{1+N}\,\text{Im } \phi_1' - \frac{2}{1+N}\, y\, \text{Re } \phi_1'' \end{aligned}\right\} \text{------ A.1}$$

and similarly, the displacements can be written as

$$\left.\begin{aligned} 2\mu u &= \frac{(\kappa - N)}{1+N}\,\text{Re } \phi_1 - \frac{2}{1+N}\, y\, \text{Im } \phi_1' \\ \text{and} \qquad & \\ 2\mu v &= \frac{(\kappa + N)}{1+N}\,\text{Im } \phi_1 - \frac{-2}{1+N}\, y\, \text{Re } \phi_1' \end{aligned}\right\} \text{----- A.2}$$

where N is a constant to be determined from the boundary conditions of the problem. Equations (A.1) and (A.2) can be obtained from equations (2.3.7) to (2.3.11).

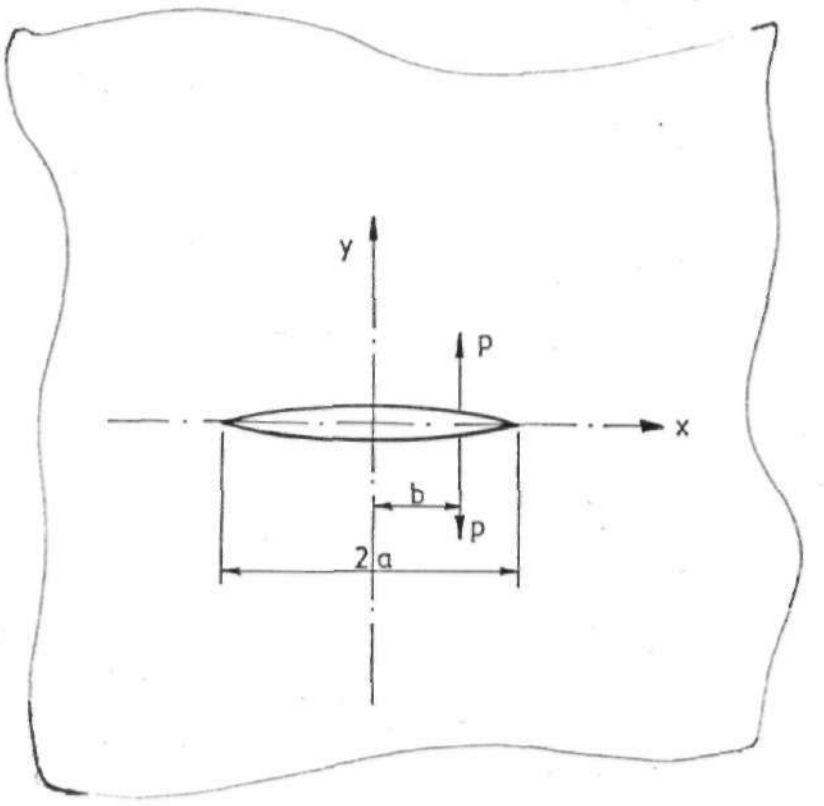


FIG 25:. A Large plate with a central crack of length 2a loaded by point loads..

From Fig. 25, the boundary conditions of the problem can be stated as

$$\sigma_{xx}^{\infty} = \sigma_{yy}^{\infty} = \tau_{xy}^{\infty} = 0$$

and $\}$, ----------A.3

$$\sigma_{xx}(X,0) = 0, \quad |X| \leq a$$

With an assumed stress function ϕ_1, after Irwin (1957) and Westergaard (1939) as

$$\phi_1' = \frac{P}{\pi} \frac{1}{z - b} \sqrt{\frac{a^2 - b^2}{z^2 - a^2}} \ , \text{----------A.4}$$

and N = 3, the boundary conditions stated in equation (A.3) are then all satisfied. The asymptotic stress and displacement distributions for the problem can be obtained from equations (A.1) and (A.2). These are given by equations (3.2.31) to (3.2.35) but with the stress intensity factor, K_1, defined by

$$K_1^P = \frac{P}{\sqrt{\pi a}} \sqrt{\frac{a + b}{a - b}} \ , \text{----------A.5}$$

Similarly, the strain energy-release rate, defined by equation (1.3.3), the new Irwin crack-tip parameter defined by equation (4.4.3) and the J-integral defined by equation (1.3.5) are respectively obtained as equations (4.2.17), (4.4.8) and (5.2.34) with K_1^P given by equation (A.5). K_1^P is as reported in the literature.

The next problem solved is that shown in Fig. 25 but with an additional pair of point loads at X = - b.

The boundary conditions for the problem again as stated by equations (A.3) which, after Irwin (1957) gave

$$\phi_1' = \frac{P}{\pi} \frac{2Z}{(z^2-a^2)} \sqrt{\frac{a^2 - b^2}{z^2 - a^2}} \quad \text{----------A.6}$$

and N = 3, and in the new formulae, equations (A.1) and (A.2), are then satisfied. The stress and displacement distributions, the strain energy-release rate, the new Irwin crack-tip parameter and the J-integral are respectively given by equations (3.2.31) to (3.2.35), equations (4.2.17), (4.4.8) and (5.2.34), with the stress intensity factor K_1^P given by

$$K_1^P = \frac{2P}{\pi} \sqrt{\frac{\pi a}{a^2 - b^2}}, \quad \text{----------A.7}$$

The next problem is again shown in Fig. 26 but instead of the point forces, there are equilibrating concentrated moments at X = b. By employing equation (A.4) as a Green's function for this problem, one can arrive at the stress function, ϕ_1 as

$$\phi_1' = \frac{M}{\pi} \frac{1}{(z - b)^2} \sqrt{\frac{a^2 - b^2}{z^2 - a^2}}, \quad \text{----------A.8}$$

The stress distribution, the strain energy-release rate, the new Irwin crack-tip parameter and the J-integral are respectively obtained as in equations (3.2.31) to (3.2.35), equations (4.2.17), (4.4.8) and (5.2.34) with the stress intensity factor, K_1^P, defined as

$$K_1^P = \frac{M}{\sqrt{\pi a}} \frac{\sqrt{a + b}}{(a-b)^{3/2}}, \quad \text{----------A.9}$$

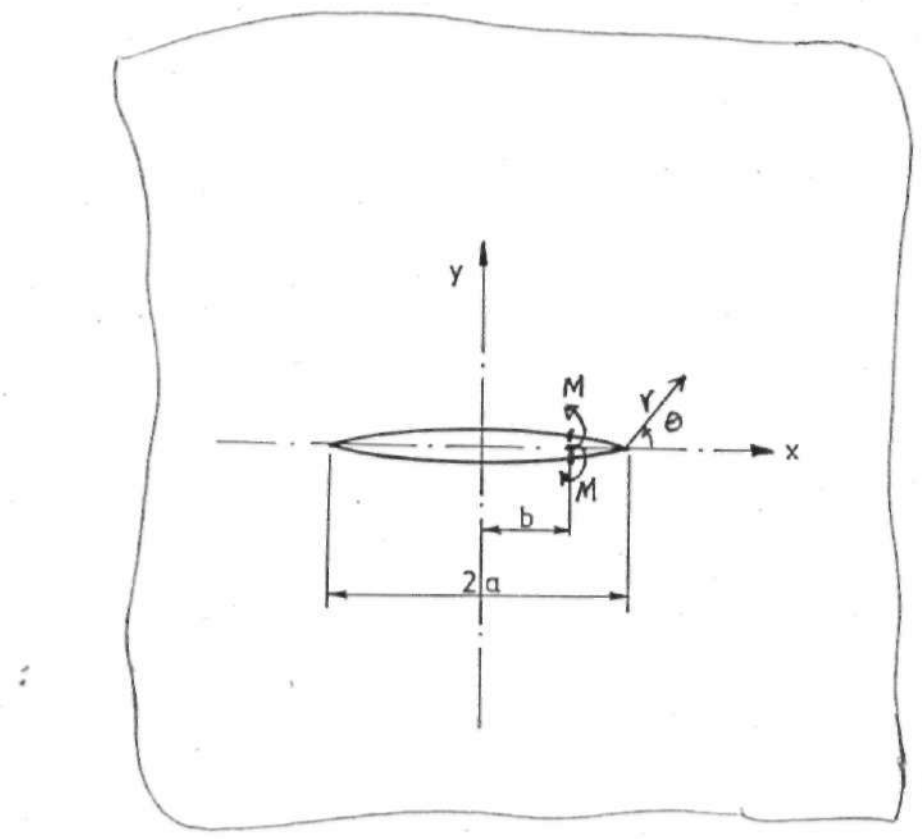


FIG 26:. A Large plate with a central crack of length 2a loaded by Concentrated Couple

The next problem is similar to the one considered above but with concentrated equilibrating moments M at $X = \pm b$. With equation (A.8) as the Green's function for this problem, one can obtain the stress function ϕ_1 as

$$\phi_1' = \frac{2M}{\pi} \frac{z^2 + b^2}{(z^2 - b^2)^2} \sqrt{\frac{a^2 - b^2}{z^2 - a^2}}, \quad \text{--------A.10}$$

The stresses, the strain energy-release rate, the new Irwin crack-tip parameter and the J-integral are respectively obtained as in equations (3.2.31) to (3.2.35), equations (4.2.17), (4.4.8) and (5.2.34) with the stress intensity factor, K_1^P given by

$$K_1^P = \frac{2M}{\sqrt{\pi a}} \frac{a^2 + b^2}{(a^2 - b^2)^{3/2}}, \quad \text{----------A.11}$$

Next, by employing the stress function in equation (A.4) as Green's function, it is intended to derive the stress function for a uniform pressure loading along the crack faces. The problem was defined by equation (3.2.54) and was solved in that section via the new formulae. We intend now to derive equation (3.2.61) instead of assuming it. With equation (A.4) as Green's function, the stress function for uniform pressure loading, σ_o can be written as,

$$\phi_1' = \frac{1}{2a} \int_{-a}^{a} \frac{P}{\pi} \frac{1}{z - b} \sqrt{\frac{a^2 - b^2}{z^2 - a^2}}\, db, \quad \text{-----A.12}$$

Then, let

$$\sigma_o = -\frac{P}{2a} = \text{Constant}. \quad \text{----------A.13}$$

The stress function, ϕ_1, then becomes

$$\phi_1' = \frac{-\sigma_o}{\pi\sqrt{z^2 - a^2}} \int_{-a}^{a} \frac{\sqrt{a^2 - b^2}}{(z - b)}\, db, \quad \text{-----A.14}$$

After substituting,

$$b = z - B,$$

therefore, $db = -dB$

in equation (A.14), and integrating, one obtains,

$$\phi_1' = \frac{\sigma_o}{\pi\sqrt{z^2 - a^2}} \left[\sqrt{a^2 - z^2 + 2Bz - B^2} - iz \sinh^{-1} \frac{2z-2B}{2ai}\right.$$

$$\left. - \sqrt{a^2 - z^2} \sinh^{-1} \frac{2zB + 2a^2 - 2z^2}{2ai|B|}\right]_{z+a}^{z-a}, \quad \text{------A.15}$$

Equation (A.15) gives

$$\phi_1' = \sigma_o\left[\frac{z}{\sqrt{z^2 - a^2}} - 1\right], \quad \text{----------A.16}$$

which is the same as equation (3.2.62). The stress distribution for this problem is given by equations (3.2.63) to (3.2.65).

The next problem considered is shown in Fig. 27. There are two equal straight cracks of length a(1-K), where $0 < K < 1$, along the x-axis. These cracks are subjected to farfield stresses $\sigma_{yy}^{\infty} = \sigma_o$ and $\sigma_{xx}^{\infty} = \alpha\sigma_o$. The new formulae i equations (A.1) and (A.2) can be used to give the stress and displacement distributions. The boundary conditions of the problem can be stated as

$$\left.\begin{aligned} &\sigma_{xx}(z\to\infty) = \alpha\ \sigma_o \\ &\sigma_{yy}(z\to\infty) = \sigma_o \\ &\tau_{xy}(z\to\infty) = 0 \\ &\sigma_{xx}(X,0) = 0, \qquad aK \le |X| \le a \end{aligned}\right\}, \quad \text{----------A.17}$$

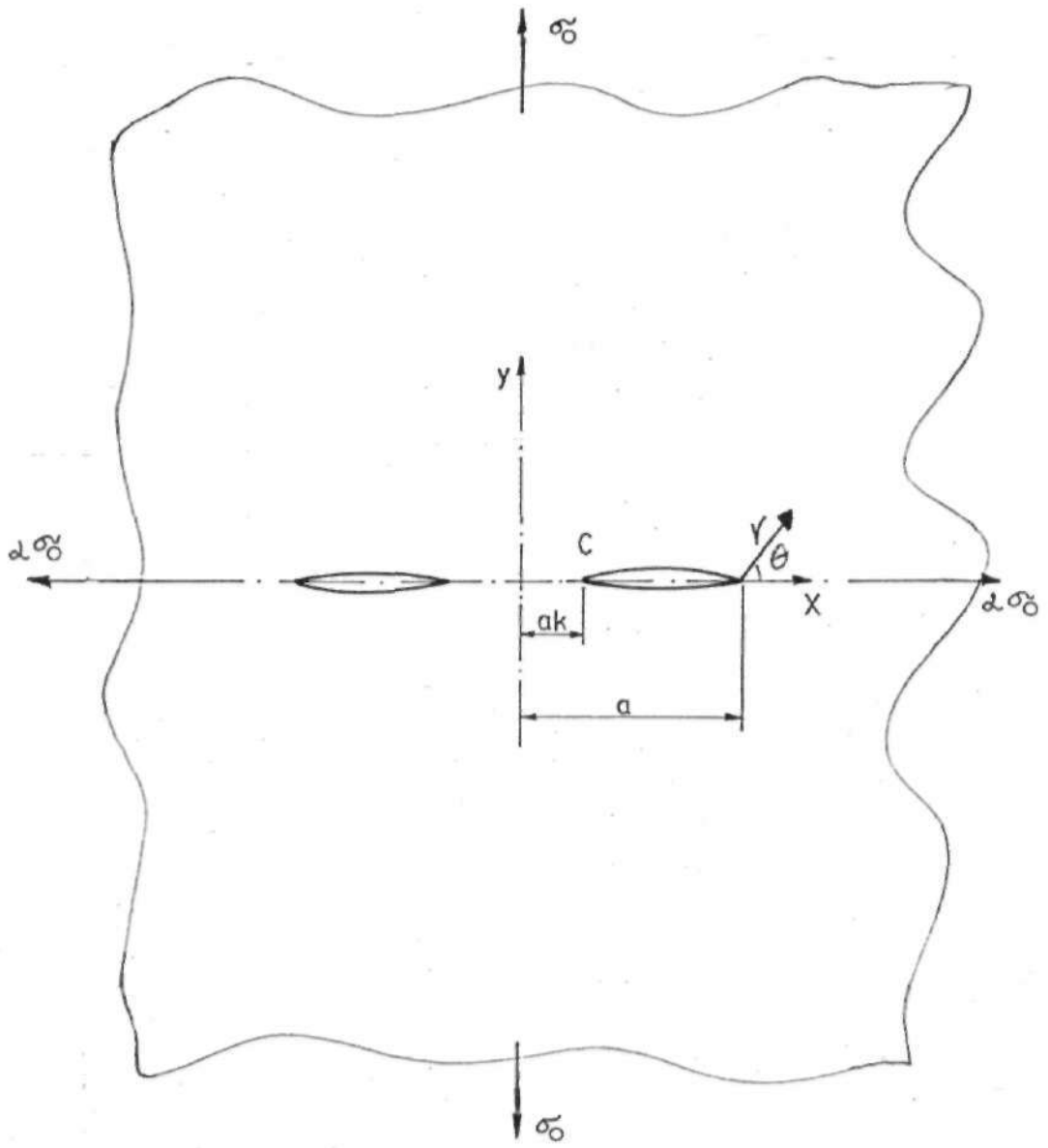


FIG . 27 . A Large plate with two equal collinear cracks .

Sneddon and Lowengrab (1969) gave the stress function, ϕ_1', as,

$$\phi_1' = \sigma_o \frac{z^2 - \lambda^2 a^2}{\sqrt{(z^2 - a^2)(z^2 - K^2 a^2)}}, \quad \text{----------A.18}$$

where

$$\lambda^2 = E'/K', \quad \text{----------A.19}$$

where K',E', are the complete elliptical integrals of the first and second kinds, respectively. K' and E' are then defined as,

$$K' = \int_0^{\pi/2} \frac{d\theta}{\sqrt{1 - K_s^2 \sin^2\theta}}, \quad \text{----------A.20}$$

and

$$E' = \int_0^{\pi/2} \sqrt{1 - K_s^2 \sin^2\theta}\, d\theta, \quad \text{----------A.21}$$

with K_s defined as

$$K_s = \sqrt{1 - K^2}, \quad \text{----------A.22}$$

By employing the new formulae, and the stress function in equation (A.18), the stress and displacement distributions, the strain energy-release rate, the new Irwin crack-tip parameter and the J-integral at the crack-tip C can be obtained respectively as in equations (3.2.19) to (3.2.23), equations (4.2.10), (4.4.6) and (5.2.17), with the stress intensity factor, K_1 given by

$$K_1 = \sigma_o \sqrt{\pi a}\ \frac{\lambda^2 - K^2}{\sqrt{K(1 - K^2)}}, \quad \text{----------A.23}$$

For the stress and displacement distributions at the other crack-tip, equations (3.2.19) to (3.2.23) are still arrived at but the stress intensity factor is less than that given by equation (A.23).

The next problem to be considered is shown in Fig. 28, where there are three cracks along the x-axis in an infinite plane. The body is subjected to some farfield stresses defined as $\sigma^{\infty}_{yy} = \sigma_o$ and $\sigma^{\infty}_{xx} = \alpha\sigma_o$. The stress function for the problem can be assumed as,

$$\phi_1' = \sigma_o \frac{z^3}{\sqrt{(z^2-a^2)(z^2-K_1^2a^2)(z^2-K_2^2a^2)}}, \quad \text{------- A.24}$$

where K_1 and K_2 are some constants greater than unity. By employing the new formulae and the above stress function, the stress and displacement distributions, the strain energy-release rate, the new Irwin crack-tip parameter and the J-integral at the crack-tip, C are obtained as in equations (3.2.19) to (3.2.23), (4.2.10), (4.4.6) and (5.2.17) respectively, but with K_1 defined as,

$$K_1 = \sigma_o\sqrt{\pi a}\ \frac{1}{\sqrt{(K_1^2-1)(K_2^2-1)}}. \quad \text{----------A.25}$$

Again at the other crack tips, the same equations can be arrived at but the stress intensity factors are less than that given by equation (A.25).

Finally, the next problem is shown in Fig. 29. It is an infinite plane body with an equally spaced infinite crack along the x-axis. In one problem the body is subjected to some farfield stresses as $\sigma^{\infty}_{yy} = \sigma_o$ and $\sigma^{\infty}_{xx} = \alpha\,\sigma_o$. In another problem, the body is subjected to an equilibrating point force P at x = 0, y = ± 0. In the problem with farfield applied stresses, Irwin (1957) gave the stress function as,

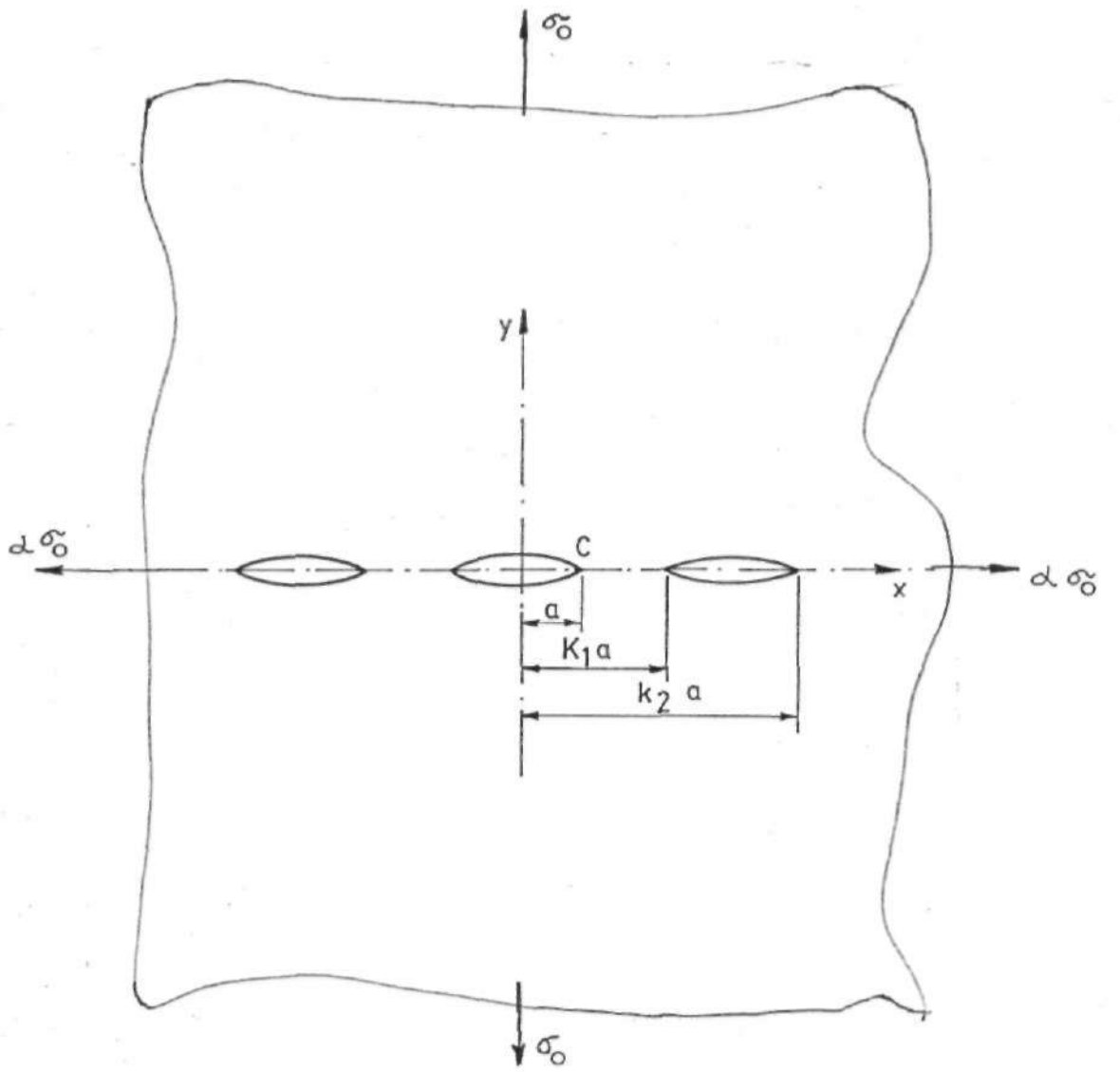


FIG . 28 . A Large plate with three cracks along the x - axis .

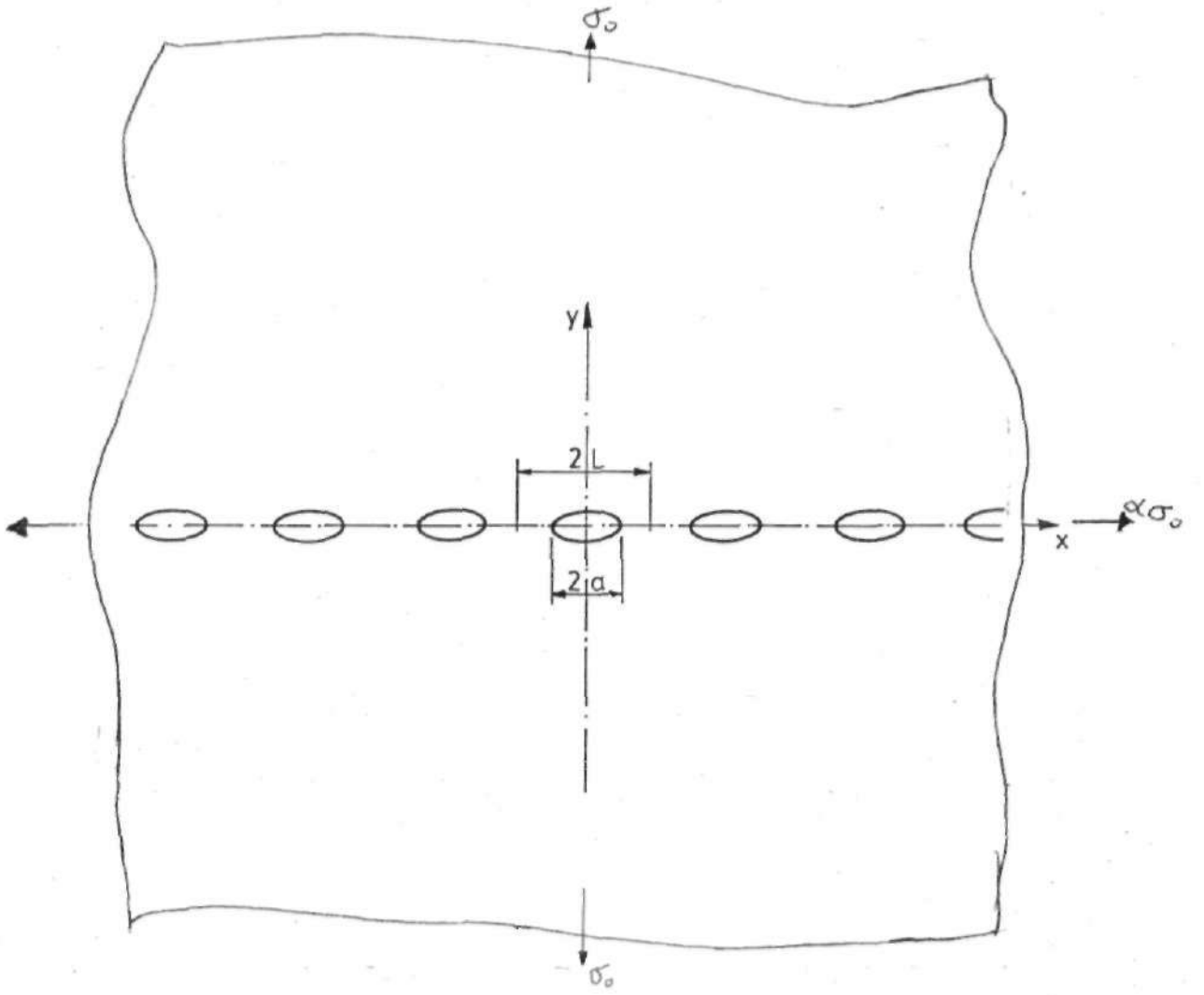


FIG .29 . A Large plate with infinte raw of cracks along the x – axis .

$$\phi_1' = \sigma_o \frac{\text{Sin } \frac{\pi z}{L}}{\sqrt{\text{Sin}^2 \frac{\pi z}{L} - \text{Sin}^2 \frac{\pi a}{L}}}, \quad \text{----------A.26}$$

while he gave that of the point force P as,

$$\phi_1' = \frac{P}{L} \frac{\text{Sin } \frac{\pi z}{L}}{\sqrt{\text{Sin}^2 \frac{\pi z}{L} - \text{Sin}^2 \frac{\pi a}{L}}}. \quad \text{---------- A.27}$$

For the farfield applied stress problem, the stress and displacement distributions, the strain energy-release rate, the new Irwin crack-tip parameter and the J-integral at the crack-tip, C can be obtained as in equations (3.2.19) to (3.2.23), (4.2.10), (4.4.6) and (5.2.17), respectively, but with the stress intensity factor defined as,

$$K_1 = \sigma_o \sqrt{L \tan \frac{\pi a}{L}}. \quad \text{---------- A.28}$$

For the concentrated force loading problem, the stress and displacement distributions, the strain energy-release rate, the new Irwin crack-tip parameter and the J-integral at the tip, C, are respectively obtained as in equations (3.2.31) to (3.2.35), (4.2.17), (4.4.8) and (5.2.34), with the stress intensity factor $K_1 = K_1^P$ defined as

$$K_1^P = P \frac{\text{Sin}^{\frac{1}{2}} \frac{\pi a}{L}}{\sqrt{L}}. \quad \text{----------A.29}$$

These problems reconsidered and those solved in Chapter III are used in arriving at some final conclusions on the strain energy-release rate and the J-integral.

It should be noted that in all the above problems re-examined, the stress distributions obtained by employing the new formulae are not as reported in the literature. These problems were re-examined because the reported old model solutions introduced some unrealistic stress distributions and displacements at the crack tips in almost the same manner as the problems discussed in pages 6 - 13. But the stress intensity factors for these problems given respectively in equations A.5, A.7, A.9, A.11, A.23, A.25, A.28 and A.29, are all as reported in the literature.

APPENDIX B: SAMPLE CALCULATIONS OF G_1 AND J

In this appendix some detailed derivations of the crack extension force G_1 and the J-integral J for some of the problems discussed in Chapters Four and Five are shown.

For the derivation of equation (4.2.10), two equations from which it could be obtained were given. These are equations (4.2.6) and (4.2.7). From equation (4.2.6) with v(x,o) given by equation (4.2.8), one obtains

$$G_1 = \frac{\partial}{\partial a}\left[\int_0^a \sigma_o^2 \frac{(\kappa + \alpha\kappa + 3 - \alpha)}{8\mu}\sqrt{a^2-x^2}\, dx\right], \quad \text{---B.1}$$

Substituting

$$x = a \operatorname{Sin} t$$

Therefore, $dx = a \operatorname{Cos} t\, dt$

in equation B.1, one obtains,

$$G_1 = \frac{\partial}{\partial a}\left[\int_0^{\pi/2} \frac{(\kappa + \alpha\kappa + 3 - \alpha)}{8\mu} \sigma_o^2 a^2 \operatorname{Cos}^2 t\, dt\right]$$

$$= \frac{\partial}{\partial a}\left[\frac{(\kappa + \alpha\kappa + 3 - \alpha)}{16\mu}\sigma_o^2 a^2 \int_0^{\pi/2}(1 + \operatorname{Cos} 2t)dt\right]$$

$$= \frac{(\kappa + \alpha\kappa + 3 - \alpha)}{8\mu}\sigma_o^2 a\left[t + \frac{\operatorname{Sin} 2t}{2}\right]_0^{\pi/2}$$

$$= (\kappa + \alpha\kappa + 3 - \alpha)\frac{\sigma_o^2 \pi a}{16\mu},$$

which gives the result quoted in equation (4.2.9).

If one goes through equation (4.2.7), then from equations (4.2.11) and (4.2.12),

$$G_1 = \lim_{\Delta a \to o} \frac{1}{\Delta a} \int_0^{\Delta a} \frac{K_1^2}{\sqrt{2\pi r'}} \cdot \frac{(\kappa + \alpha\kappa + 3 - \alpha)}{4\mu}\sqrt{\frac{\Delta a - r'}{2\pi}}\, dr'$$

$$= \lim_{\Delta a \to o} \frac{1}{\Delta a} \frac{(\kappa + \alpha\kappa + 3 - \alpha) K_1^2}{8\mu\pi} \int_0^{\Delta a} \sqrt{\frac{\Delta a - r'}{r'}}\, dr', \text{---B.2}$$

In equation B.2, let

$$t = \sqrt{\frac{\Delta a - r'}{r'}}$$

Therefore,

$$dr' = -2\Delta a \frac{t}{(1+t^2)^2}\, dt,$$

then,

$$G_1 = \lim_{\Delta a \to o} - \frac{(\kappa + \alpha\kappa + 3 - \alpha)\sigma_o a}{8\mu} \int_{\infty}^{o} \frac{2\Delta a t^2}{(1+t^2)^2}\, dt$$

$$= - \frac{(\kappa + \alpha\kappa + 3 - \alpha)\sigma_o^2 a}{8\mu} \int_{\infty}^{o} \frac{2t^2}{(1+t^2)^2}\, dt, \text{ ------B.3}$$

In equation B.3, let

$$t = \tan w,$$

Therefore,

$$dt = \sec^2 w\, dw,$$

then B.3, becomes

$$G_1 = - (\kappa + \alpha\kappa + 3 - \alpha) \frac{\sigma_o^2 a}{8\mu} \int_{\pi/2}^{o} \frac{2 \tan^2 w}{\sec^2 w}\, dw$$

$$= -(\kappa + \alpha\kappa + 3 - \alpha) \frac{\sigma_o^2 a}{8\mu} \int_{\pi/2}^{o} 2 \operatorname{Sin}^2 w\, dw$$

$$= -(\kappa + \alpha\kappa + 3 - \alpha)\frac{\sigma_o^2 a}{8\mu} \int_{\pi/2}^{o} [1 - \operatorname{Cos} 2w]dw$$

$$= -(\kappa + \alpha\kappa + 3 - \alpha)\frac{\sigma_o^2 a}{8\mu} \left[w - \frac{\operatorname{Sin} 2w}{2}\right]_{\pi/2}^{o}$$

$$= (\kappa + \alpha\kappa + 3 - \alpha)\frac{\sigma_o^2 \pi a}{16\mu},$$

which is again equal to the result quoted in equation (4.2.9).

These derivations were also carried out before arriving at equations (4.2.10), (4.2.14) and (4.2.20).

Similarly for the evaluation of the J-integral some lengthy algebra were jumped especially between equations (5.2.16) to (5.2.17). This algebra is shown in some detail below. From equations (5.2.10, (5.2.15) and (5.2.16), one obtains,

$$J = \int_{-\pi}^{\pi} \{ \frac{K_1^2}{4\pi Er} [(1+\alpha^2-2\nu\alpha)(2\ \mathrm{Cos}^4 \tfrac{1}{2}\theta - \mathrm{Cos}^2\ \tfrac{1}{2}\theta)$$

$$+ \frac{(1+\alpha)^2(a+\nu)}{8} \mathrm{Sin}^2\theta\ \ \mathrm{Cos}\ \theta + \frac{(1+\alpha^2)(1+\nu)}{2} \mathrm{Sin}^2\theta\ \mathrm{Cos}\ \theta$$

$$+ \frac{(1+\alpha)^2(1+\nu)}{2} [\mathrm{Sin}^2\theta - \mathrm{Sin}^4\ \tfrac{1}{2}\theta)]$$

$$- \frac{K_1^2}{32\pi\ \mu r} [\alpha(\kappa+\alpha\kappa-3+\alpha)(\mathrm{Cos}^2\theta+\mathrm{Cos}\ \theta)+(1-\alpha)(\kappa+\alpha\kappa+3-\alpha)$$

$$(\mathrm{Sin}^2\ \tfrac{1}{2}\theta - 2\ \mathrm{Sin}^4\ \tfrac{1}{2}\theta) - \frac{(4\kappa+4\kappa\alpha+3-2\alpha-\alpha^2)}{2} \mathrm{Sin}^2\theta$$

$$- \frac{\alpha(1+\alpha)}{2} (\mathrm{Cos}^2\ \tfrac{1}{2}\theta - \mathrm{Cos}\ \tfrac{1}{2}\theta\ \mathrm{Cos}\ \tfrac{7}{2}\theta)$$

$$- \frac{(1-\alpha)(1+\alpha)}{4} (\mathrm{Sin}^2\ \tfrac{1}{2}\theta + \mathrm{Sin}\ \tfrac{1}{2}\theta\ \mathrm{Sin}\ \tfrac{7}{2}\theta)$$

$$+ \frac{(3-\alpha)(1+\alpha)}{8} (\mathrm{Cos}^2\ \tfrac{1}{2}\theta - \mathrm{Cos}\ \tfrac{1}{2}\theta\ \mathrm{Cos}\ \tfrac{5}{2}\theta$$

$$- \mathrm{Cos}\ \tfrac{1}{2}\theta\ \mathrm{Cos}\ \tfrac{3}{2}\theta + \mathrm{Cos}\ \tfrac{3}{2}\theta\ \mathrm{Cos}\ \tfrac{5}{2}\theta)$$

$$+ \frac{(5+\alpha)(1+\alpha)}{8} (\mathrm{Sin}\ \tfrac{1}{2}\theta\ \mathrm{Sin}\ \tfrac{5}{2}\theta - \mathrm{Sin}^2\ \tfrac{1}{2}\theta - \mathrm{Sin}\ \tfrac{1}{2}\theta\ \mathrm{Sin}\ \tfrac{3}{2}\theta$$

$$+ \mathrm{Sin}\ \tfrac{3}{2}\theta\ \mathrm{Sin}\ \tfrac{5}{2}\theta)] \} r d\theta, \quad \text{----------B.4}$$

or

$$J = \int_{-\pi}^{\pi} \{ \frac{K_1^2}{4\pi E} [(1+\alpha^2-2\nu\alpha)(2\ \mathrm{Cos}^4\ \tfrac{1}{2}\theta - \mathrm{Cos}^2\ \tfrac{1}{2}\theta$$

$$+ \frac{(1+\alpha)^2(1+\nu)}{16} (\mathrm{Cos}\ \theta - \mathrm{Cos}\ 2\theta\ \mathrm{Cos}\ \theta)$$

$$+ \frac{(1+\alpha^2)(1+\nu)}{4} (\mathrm{Cos}\ \theta - \mathrm{Cos}\ 2\theta\ \mathrm{Cos}\ \theta)$$

$$+ \frac{(1+\alpha)^2(1+\nu)}{2}(\sin^2\tfrac{1}{2}\theta - \sin^4\tfrac{1}{2}\theta]$$

$$- \frac{K_1^2(1+\nu)}{16\pi E}[\alpha(\kappa + \alpha\kappa - 3 + \alpha)(\cos^2\theta + \cos\theta)$$

$$+ (1-\alpha)(\kappa + \alpha\kappa + 3 - \alpha)(\sin^2\tfrac{1}{2}\theta - 2\sin^4\tfrac{1}{2}\theta)$$

$$- \frac{(4\kappa + 4\kappa\alpha + 3 - 2\alpha - \alpha^2)}{2}\sin^2\theta$$

$$- \alpha\frac{(1+\alpha)}{2}(\cos^2\tfrac{1}{2}\theta - \cos\tfrac{1}{2}\theta\cos\tfrac{7}{2}\theta)$$

$$- \frac{(1-\alpha)(1+\alpha)}{4}(\sin^2\tfrac{1}{2}\theta + \sin\tfrac{1}{2}\theta\sin\tfrac{7}{2}\theta)$$

$$+ \frac{(3-\alpha)(1+\alpha)}{8}\cos^2\tfrac{1}{2}\theta - \cos\tfrac{1}{2}\theta\cos\tfrac{5}{2}\theta$$

$$- \cos\tfrac{1}{2}\theta\cos\tfrac{3}{2}\theta + \cos\tfrac{3}{2}\theta - \cos\tfrac{5}{2}\theta)$$

$$+ \frac{(5+\alpha)(1+\alpha)}{8}(\sin\tfrac{1}{2}\theta\sin\tfrac{5}{2}\theta - \sin^2\tfrac{1}{2}\theta$$

$$- \sin\tfrac{1}{2}\theta\sin\tfrac{3}{2}\theta + \sin\tfrac{3}{2}\theta\sin\tfrac{3}{2}\theta)]\}d\theta. \quad \text{---- -- B.5}$$

These integrals were evaluated as:

$$\int\cos^2\theta\,d\theta = \frac{\theta}{2} + \frac{\sin 2\theta}{4},$$

$$\int\sin^2\theta\,d\theta = \frac{\theta}{2} - \frac{\sin 2\theta}{4},$$

$$\int\cos^4\theta\,d\theta = \frac{3\theta}{8} + \frac{\sin 2\theta}{4} + \frac{\sin 4\theta}{32},$$

$$\int\sin^4\theta\,d\theta = \frac{3\theta}{8} - \frac{\sin 2\theta}{4} + \frac{\sin 4\theta}{32},$$

$$\int\cos q_1\theta\cos q_2\theta\,d\theta = \frac{\sin(q_1-q_2)\theta}{2(q_1-q_2)} + \frac{\sin(q_1+q_2)\theta}{2(q_1+q_2)},$$

$$\int\sin q_1\theta\sin q_2\theta\,d\theta = \frac{\sin(q_1-q_2)\theta}{2(q_1-q_2)} - \frac{\sin(q_1+q_2)\theta}{2(q_1+q_2)}.$$

Then equation (B.5) gives

$$J = \frac{K_1^2}{2E}[\frac{(1+\alpha^2-2\nu\alpha)}{4} - \frac{(1-\alpha)^2(1+\nu)}{8}]$$

$$- \frac{K_1^2(1+\nu)}{8E}\left[\alpha\left(\frac{\kappa+\alpha\kappa-3+\alpha}{2}\right) - \left(\frac{(1-\alpha)(\kappa+\alpha\kappa+3-\alpha)}{4}\right)\right.$$

$$- \left(\frac{4\kappa+4\alpha\kappa+3-2\alpha-\alpha^2}{4}\right) - \alpha\left(\frac{1+\alpha}{4}\right) - \left(\frac{1-\alpha)(1+\alpha)}{8}\right)$$

$$\left. + \left(\frac{(3-\alpha)(1+\alpha)}{16}\right) - \left(\frac{(5+\alpha)(1+\alpha)}{16}\right)\right], \quad \text{B.6}$$

With $\kappa = \frac{3-\nu}{1+\nu}$ in equation (b.6), one could simplify J to,

$$J = \frac{(1+\alpha)(3-\alpha)}{4E} K_1^2, \quad \text{B.7}$$

Expanding equation (B.7), equation (5.2.17) is obtained.

REFERENCES

ALJYU, A.A. and DANIEL, I.M.(1985):"Effects of Strain Rate on Delamination Fracture Toughness of Graphite/ Epoxy". Delamination and Debonding of Materials, ASTM STP 876, American Society for Testing and Materials; Philadelphia, 1985, pp. 336 - 348.

ALIYU, A.A., DANIEL, I.M. and SHAREEF, I.(1985):"Delamination Fracture Toughness of F185-T300". Presented at ASTM Symposium on Toughness of Composites, U.S.A., March, 1985.

AOKI, S., KISHIMOTO, K. and SAKATA, M.(1981):"Energy-Release Rate in Elastic-Plastic Fracture Problems". ASME Journal of Applied Mechanics, 48: pp. 825 - 829.

ATKINSON, C. and ESHELBY, J.D.(1968):"The Flaw of Energy Into the Tip of a Moving Crack". International Journal of Fracture Mechanics, 4: pp. 3 - 8.

BEGLEY, J.A. and LANDES, J.D.(1972): In: "Fracture Toughness". ASTM STP 514: pp. 1 - 23.

BROWN, W.F. and STRAWLEY, J.E.(1967):"Plane Strain Crack Toughness Testing of High Strength Metalic Materials". ASTM STP 410, American Society for Testing and Materials; pp. 8 - 16.

BUDIANSKY, B. and RICE, J.R.(1973):"Conservation Laws and Energy-Release Rates". ASME Journal of Applied Mechanics, 40: pp. 201 - 203.

CLAUSING, D.P.(1969):"Crack Stability in Linear Elastic Fracture Mechanics". International Journal of Fracture Mechanics, 5: pp. 211 - 227.

DALLY, J.W.(1979):"Dynamic Photoelastic Studies of Fracture", William M. Murray lecture. Experimental Mechanics, 19: pp. 349 - 361.

DANIEL, I.M.(1983):"Experimental Methods in Applied Mechanics". ASME Journal of Applied Mechanics, 50: pp. 963 - 976.

EFTIS, J. and LIEBOWITZ, H.(1972):"On the Modified Westergaard Equation for Certain Plane Crack Problems". International Journal of Fracture Mechanics, 4: pp. 383 - 392.

ERDOGAN, F.(1983):"Stress Intensity Factors". ASME Journal of Applied Mechanics, 50: pp. 992 - 1000.

GRIFFITH, A.A.(1920):"The Phenomena of Rapture and Flow in Solids". Phil. Transactions, A221: pp. 163 - 198.

HAYES, D.J.(1975):"Origins of the Energy Balance Approach to Fracture". Journal of Strain Analysis, 10: pp. 195 - 200.

HERRMAN, A.G. and HERRMAN, G.(1981):"On the Energy-Release Rates for a Plane Crack". ASME Journal of Applied Mechanics, 48: pp. 525 - 528.

HEYER, R.H.(1973):"Crack Growth Resistance Curves (R-Curves) - Literature Review". Fracture Toughness Evaluation, ASTM STP 527: pp. 3-16.

ICHIKAWA, M. and TANAKA, S.(1982):"A Critical Analysis of the Relationship between the Energy-Release Rate and the Stress Intensity Factor for Non-Coplanar Crack Extension Under Combined Mode Loading". International Journal of Fracture, 18: pp. 19 - 28.

IRWIN, G.R.(1957):"Analysis of Stresses and Strains Near the End of a Crack Traversing a Plate". ASME Journal of Applied Mechanics, 24: pp. 361 - 364.

IRWIN, G.R.(1960):"Fracture Mechanics", in: Structural Mechanics , Goodier, J.N. and Hoff, N.J., eds., Pergamon Press, New York: pp. 557 - 591.

IRWIN, G.R., DALLY, J.W., KOBAYASHI, T., FOURNEY, W.L., ETHERRIDGE, M.J. and ROSSMANITH, H.P.(1978):"On the Determination of the $\dot{a}$-k Relationship for Birefringent Polymers". Paper presented at the 1978 SESA Spring Meeting at Wichita, Kansas State, U.S.A.

MUSKHELISHVILI, I.N.(1953): "Some Basic Problems of the Mathematical Theory of Elasticity". Groningen, P. Noordhoff Ltd. pp. 1-711.

PARIS, P.C.(1977):"Fracture Mechanics in the Elastic-Plastic Regime". Flaw Growth and Fracture, ASTM STP 631: pp. 3 - 27.

PARIS, P.C., TADA, H., ZAHOOR, A. and ERNST. H.(1979): The Theory of Instability of the Tearing Mode of Elastic-Plastic Crack Growth". Elastic Plastic Fracture, ASTM STP 668: pp. 5 - 36.

RICE, J.R.(1968):"A Path-Independent Integral and the Approximate Analysis of Strain Concentration by Notches and Cracks". ASME Journal of Applied Mechanics, 35: pp. 379 - 386.

SANDERS, J.L.(1960):"On the Griffith-Irwin Fracture Theory". ASME Journal of Applied Mechanics, 27: pp. 352 - 353.

SANFORD, R.J.(1979):"A Critical Re-Examination of the Westergaard Stress Function". Mechanics Research Communications, 6: pp. 289 - 294.

SIH, G.C.(1974):"Strain Energy-Density Factor applied to Mixed Mode Crack Problems". International Journal of Fracture, 10: pp. 305 - 321.

SNEDDON, I.N. (1946): "The Distribution of Stress in the Neighbourhood of a Crack in an Elastic Solid". Production of Royal Society of London, Series A, 187: pp. 229 - 260.

SNEDDON, I.N. and LOWENGRUB, M. (1969): "Crack Problems in the Classical Theory of Elasticity". John Wiley and Sons, Inc., pp. 1 - 129.

SOKOLNIKOFF, I.E. (1956): "Mathematical Theory of Elasticity". MacGraw-Hill, Inc., pp. 1 - 476.

TURNER, C.E. (1975): "Yielding Fracture Mechanics". Journal of Strain Analysis, 10: pp. 207 - 216.

WESTERGAARD, H.M. (1939): Bearing Pressures and Cracks". ASME Journal of Applied Mechanics, 24: pp. 361-364.

WHEELER, C., EASTABROOK, J.N., ROOKE, D.P., SCHWALBE, K.H., SETZ, W. and KONING, A.U. (1982): "Recommendations for the Measurement of R-Curves Using Centre-Cracked Panels". Journal of Strain Analysis, 17: pp. 205 - 213.

WILLIAMS, M.L. (1956): "On the Stress Distribution at the Base of a Stationary Crack". ASME Journal of Applied Mechanics, No. 56: pp. A16.

WILLIAM, G. (1962): "Stress Distribution about a Slowly Growing Crack Determined by Photoelastic-Coating Method". 2, pp. 359 - 365, Experimental Mechanics.